NTNU
Norwegian University of
Science and Technology

Harmonic analysis of collection grid in offshore wind installations

Chan Shan

Harmonic Analysis of Collection Grid in Offshore Wind Installation
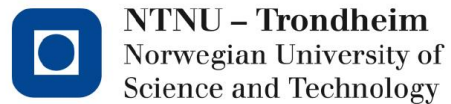
By Chan Shan

For obtaining the degree of Master of Science in

Electrical Engineering at Delft University of Technology (TU Delft)

& Wind Energy at Norwegian University of Science and Technology (NTNU)

TUDelft
Delft
University of
Technology

EWEM

NTNU – Trondheim
Norwegian University of
Science and Technology

Acknowledgements

Chan Shan

Oct 10, 2017

Abstract

Wind power as a green and low-carbon renewable energy could effectively mitigate the energy crisis and reduce environmental pollution, including the rapid developing offshore wind power with its rich reserves, wind stability, high wind speed, less interference, noise and other advantages. The trend for development of offshore wind farms is towards a growing size of installed power. This together with higher distances from the shore leads in many cases to HVDC connection as a preferred choice for power export. Thus, the wind turbines are connected through a collection grid to an offshore platform. As the offshore wind farm contains a large number of power electronic devices and submarine cables, it will inevitably lead to the occurrence of harmonic resonance. Offshore wind farm harmonic and resonance will affect the power quality, while poses a huge challenge to the power grid and wind power.

In this thesis work, a comprehensive harmonic analysis in offshore wind farm was studied. Firstly, a detail configuration of the wind energy conversion system and harmonic analysis basics are described and interpreted. Next, a suitable model of one offshore wind farm is built and validated in Matlab/Simulink. The equivalent circuit is calculated for the components in the aggregated wind farm based on their harmonic model. And potential resonance problems are analyzed by frequency scan method to calculate the resonance impedance and frequency. Afterwards, based on the self-built system model, potential harmonic issues that arise in the system are investigated in time domain to interpret the THD at PCC between the collection grid and the onshore grid. As well, a few effective strategy for suppressing harmonics are simulated to evaluate the various influence on the harmonic issue. Both the designed C-type filter and active power filter performed a satisfying results on harmonics suppression. The main contents are as follows:

1) Study on the basics of harmonics and discuss the potential sources and the mechanism of harmonic resonance in offshore wind farms. The simulation model of PMSG Wind Energy Generation System is established. Harmonic characteristics of machine-side converter, grid-side converter and line filter capacitor are analyzed. It could be deducted that machine-side converter current is mainly influenced by wind speed and mechanical control system. Grid-side current, which has a lower harmonic to the machine-side current, are mainly affected by PWM control system of converter. Thus, harmonic current injected from PMSG to grid is mainly determined by gird side converter and filter in wind turbine out port.
2) System resonance problem of OWF was analyzed in equivalent circuit models.

And then the frequency scan method is applied to detect the influence components which potentially affect the harmonic resonance. From the simulation results, the main resonance points are similar at collection grid bus of wind farm in HVAC transmission system and HVDC transmission system, which are around 7th order frequency. Resonance points are also influenced by length, inductance and capacitance of submarine cable, due to the high distributed capacitance of submarine cable.

3) Study on the strategy for suppressing harmonics at an offshore wind farm. The harmonics distribution in cases with C-type filter or active power filter adopted are designed and analyzed in the simulation models. The C-type passive filter performed satisfying results on harmonics suppression.

Keywords

Contents

List of figures

List of tables

Chapter 1 Introduction

1.1 Background and Motivation

As we all know, wind power is a kind of intermittent and random energy affected by varied wind speed, season, region and climate. With the increasing scale of offshore wind farms, a series of power quality problems will be produced for the onshore grid [1]. The power fluctuation has great influence on the power flow, especially when the wind power output fluctuation is strong, it is easy to cause the voltage fluctuation. At the same time, the interaction between the transient change of power and the voltage feedback control devices in the system will probably lead to voltage flicker problems [2]. In addition, the power electronic equipment is another potential source of harmonics. The generated harmonics will cause great threat to the safety and stability of the system [3].

At present, the non-linear power electronic devices in the process of wind energy conversion play a very important role [4]-[6]. The most common types of wind turbine applied in the large scale offshore wind farm system are the variable speed wind turbine generator with partial scale power converter or with full scale power converter. For the offshore wind farm, a large number of submarine cables with high distributed capacitance are used in the transmission system, which will cause the system harmonic problems more serious [7]. In addition, when the cables are connected with the transformers or other inductive components, the parallel resonance is easy to occur in the system, which will increase the harmonic current distortion rate and distortion level.

In large scale offshore wind farm, full-rated converters are applied in the offshore wind farm construction, which makes the harmonics generated from those power electronic devices more complex compared with the conventional harmonic components. The difference of harmonic response is mainly reflected in the different frequency range of the output harmonics. In addition, the complexity of the response characteristic of the power electronic devices around low-frequency band is also very high, and the harmonic impedance also has a great influence on the resonance point of the offshore grid system. The resonance phenomena has amplification impact on the harmonic characteristics of the system. This will cause the harmonic level injected into the onshore grid several times higher than that of the individual turbines [8]. A large area of cable laying also cause the resonance point more complex to be estimated.

The trend for development of offshore wind farms is towards a growing size of installed power. This together with higher distances from the shore leads in many cases to HVAC and HVDC connection as a preferred choice for power export [9]. The complex non-linear electronic devices for the control system of these transmission systems are also challenging the existing system. At the same time, the grid topology applied in offshore wind farm determines the length, electrical parameters and connection methods of the cable, and directly affects the harmonic generation,

resonance frequency and its intensity. The lack of consideration of collection grid will lead to less accurate harmonic analysis. The harmonic subject is however rarely taken up in discussion about the effect of the collection grid of the offshore wind farm, which could be an interesting study direction.

In electrical power system, a harmonic is defined as the content of the signal with an integral multiple of the fundamental frequency. Non-linear components, including transformers, converters, electrical machines, non-linear load, produce harmonics in the system. Since the system is interconnected together, the harmonics can create unpredicted stresses to the system and they can propagate over great distances within the whole network, especially in an offshore wind farm. The harmonics in the system could attenuate the stability of the system control and reduce the voltage quality. The harmonic levels in the network could be amplified by resonance phenomenon [3]. Moreover, harmonics could also cause the overheating of the electrical components in the network which may damage their insulation. These bad effects show that harmonics reduce the efficiency of both the wind energy conversion system (WECS), and the power utilization.

Since the uncertainty of wind resources and the characteristics of the wind turbine generator, the output power of WECS exhibits fluctuation and intermittent nature, which easily results in harmonic problems. Furthermore, offshore wind farms are installed in remote sea, far from conventional generations. Therefore, in order to have high quality power supplies from offshore wind farms, evaluating the harmonic emission levels at the point of common coupling (PCC) has already been an urgent demand. However, directly measuring and monitoring harmonics, particularly on high voltage transmission network, can be very challenging [10]. Thus, the system modeling and harmonic analysis in computer simulation programs can be a proper way to estimate the potential harmonics and help to find solutions to improve the power quality based on the study results.

1.2 Problem Description

The trend for offshore development of wind farms is towards a growing size of installed power. This together with higher distances from the shore leads in many cases to HVDC connection as a preferred choice for power export. In this thesis work, an offshore wind farm model consisting of full-scale converter wind turbines, is proposed in MATLAB/Simulink. It is important that the models built for analyzing the harmonics are practical and appropriate. However, offshore wind farms involve multiple suppliers of wind turbines, cables, transformers and other devices. The design details of each components in the system required by system modeling and analysis are kind of impossible to get. Majority of related research work assume the wind farm as an ideal voltage source or an equivalent constant power grid, which ignore the fluctuation and intermittent nature of wind farms and the collection grid network. This thesis work is considered to build a numerical model for a large scale offshore wind farm and to investigate the potential influence factors in the wind farm,

such as the individual wind turbine, the collection grid network, the transmission system type. Hopefully after the thesis work, an overall scope and understanding of the harmonic problems and resonance phenomenon in the large scale wind farm could be established. And finally some effective methods should be recommended to reduce the harmonic problems.

1.3 Objective and Scope

The objective of this master thesis is to discuss the harmonic problems which may occur in the collection grid of the large scale offshore wind farm (OWF) and try to validate a practical simulation modelling and harmonic analysis approach for OWF.

This topic can furthermore be divided into several sub-topics:
- Wind farm collection grid and transmission system modeling
- Harmonic resonance analysis by frequency scan method
- Time-domain circuit simulation and harmonic FFT analysis

The scope of the thesis work is set as follows:
- Target System- a simple offshore wind farm collection grid in radial topology is modeled and studied in MATLAB/SIMULINK. The wind farm employs a 2MW permanent-magnet synchronous generator and a back-to-back full power conversion system (Type 4 turbine). The offshore transmission system is equipped with 100kV HVDC export submarine cables and substation converters. The onshore transmission system and the ac power grid is assumed to be a stable and ideal infinite power supply.
- Testing Method- all the analysis are performed in MATLAB/SIMULINK and the conclusions drawn from the simulation results. No practical experiments are involved.
- Harmonic field- the investigation scope of harmonics limits to maximum of 30th order. And the study will only focus on odd order harmonics. No considering of inter-harmonics.
- Analysis Method- FFT analysis tool for measuring THD at the connection point between the target offshore wind farm collection grid and the onshore power grid. Frequency scan method for harmonic resonance analysis on the equivalent harmonic model of the target offshore wind farm collection grid.
- Exclusions- the following aspects are not considered in the project:
  - ✓ The effect of control strategy to the harmonic emission
  - ✓ The detailed modeling of the collection grid assumes ideal switches and well protected

1.4 Report Layout

This thesis report is organized as follows:

Chapter 1 introduces an overview of the work objective and background.

Chapter 2 gives an overview about the essential definitions and basics referred to harmonics. The subsequent part shows the theory of harmonic resonance and potential causes in offshore wind farm. The frequency scan method and time domain harmonic

analysis based on FFT calculation in numerical simulation model are introduced, for further analysis foundation.

Chapter 3 interprets the basic of wind turbine and offshore wind farm installation. It describes the composition and structure of collection grid for offshore wind farms, including the common collection grid topology, MVAC or MVDC collection grid, transmission system category, and compares the advantages and disadvantages introduced followed.

Chapter 4 establishes the type 4 PMSG wind turbine based on the model example from MATLAB. Harmonic current output characteristics of the machine-side converter and the grid-side converter are analyzed by the FFT analysis tool in Simulink. The model for an investigated offshore wind farm is validated in simulation. Harmonic output characteristics of the offshore wind farm is also analyzed.

Chapter 5 builds the harmonic model of offshore wind farm installation, simulates the system in equivalent impedance circuit. And then the frequency scan method is applied to detect the influence components which potentially affect the harmonic resonance. Give an approximate forecast of the theoretical resonance point.

Chapter 6 studies on the strategy for suppressing harmonics at the offshore wind farm. By introducing the characteristics and working principle of filters, a C-type filter and an active power filter adopted in the system are designed and analyzed with simulation models. We have also mentioned three effective methods to optimize the system network structure to help suppressing harmonics.

Chapter 7 draws the main conclusions from this project and gives some suggestions for future research work.

Chapter 2 Basic of Harmonics

The fundamental theory about harmonics are introduced in this chapter, including the definition and several indices referred to harmonics, such as Total Harmonic Distortion. The potential harmonic sources in the offshore wind farm are discussed and investigated as follows. The subsequent part shows the theory of harmonic resonance and potential causes in offshore wind farm. The last part explains the research method related to the analysis of the harmonics and resonance.

2.1 The Definition of Harmonic

Harmonics are steady-state distortions to current and voltage waves and repeat every cycle in power system. The harmonic can be simply expressed as

$$f_h = h \cdot f \tag{2-1}$$

Terms that have represent the harmonic components of the current (or voltage). Several points need to be emphasized:

1) The harmonic order h is a positive integer ($h = 1, 2, 3, \dots n$). And the term f_h is the frequency of the h order harmonic. When $h = 1$, it represents the fundamental frequency, which is usually 50Hz in Europe countries or 60 Hz in America countries.

2) When $h < 1$, which means the sinusoidal waves are the below the fundamental frequency, those kind of components are called the sub-harmonics. When any non-integer values of h occur, it means that the voltages or the currents have frequency between the harmonics, those kind of components are called inter harmonics [11]. Both sub-harmonics and inter harmonics will not be included in the research scope of this thesis paper.

3) According to the basic concept of Fourier series, the waveform of transformation must be periodic and relatively unchangeable. Although in the actual operation situation, due to the complex changes in power system conditions, it is impossible to achieve infinite waveform unchanged, thus it will take some time to apply the Fourier transform. Therefore, harmonic phenomena and transient phenomena need to be distinguished.

4) It is necessary to distinguish between short time harmonics (such as impulse currents, etc.) and steady-state or quasi-steady-state harmonics.

2.2 Total Harmonic Distortion (THD)

The total harmonic distortion (THD) is an important parameter that could represent the harmonic distortion level of voltage or current signals. It is defined as the ratio of the sum of the powers of all harmonic components to the fundamental frequency component. Taking voltage as an example, THD is an index to compare the harmonic voltage components with the fundamental voltage component, as the following

equation defines it mathematically.

$$THD = \frac{\sqrt{\sum_{h=2}^{n} V_h^2}}{V_1} = \frac{\sqrt{V_2^2 + V_3^2 + \cdots + V_n^2}}{V_1} \qquad (2\text{-}2)$$

Where the variable h is the number of harmonic, and n is the maximum harmonic order of voltage, V_1 is the nominal system voltage at the fundamental frequency [12]. Generally, the analysis of harmonics is considered below the 51th order, since the higher range of frequency components have little power to influence the stability of the power grid. Total harmonic distortion can be expressed also in per cents. Theoretically, the smaller the value of THD measured in any output signal of one system, the degree of distortion is lower at that signal.

On the analogy of this, the similar parameter for measuring the current distortion is called the total harmonic current distortion (THDI), as following equation [13]

$$THDI = \frac{\sqrt{\sum_{h=2}^{n} I_h^2}}{I_1} = \frac{\sqrt{I_2^2 + I_3^2 + \cdots + I_n^2}}{I_1} \qquad (2\text{-}3)$$

For the evaluation of power quality related to levels of harmonic distortion, there is recommended limits standard for THD (and THDI) in an electrical distribution system at the point of common coupling (PCC) that must be obeyed in industry facility. The PCC is the point between the non-linear load and its connection to a power source, either the serving utility or an on-site generator. [6].

The ANSI/IEEE 519-1992 standard lists is recommended to be one of the most widely used guide for THD limits in a power grid system [36]. Thus, one objective of harmonic analysis is to assist the system design and installation in meeting IEEE 519-1992 requirements limiting THD, as shown in Table 2-1.

Table 2-1: THD Limits (% of the fundamental)

PCC Voltage	THD (%)
V ≤ 69 kV	5
69 kV < V < 161 kV	2.5
V > 161 kV	1.5

2.3 Fast Fourier Transform (FFT)

As previously described, the total harmonic distortion (THD) interprets the distortion degree between the waveform and the pure sine wave, characterized mainly by the amplitude of voltage harmonics in the system, which is defined as the percentage of the total harmonic content of the RMS value and fundamental RMS ratio.

The analysis and calculation of harmonic distortion level is based on the algorithm called Fast Fourier Transformation (FFT), proposed by American scientists in 1965. In general, any periodic waveform could be expanded into Fourier series. For instance, a periodic current signal could be expressed as following equation

$$i(t) = \sum_{h=1}^{M} I_h \cos(h\omega_0 t + \theta_h) \qquad (2\text{-}4)$$

In which, I_h is the h order harmonic peak current, θ_h is the phase of the h order harmonic current [14], ω_0 is the fundamental angular frequency, M is the considered highest order of harmonics, normally less than 50.

Fast Fourier Transformation is simply an algorithm that can compute the discrete Fourier transform (DFT) much more rapidly and efficiently than other available algorithms [14]. It does not require a detail understanding in the algorithm itself, but rather be treated as a particular method and computation tool to obtain the amplitude, frequency and phase etc. information of the harmonic signal [14], which has the advantages of high precision, strong practicability. Thus, the FFT algorithm will not be interpreted in detail in this thesis.

In the harmonic analysis of offshore collection grid, FFT can describe curves that show the relationship between the orders of harmonics and interprets the THD values at each order harmonic of the system. Thus FFT method laid a theoretical foundation for exploring the factors affecting harmonics. And it is one of the most important and widely used methods to research harmonics in the current stage.

2.4 Sources of Harmonics in Offshore Wind Farms

Harmonic problem is one of the main concern in the offshore wind farm installation, where large number of subsea cables and converters are equipped. Wind farms are known as sources of harmonic distortion. When analyzing the harmonics from a wind farm system, two main emission sources of harmonics should be considered.

- **Harmonic Emission from Individual Wind Turbine**

The first common concern is the harmonic emissions from individual wind turbines [8]. Theoretically, the harmonics generated from wind turbine generators will flow into the entire collection grid of the offshore wind farm, and will cause the harmonic distortion level more severe into the onshore grid. Generally, the harmonic emission from individual wind turbines mainly comes from power-electronic converters, induction machines and power transformers. Nowadays large size wind turbines in MW capacity usually contain converters, normally could be a full scale power converter or a partial-size converter. However, quite a lot research have already focused on this topic. And it turns out that the level of harmonic output from wind turbines is relatively small [8]. The harmonics are influenced by the converter control strategy and switching frequency of electronic devices. Only some relatively high emission occurs at higher harmonic orders, which is lack of enough power to influence the voltage quality of the whole grid system, and for other frequencies where the distortion levels are traditionally lower.

- **Harmonic Emission from the Wind Farm Collection Grid**

The impact of the wind farm collection grid on the harmonic emission has not been studied in very detail, but harmonic resonances have been widely studied [27]-[29]. The collection grid in one offshore wind farm can consist capacitance of large amount of subsea cables and the inductance of the transformers, which will induce the resonance problem occur. In this case, the harmonic emission from the wind farm into the onshore grid is several times higher than that of the individual turbines. In this

thesis work, the one consideration target is on the potential influence of the collection grid to the harmonic propagation and related resonance issues.

2.5 Harmonic Resonance

2.5.1 Introduction

In an electrical system, the capacitance appears in the form of cables, overhead lines, or capacitor banks, while the inductance appears in the form of cable lines, transformers. A reactance of an electrical network is dependent on the frequency. At certain frequencies the inductive and capacitive components of the network start to resonate with each other at the resonance frequency. When the harmonic current is the same as the resonant frequency, the harmonic current or voltage will be amplified. In that way, the harmonic problem will become more severe [30]. The resonance frequency can be calculated as

$$f = \frac{1}{2\pi}\sqrt{\frac{1}{LC}} \; , \tag{2-4}$$

Where L is the inductance and C is the capacitance of the network.

Two different types of harmonic resonances can be distinguished: parallel resonances and series resonances [8], discussed in Sections 2.5.2 and 2.5.3. The components that make the power system more likely to experience resonances are discussed in Section 2.5.

2.5.2 Parallel Resonance

At parallel resonance, the parallel LC tank circuit acts like an open circuit with the circuit current being determined by the resistor, R only. At resonance, the impedance of a parallel resonance circuit at resonance is at its maximum value and equal to the value of the resistance R in the circuit. Also at resonance, as the impedance of the circuit is now that of resistance only, the total circuit current, I will be "in-phase" with the supply voltage.

When the parallel resonance occurs, the harmonic current is excited to oscillate between the inductive energy storage and the capacitor energy storage. Then parallel circuits produce current resonance. Then overvoltage become easier to occur. At the same time, it could result in an amplification of the harmonic current, thus the current elsewhere in the gird could be higher than that close to the source of the distortion [8], as illustrated in Fig. 2-1.
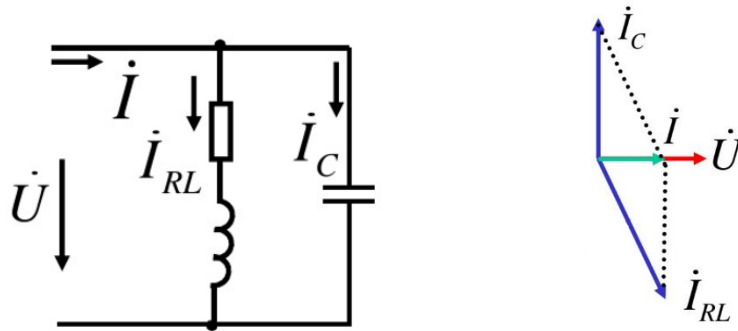
Fig. 2-1: Parallel resonance circuit and phase diagram
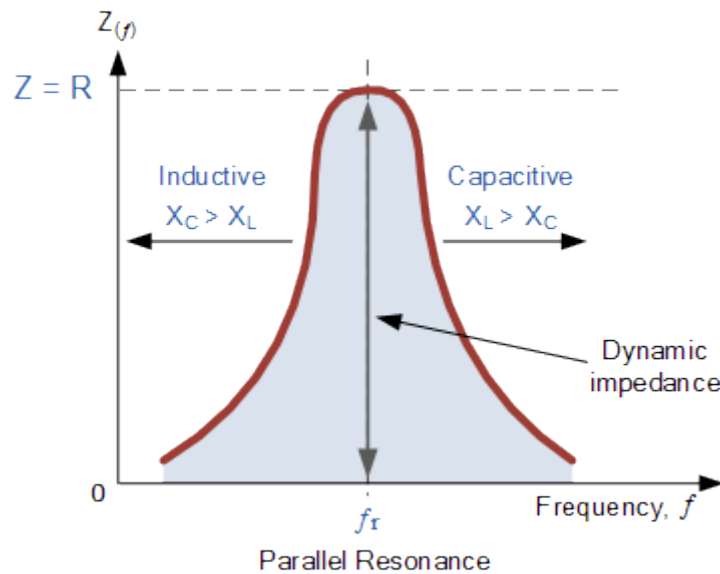
Fig. 2-2: Impedance in a parallel resonance circuit

It has a negative impact on every wind farm component, and eventually it will damage the system. The parallel resonance is common when there are capacitor banks or long AC lines connected with large transformers. Hence, for the offshore wind farm collection grid with large amount of those nonlinear components, the parallel resonance is a hidden danger that can result in the harmonic distortion level at PCC several times higher than that of individual turbines [8]. In an extreme case, even a relatively small harmonic current can cause destructively high voltage peaks at resonance frequency.

2.5.3 Series Resonance

During series resonance, the inductive reactance of system components (such as transformers) is equal to the capacitive reactance of system components (such as cables or capacitor banks) as shown in following equations. This would cause the impedance of the circuit very low.

$$\omega L = \frac{1}{\omega C} \tag{2-5}$$

The natural resonant frequency will be:

$$f = \frac{1}{2\pi\sqrt{LC}} \tag{2-6}$$

When $X_L = X_C \gg R$, then $U_L = I_0X_L = U_C = I_0X_C \gg U = I_0R$, where U represent the system equivalent voltage source. Though these inductive and capacitive high voltages drop U_L, U_C will have opposite signs, which makes the sum of the two voltages be zero, but each of them will still have high amplitude, as presented in the phase diagram below. The point at which this occurs is called the resonant frequency point of the circuit.
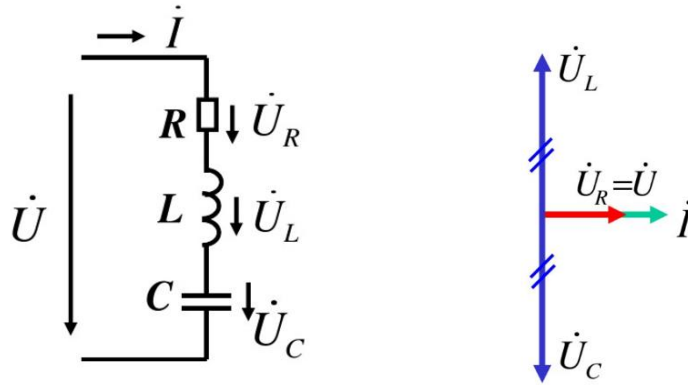
Fig. 2-3 Series resonance circuit and phase diagram

2.6 Harmonic Analysis Methods

2.6.1 Introduction

Harmonics analysis in this thesis report has two main stages. The first step is the frequency scan method to identify resonance frequencies [15]. The second one is to perform time-domain simulation to calculate harmonic distortion indices, mainly refer to THD values at the collection point.

2.6.2 Frequency Scan Method

The usual method for analyzing harmonic impedance characteristic is the impedance scan method, which is also called frequency scan method. It is an approximate linearization analysis method. The core of impedance scan method is to describe the whole system impedance versus frequency curve from the studied component sight, which includes two kinds curve plot, reactance versus frequency curve and resistance versus frequency curve. Its principal objective is to detect the possible resonance frequencies at which parallel and/or series resonance can occur in the electrical network.

The impedance seen at a bus is calculated at all frequencies, sweeping or scanning the frequency spectrum of interest. It can be treated as being performed by injecting a 1A sinusoidal current with a certain frequency at this bus and calculating the corresponding voltage which consequently corresponds to the impedance at this bus.

This process is repeated for all frequencies within the range of interest [15]. The result of this calculation is a plot of the magnitude of the driving point impedance at a certain bus (on the vertical axis) versus the harmonic frequency (or the harmonic order) (on the horizontal axis). Then the relation between the magnitude of impedance and the frequency (or harmonic order) is obtained, and the potential resonance point of the system could be observed. A high value (a sharp peak) of impedance at certain frequency means the network is having parallel resonance at this frequency. When parallel resonance happens, relatively small excitation current can generate large voltage amplification. A near zero value (a sharp dip) of impedance at certain frequency means the network is having series resonance at this frequency [15]. When series resonance happens, relatively small excitation voltage can cause large current amplification.

In this thesis, the frequency sweep impedance plot presents the magnitude and angle of the network impedance calculated at PCC (Power Collection Point). In another word, this method measures impedance of circuit as function of frequency. In Chapter 4, frequency scan method is used to monitor these possible dangerous resonance phenomenon, and also to analyze the potential influence of those electric devices in the OWF system.

2.6.3 Time-Domain Harmonics Analysis

Time-domain analysis is also called transient simulation. The time domain formulation consists of differential equations representing the dynamic behavior of the interconnected power system components. The resulting system of equations, generally non-linear, is normally solved using numerical integration [16]. It is normally used to verify results of other frequency analysis algorithms.

Time-domain analysis requires considerable computation even for relatively small systems. Another problem attached to time domain algorithms for harmonic studies is the difficulty of modelling components with distributed or frequency-dependent parameters [17].

In the time domain analysis, simulation is performed for sufficient time to reach steady state conditions using digital simulators, such as PSCAD, MATLAB, PowerFactory. The resulting waveforms are then analyzed using FFT to determine harmonic components of currents and voltages under investigation. Consequently harmonic distortion indices are calculated. In this thesis, MATLAB/Simulink software is applied in time domain harmonic analysis. Simulink provides an integrated environment for modeling, simulation, and integration of dynamic systems. In this environment, a complex system can be constructed without a large number of writing programs, and only by simple mouse operations.

2.7 Summary

All in all, this chapter gives an overview about the basics of harmonics, including some essential definitions and indices, such as Total Harmonic Distortion (THD). The

subsequent part shows the theory of harmonic resonance and then discuss the potential causes in the offshore wind farm (OWF). The last part explains the research method for harmonics and resonance analysis. The frequency scan method and time domain harmonic analysis based on FFT calculation in numerical simulation model are introduced, for further analysis foundation.

Chapter 3 Basics of Offshore Wind Farm System

In general, an offshore wind farm (OWF) mainly consists of wind turbine generator (WTG), collection grid, transmission system. Thus, the harmonic characteristics from OWF will be complicated cases of different categories of wind turbine generators, the electric configuration of converters, the collection grid topology and the transmission system in either HVAC or HVDC. This chapter, the basic theory about offshore wind farm system is described as the fundamental for the model building and harmonic analysis of the offshore wind farm system.

3. 1 Wind Turbine Fundamentals

3.1.1 Wind Turbine Characteristics

The model is based on the steady-state power characteristics of the turbine. The output power equation of the wind turbine is given by the following equation:

$$\text{P} = \frac{1}{2}\rho V_0^3 A C_p(\beta, \lambda) \tag{3-1}$$

Where V_0 represents the wind speed (m/s), ρ is the air density (kg/m^3), A is the turbine swept area (m^2), C_p is the performance coefficient of the turbine. C_p is a function of pitch angle β (degree) and tip speed ratio of the rotor blade tip speed to wind speed $\lambda = \frac{\omega R}{V_0}$, where ω is the angular rotor speed for the wind turbine.
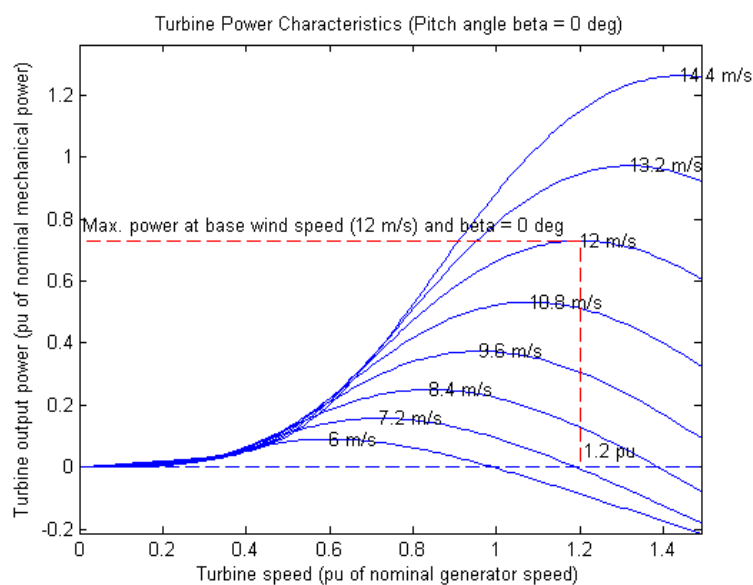
Fig. 3-1: Wind turbine power characteristics

The analytical approximation method used to calculate C_p is given by the following equations:

$$C_p(\beta, \lambda) = 0.5176 \left(\frac{116}{\lambda_i} - 0.4\beta - 5 \right) e^{\frac{-21}{\lambda_i}} + 0.0068\lambda \qquad (3\text{-}2)$$

$$\frac{1}{\lambda_i} = \frac{1}{\lambda + 0.08\beta} - \frac{0.035}{\beta^3 + 1} \qquad (3\text{-}3)$$
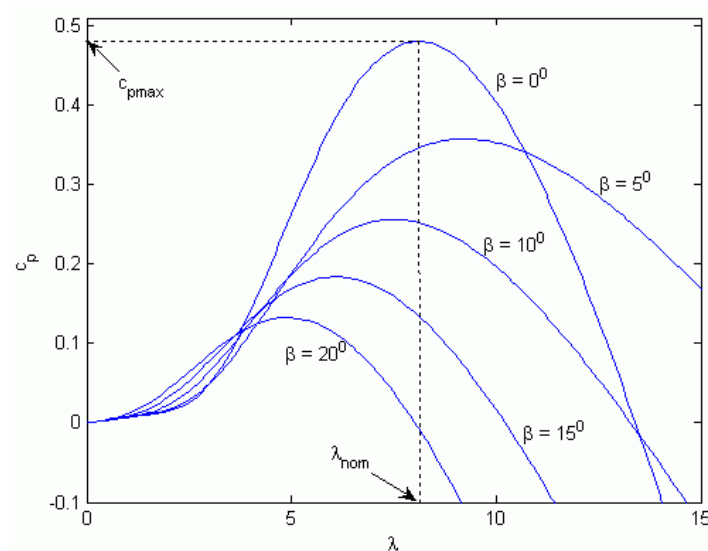
Fig. 3-2: C_p-β characteristics for different values of the pitch angle β

3.1.2 Operation Modes of Wind Turbine

The tasks of the turbine's control system include the start and stop of the turbine, power output limitation, optimization of power output and efficiency, keeping the rotational speed within a certain range, minimization of power fluctuations and mechanical loads. The following figure shows the ideal operation status under the changing of wind speed, which can be categorized to three operation modes.
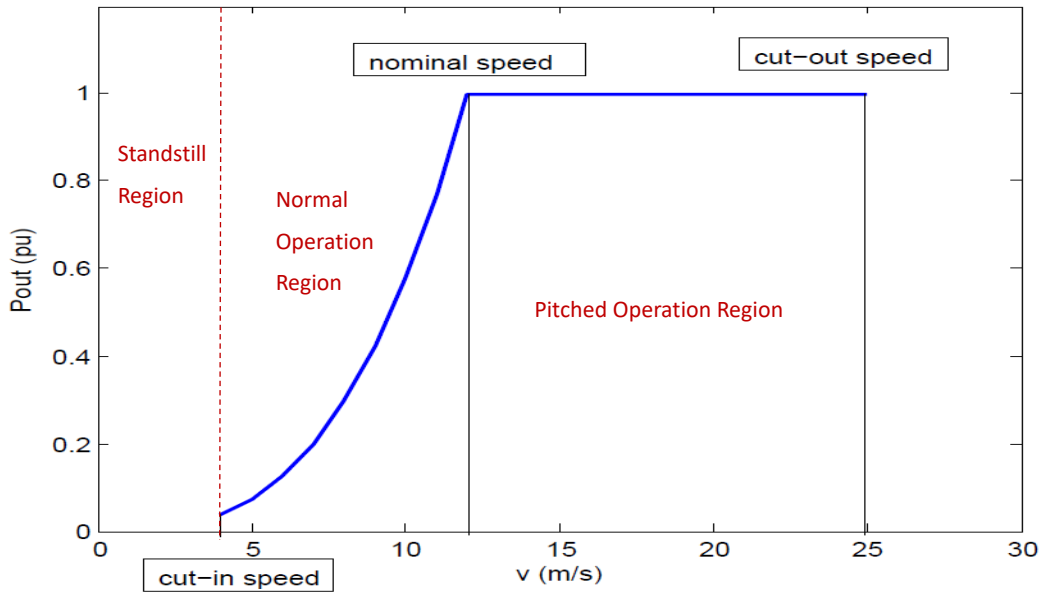
Fig. 3-3: Power Curve vs Wind Velocity

Zone 1: $V_{wind} < V_{cut-in}$ or $V_{wind} > V_{cut-out}$
The power output of turbine should be zero. In this operation mode, the task of the control system is the start and stop of the turbine.

Zone 2: $V_{cut-in} \leq V_{wind} \leq V_{rated}$
The blade pitch angle is set fixed to its optimal value that allows the turbine to extract maximum energy from incident wind [18]. The wind turbine rotational speed ω is controlled to keep the tip speed ratio λ at its optimal value. In this operation zone, the wind turbine is controlled by MPPT control scheme to optimize the power output. Speed control loop bandwidth must be limited within around 2 rad/s in order to obtain a smooth power output [19].

Zone 3: $V_{rated} < V_{wind} \leq V_{cut-out}$
When the wind speed is greater than the rated wind speed, in order to limit the power output, the wind turbine is controlled by the pitch regulation. To avoid over rated power excursions due to wind gusts, a constant power reference is obtained by reducing torque (with the increase of rotational speed). In another words, if the wind speed is larger than the rated speed, then the output power command of the PMSG $P_g{}^*$ is set to 1pu [20].

3.1.3 Category of Wind Turbine Generators

As the fast development of offshore wind farm technology, the harmonic problems turn out to be more complicated and severe. The harmonic and resonance problems of offshore wind farms vary from each other according to the various types of wind turbine generators, electric configuration and control strategy of converters, the

capacitance to earth from undersea transmission cables, etc. The technology of wind turbine generators change from previous fixed-speed induction generator with small rating power to various speed wind turbine generator with much larger rating power.

The generators for wind turbines are categorized into following four major types, fixed-speed induction generator (FSIG), doubly fed induction generator (DFIG), and full power converter (FPC) synchronous or asynchronous generators [21]. The overview of wind turbine concepts are described as following.

Fixed Speed Wind Turbine Generator

Fixed speed wind turbines comprise of squirrel cage asynchronous generator (SCIG). Its rotor is driven by the turbine and its stator is directly connected to the grid. This type wind turbine generator has the limitation that any wind fluctuation will result into the fluctuations of the mechanical torque and the electrical power, which lead to voltage fluctuation and flicker effects in the case of weak grid.
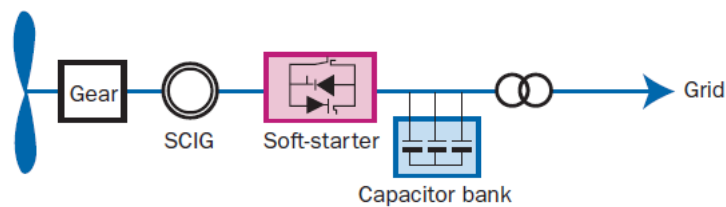
Fig. 3-4: Fixed Speed Wind Turbine Generator

Limited Speed Wind Turbine Generator

Limited variable speed wind turbines are usually equipped with a wound rotor induction generator (WRIG). The rotor electrical resistance is changed through power electronics to allow both the rotor and the generator to vary their speed up and down to $\pm 10\%$ of synchronous speed. It's also called variable slip operation. And this type design concept helps reduce the mechanical stress of the turbine and maximize the power quality. Aerodynamic control method of limited speed wind turbine is active blade pitch control.
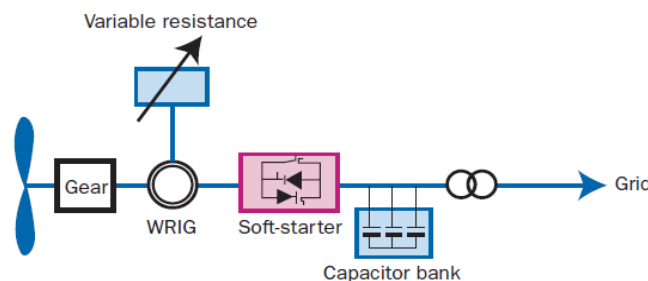
Fig. 3-5: Limited Speed Wind Turbine Generator

Variable Speed Wind Turbine Generator with Partial Scale Power Converter

This type turbine generator is also known as doubly-fed induction generator (DFIG). The stator of the generator is connected directly to the grid and the windings of the rotor are connected to a partial scale power converter [22], as shown in Fig. 3-6.
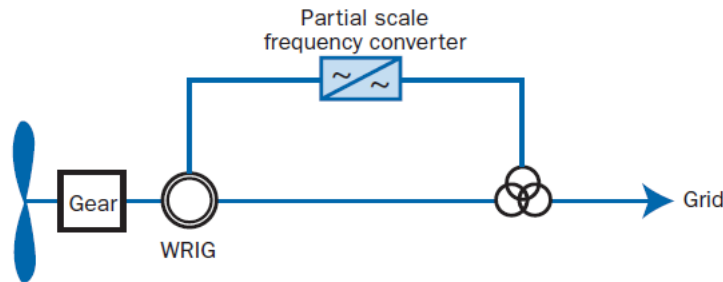
Fig. 3-6: Variable Speed Wind Turbine with Partial Scale Power Converter

The harmonics in DFIG mainly come from three aspects: the first is the natural slot harmonic and saturated air gap in the structure of asynchronous generator. Secondly, the AC excitation flowing to the grid network provided by the various speed generation system with large rating power will potentially threaten the grid. Thirdly, harmonics from the grid network could also be a source.

DFIG type wind turbine is commonly used because of its small capacity excitation converter, low cost and high efficiency. But the use of DFIG will lead to serious harmonic problem, many studies have been done about it in recent years.

Variable Speed Wind Turbine Generator with Full Scale Power Converter

While a partial scale power converter is needed for DFIG, the full scale power converter is needed for this Type D generator configuration [13]. The wind turbines are equipped with the classical drive-train (geared), in the direct drive concept (without gear box, slow running generator). And various types of generators could be used in this type wind turbines: permanent magnet synchronous generator (PMSG), wound rotor synchronous generator (WRSG), and wound rotor induction generator (WRIG) [23], shown as Fig. 3-8. Since being completely decoupled from the grid, it can provide wider range of operating speed than type C, and has a broader range of reactive power and voltage control capacities [24].
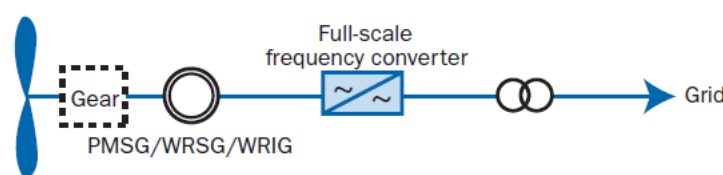
Fig. 3-7: Variable Speed Wind Turbine with Full Scale Power Converter

Compared to the DFIG, PMSG has lower operation and maintenance cost, simpler structure, smaller noise and higher energy conversion efficiency, especially for large rating power generators. Therefore, the market share of large capacity wind power generator based on PMSG is increasing. At the same time, more and more wind power manufacturers favor this type of wind turbines in industry market.

In the future, long distance and large scale offshore wind farms will be more inclined to adopt PMSG power generation system. At present, there is not much research on harmonic analysis of PMSG power generation system, compared to the study of DFIG. Based on the above analysis, this paper takes offshore wind farm equipped with PMSG wind turbines as the object of study, and studies the harmonic and resonance problems of the collection grid in offshore wind farm installations.

3.2 Collection Grid in Offshore Wind Farm

3.2.1 Collection Grid Topology

In common cases, the capacity of a single wind turbine in offshore wind farms is several MW, thus the total capacity of a medium or large scale offshore wind farm connected to the onshore grid could be several hundred MW or several thousand MW. They need the collection grid to interconnect all the wind turbine generators (WTG) to fulfill the long distance transmission. In fact, the collection grid topology of the offshore wind farm decides the length of undersea cables, electric parameter settings and connecting configuration, which directly influence the harmonic emission of the system, resonance frequency and intensity. Lacking the consideration of collection grid topology will lead to inaccuracy of harmonic analysis. Thus, before stepping into the harmonic analysis of the offshore wind farm connected to the grid, the collection grid topology needs to be concerned.

In recent studies in the collection grid topology, researchers often focus more on the economy and reliability, but much less on the harmonic analysis of the offshore wind farm. The offshore collection grid have three alternative configurations so far: radial (or string), ring and star cluster [41]. Considering the variety of wind farm capacity, the distance to the onshore grid, the reliability of the system and other factors, the collection grid topology of wind farm installation will have different choices. Since the collection grid topology will result in different length of undersea cables, electric parameter settings and connecting configuration of electronic devices, and those facts have relatively large influence on harmonic resonance problems, thus affecting the reliability of the offshore wind farm and its connecting onshore grid. The following three alternative configurations of the collection grid topologies are introduced in detail:

1) Radial

For radial clusters, the wind turbines inject their power into the same feeder in string configuration. The feeder bus should have high enough voltage level to have

the capacity of the total power production of the string. In order to adapt WTG and feeder bus voltages, each wind turbine need a set-up transformer.

This radial configuration has the advantages of simple operation and low cost, but the disadvantage exists in the lack of reliability. Once the network cable or the corresponding equipment needs to be repaired, the whole cable needs to be cut off. All in all, the radial collection system is currently the most economical, common collection grid topology. The radial collection grid topology has been more widely adopted in many offshore wind farms, such as Horns Rev2 wind farm in Denmark.
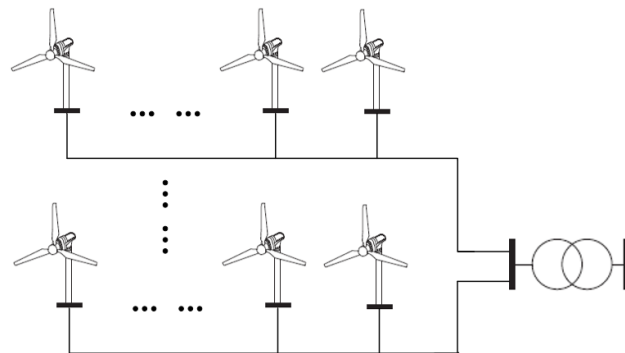
Fig. 3-8: Radial clusters configuration

2) Ring

The ring topology is quite similar to the string topology, but the collection grid connects each two independent string clusters to a closed ring cluster through cables. For ring clusters configuration, it reduces the possibility of a cable failure and allows auxiliary supplies to turbines be maintained. The system reliability is improved but apparently costs more and the operation is relatively complex.
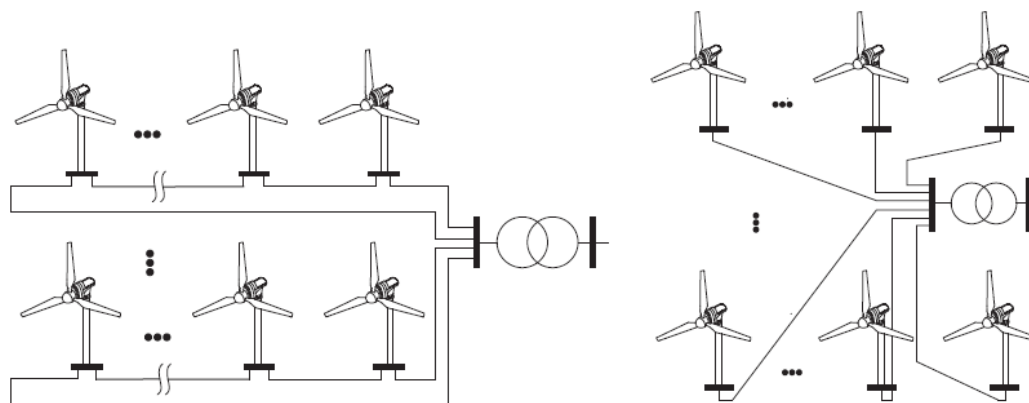
Fig. 3-9: Ring (left) and star (right) clusters configurations [61]

3) Star

For the star collection system, each single WTG is connected to a nodal point directly through cables in small or medium capacity, where a transformer is installed in the offshore platform. After the set-up transformer, the total generated power is further brought to a central collection point through large capacity cables. The star

collection grid topology has high reliability, however, the disadvantage also exists. The system needs more electric devices such as circuit breaker, isolating switch. Thus, the cost is relatively higher than other topology. The wind farms generally do not use this type of collection grid topology, unless in special demand.

Currently, the most cost effective collection voltage seems to be approximately between 30kV to 36kV [42]. Only radial connection is the most common configuration used in offshore wind farm projects thus far, therefore, this thesis work also chose the radial cluster configuration for the wind farm installation.

3.2.2 MVAC/MVDC collection grid

When wind farms adopt HVDC transmission technology, MVAC or MVDC collection grid can be used. When the power from MVAC collection system being converted to HVDC transmission system, it needs large capacity transformer, power electronic converter and other equipment as shown in Fig. 3-11. It is necessary to build a large offshore platform; and the maintenance cost of the power frequency transformer is high.
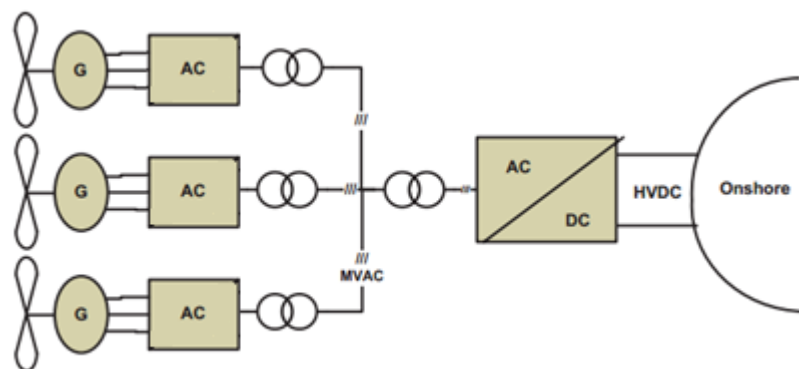
Fig. 3-10: An MVAC-collection grid for an offshore wind farm [43]

The wind farm using DC (MVDC)-collection grid has been considered as one of effective solutions to solve these problems due to recent research. Several configurations were evaluated with respect to overall system efficiency [43].
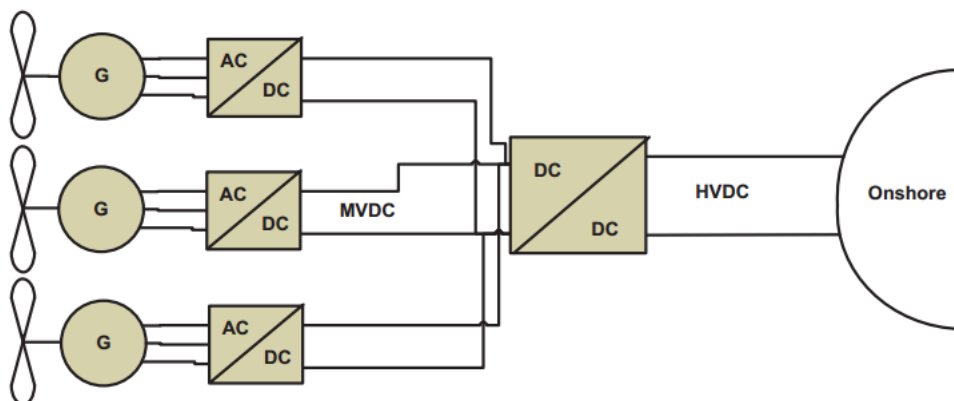
Fig. 3-11: An MVDC-collection grid for an offshore wind farm

Compared with MVAC collection grid, the layout of MVDC collection cables avoids the problems of reactive charging current and potential resonance. And it also requires that the output voltage of each turbine is at a certain level that there is no need for a step-up transformer before the central converter of the farm. As a result, switching losses are reduced [43]. Although the MVDC collection system also needs the booster station, but power electronic converter for DC boost occupies a much smaller space. Other benefits from this solution are less expensive generator drives and more reliable systems, since one VSC less is utilized in each turbine [43].

3.3 Transmission System to Shore

3.3.1 Introduction

The majority of offshore wind power plants that are currently operating have adopted an HVAC connection for the cabling to the shore (main ac grid). As the size of future wind power plants and the distance to shore is likely to increase, more and more planned offshore projects will be connected via HVDC (High voltage direct current) transmission system [44].
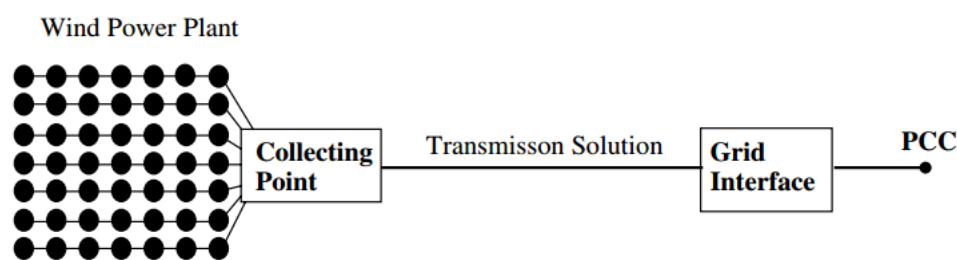
Fig. 3-12: Structure diagram of an offshore wind power plant

For HVDC transmission system, there are two technical options: line commutated converter (LCC)-based HVDC and voltage-source converter (VSC)-based HVDC technology [45]. The HVDC system has been dominated by line commutated converters (LCC); however, voltage source converters (VSCs) which include two-level, multi-level and modular multilevel converters are increasing dramatically due to having superior system performance and controllability [46].

3.3.2 HVAC Transmission

Currently, HVAC (High voltage alternating current) transmission system is the most common solution adopted by the existing offshore wind farms. HVAC technology can be economically used for the lower rated schemes over short distances [47]. And it has following features:

1) The undersea AC cable generates large reactive current, which reduces the active current carrying capacity of the cable. Limits of AC cable power ratings over longer distances will probably not be improved enough to allow utilization of this technology on larger wind farms [47].

2) Due to the long distance, the cable owns high capacitance, thus large reactive power compensation device is often needed, which increases the cost and brings troubles to the corresponding substation. Furthermore, high capacitance of the cable may lead to resonances between the offshore and onshore grids. Then voltage distortion may be a vital problem for the grid which need extra efforts to fix with.
3) Compared to HVDC connections, the substations for HVAC is low cost, because no power electronic devices (converters) are needed. But the cables are more expensive than that for dc transmission system, when the transmission distance is far away from the shore.

3.3.3 LCC-HVDC Transmission

LCC-HVDC (High voltage direct current with thyristor-based line-commutated converters) transmission systems have proven its reliability on land in practical industry for a while [48]. At present, it has gradually been used in the transmission network. Due to its large capacity, long-distance transmission and simple control strategy, LCC-HVDC technology has certain applicability for offshore wind power. The whole grid connected transmission system is shown below.
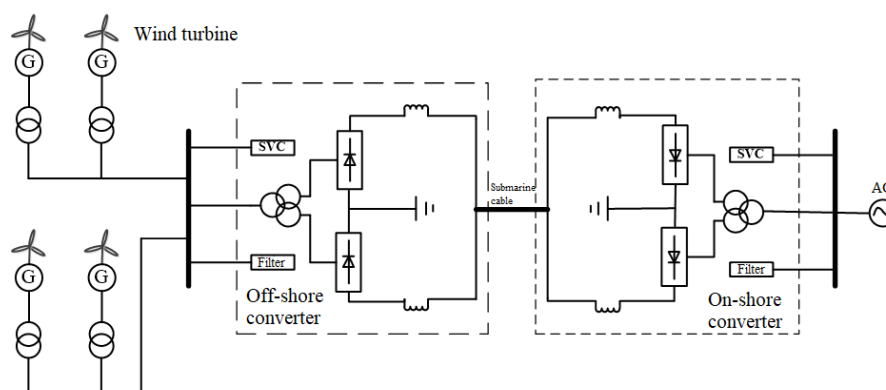
Fig. 3-13: Configuration of LCC-HVDC transmission system to shore

The LCC-HVDC transmission system mainly includes transformer, SVC, filter, thyristor converter, DC reactor, DC cable and other equipment. The normal operation of the substation is based on the thyristor converter. Due to the characteristics of the thyristor, a large number of reactive power need to be absorbed in order to operate under normal condition, thus the collecting point need to be equipped with reactive power compensation equipment, which will increase the cost and volume of the offshore substation.

The conventional HVDC transmission system has following advantage features compared to HVAC technology:
1) Frequency at the sending end can be variable. The ability to de-couple the multiple turbines, and avoid synchronizing them with the onshore network has a major advantage, as each end of the link may be allowed to operate according to its own control strategy, largely independent of the other end.

2) Transmission distance is not a technical limitation. The impact of cable charging current in AC cable interconnections is significant, even dominant, but in DC applications it is negligible.

LCC-HVDC systems have proven its reliability on land in practical industry for a while and could be cheaper than VSCs for power rating of hundreds of megawatts [42]. But for offshore wind farms, the suitability should be considered carefully.

1) Converter and other electric equipment need space to install, which means enormous offshore platform has to be built.
2) Furthermore, it is easy effected by ac network disturbances, which may lead to converter commutation failures.
3) It requires reactive power and voltage support for offshore ac bus. Usually a static synchronous compensator is essential to fulfill the network requirement [49].

3.3.4 VSC-HVDC Transmission

VSC-HVDC is a new type of power transmission and distribution technology with power electronic technology as its core, which is gaining more and more attention. It has only become possible as a result of important advances in the development of insulated gate bipolar transistors (IGBTs). In this way, pulse-width modulation (PWM) technology can be used for the VSCs as a means of control, as opposed to thyristor-based LCCs used in the conventional HVDC technology.
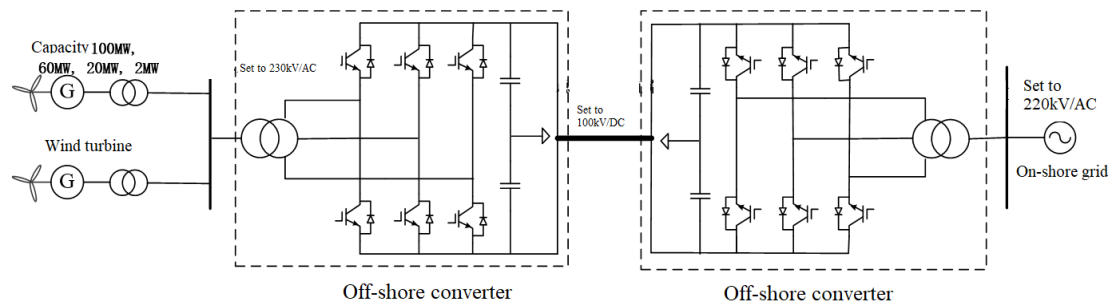
Fig. 3-14: Configuration of VSC-HVDC transmission system to shore

HVDC-VSC technology has several advantages compared with LCC-HVDC.
1) VSC technology does not require commutation voltage supplied by compensator, and the DC capacitor is enough for the reactive power provision.
2) Low order harmonics almost not existed thanks to the voltage and current control uses PWM (pulse-width modulation) with switching frequency of several times of the fundamental frequency [47]. And the harmonic distortion in ac side voltage is lower in VSC-HVDC system, and fewer auxiliary filters are required compared with LCCs.
3) The active and reactive power through undersea DC cable to the ac grid is independently controlled. Thus, the voltage regulation is more effective due to the robust control strategy. And the VSCs are able to operate in weak ac network, in another word, the reliability of the system could be guaranteed.

3.3.5 Transmission System Selection

In general, offshore wind farm installed with rating power less than 150MW and offshore distance within 100km can consider the HVAC transmission system. Compared to the other two HVDC transmission system, the cost of HVAC collection solution is much lower, which has economic superiority for industry installation.

When the installed capacity is between 100-400MW, the priority is given to the HVDC transmission system. Considering the construction cost and installation difficulty of the offshore converter substation, VSC-HVDC has more economic and technological advantages than the traditional LCC-HVDC.
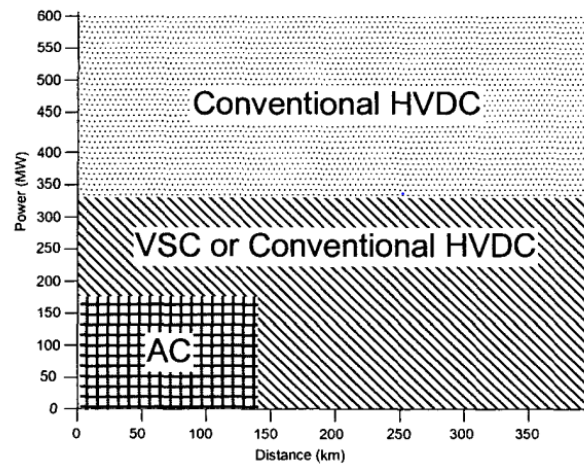
Fig. 3-15: Transmission solutions with power range vs distance [14]

For large scale offshore wind farms with power ratings above about 300 MW, it can be seen that conventional LCC-HVDC technology is the optimum solution [50]. An estimated comparison of the different transmission systems is as shown in Figure 3-16. Therefore, considering the actual situation, we need to evaluate the specific choice of transmission system connected to shore, within the consideration of installation capacity, total cost, system reliability, and harmonic issues.

Chapter 4 Modelling and Harmonic Analysis in Offshore Wind Farm

4.1 Wind Energy Generation System

4.1.1 Introduction

This following section presents the dynamic model of the individual direct drive PMSG wind energy generation system [25]. The wind turbine generator considered in this paper employs a direct-driven (without gearbox) PMSG directly coupled to the wind turbine and connected to the electric grid through offshore collection grid [26]. The stator windings of the PMSG are connected to a full scale back-to-back ac/dc/ac power converter which composed of a machine-side and grid-side converter with an intermediate dc link [26]. The system configuration is shown in Figure 4-1.
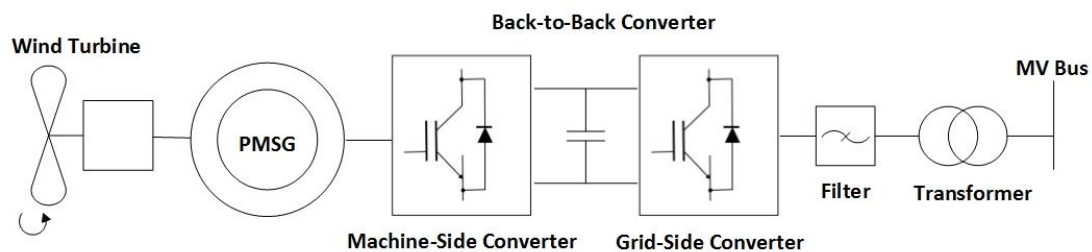
Fig. 4-1: Configuration of PMSG based wind energy generation system

Wind turbine output power is sent to PMSG. To obtain maximum energy production, the rotational speed of the PMSG is controlled by a PWM converter [27]. The machine side converter proposes the control schemes including a maximum power point tracking (MPPT) control. The grid side converter is used to regulate the dc voltage of the back-to-back converter, and the collection grid voltage. A simple LC filter is also designed to filtering the possible ripple caused by the switching [28]. And a step-up transformer is included to transform the electricity from the low voltage machine side to the medium voltage side for inter-array collection grid.

This section directly applied the detailed model of the variable speed direct-driven PMSG (Type 4) based wind energy generation system. The proposed modeling approach is developed using SimPowerSystems of MATLAB/Simulink. The dynamic performance of the proposed PMSG based wind energy generation system and especially its harmonic emission impact is discussed and evaluated through digital simulations carried out using detailed simulation method [26].

4.1.2 Parameter Setting of Wind Turbine

The Synchronous Generator and Full Scale Converter (Type 4) Wind Turbine Detailed

Model from Matlab example is the original fundamental of the model validation. The main parameters of the investigated wind turbine are shown in table 4-1.

Table 4-1: Parameters for 2MW wind turbine

Rated power	2 MW	Cpmax	0.46
Cut-in speed	3m/s	Air density	1.225kg/m3
Rated speed	12m/s	Rotor	80m
Cut-out speed	25m/s	Sweep Area	5027m2
Nominal voltage	575 V	Nominal DC voltage	1100V
Nominal Frequency	50Hz	Line filter capacitor (Q=50)	0.15MVar
Inertia Constant	4.32s	Grid-side converter nominal voltage	575V
Nominal DC bus voltage	1100	DC bus capacitor	90mF
Stator, rotor leakage inductance	0.124p.u.，0.116p.u.	Switching frequency	1950Hz
Stator, rotor resistance	0.024p.u.，0.0396p.u.	Excitation inductance	2.9p.u.

4.1.3 Model Simulation Results

A simple wind energy conversion system is built via Matlab/Simulink. In this paper, the base speed is considered as 15m/s. The output voltage is 575V at 50Hz. The simulation results show the steady state performance of the PMSG-based wind energy conversion system. The output power of the wind turbine can always approach its optimal value, while the reactive power is kept to be close enough to zero. But imperfect reacting time at the beginning and the harmonic issues could be observed from the scope plot.
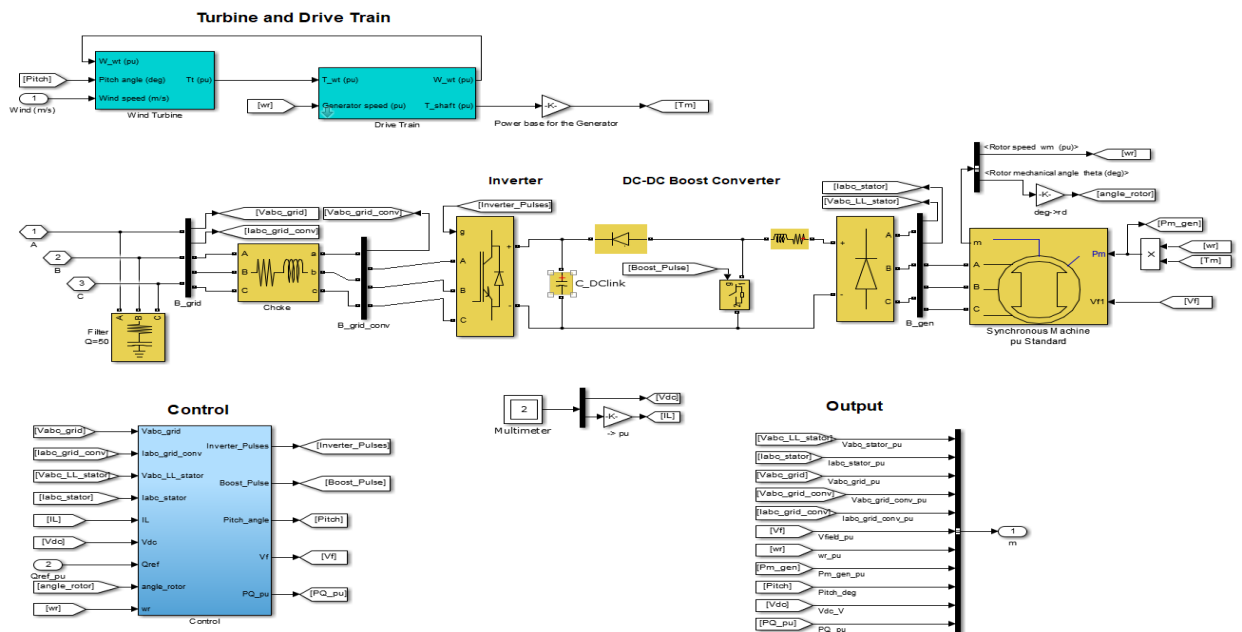
Fig. 4-2: Inner construction illustration of wind turbine

As shown in Figure above, after analyzing and compare the harmonic characteristics of the machine-side converter current Iabc_stator and the grid-side converter current Iabc_grid_conv, the result is shown below:
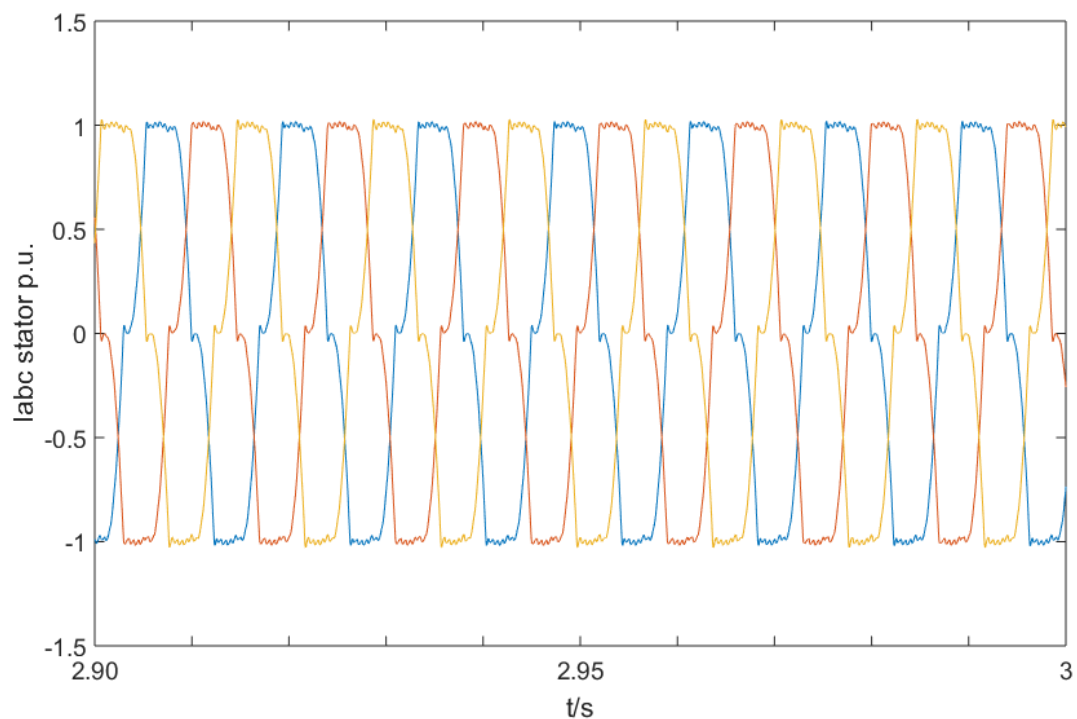
（a）wave form of machine-side converter current
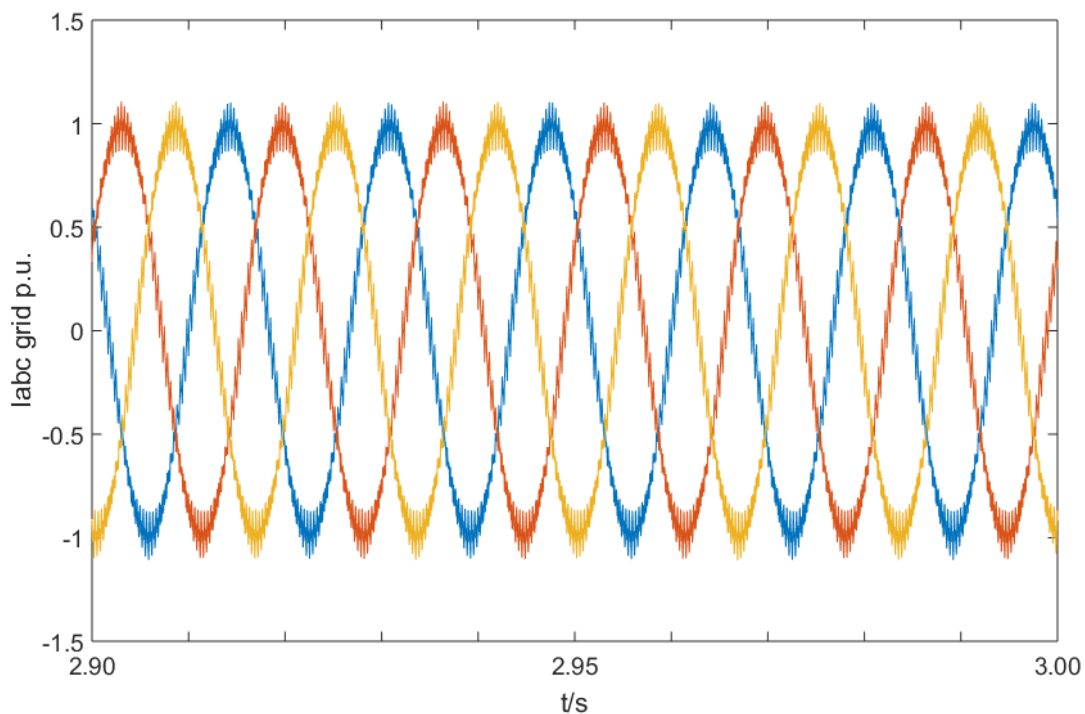
（b）wave form of grid-side converter current

Fig. 4-3: wave form of machine-side and grid-side converter current

After the FFT analysis, the harmonic characteristics of current are shown below:

Table 4-2: Harmonic characteristics of current from machine-side and grid-side converter

Harmonic	machine-side converter	grid-side converter
THD	117.32%	6.51%
3	2.08%	0.07%
5	3.84%	0.14%
7	1.16%	0.17%
9	0.75%	0.02%
11	0.66%	0.03%
13	0.31%	0.01%
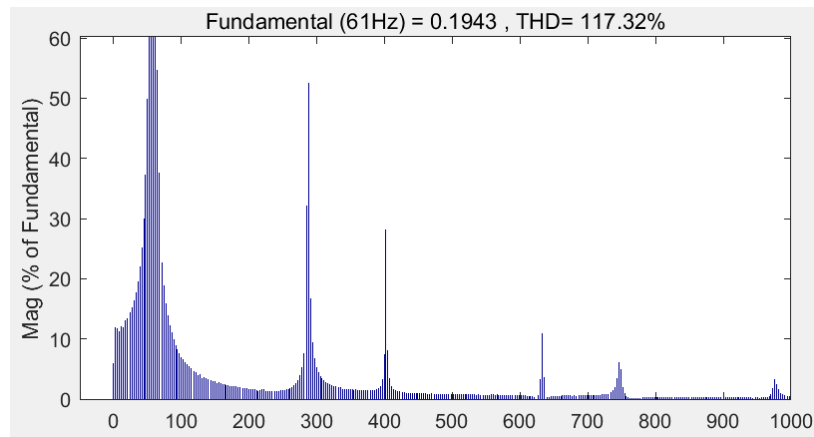
Fig. 4-4: harmonic characteristics of machine-side converter current (x-axis: harmonic frequency [Hz])
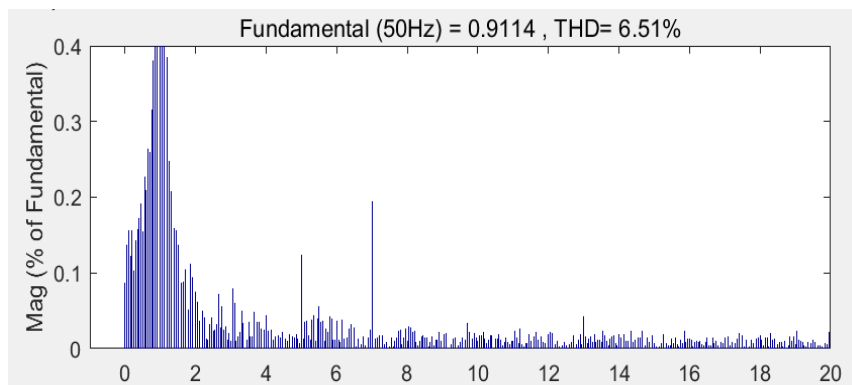
Fig. 4-5: harmonic characteristics of grid-side and grid-side converter current (x-axis: harmonic order)

It can be deducted from the figure above that machine-side converter current contain extremely high level of harmonics. It can be speculated that the machine-side output current that could only be relied on wind turbine mechanical control strategy is the main reason. The detail analysis of the reason will be left for further study in the

future. Grid-side converter current, which contains much less harmonic, is mainly influenced by the control of converter control, from which can be seen that full scale converter of PMSG could decrease influence of the fluctuation and mechanical control of wind turbine to the harmonic of gird side.

From the figure 4-5, the grid-side converter current still contains a relatively high level of 5th and 7th harmonic, after installing a 0.15MVar Line filter capacitor, the result from comparing the current before and after the filter is shown below:
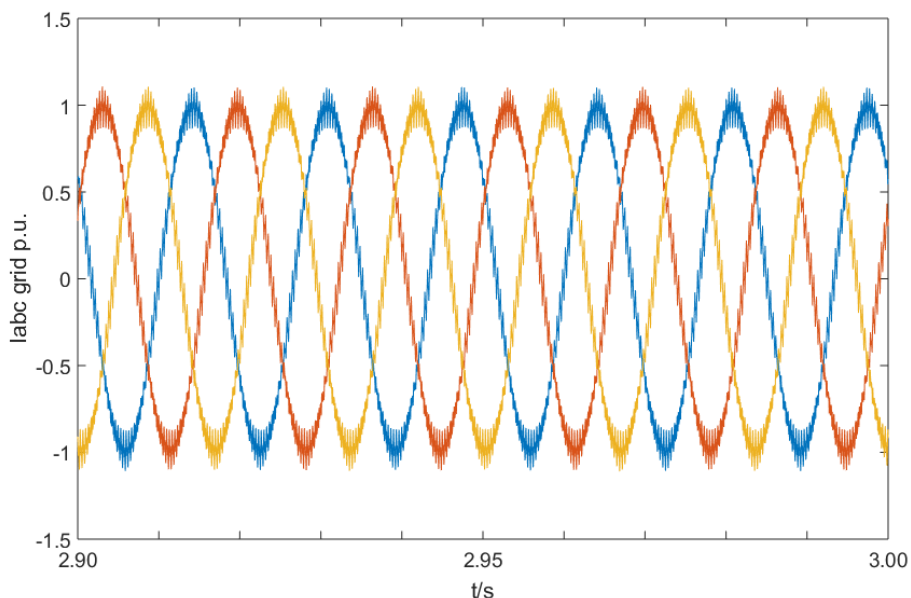
(a) Wave form of grid-side converter current before filter
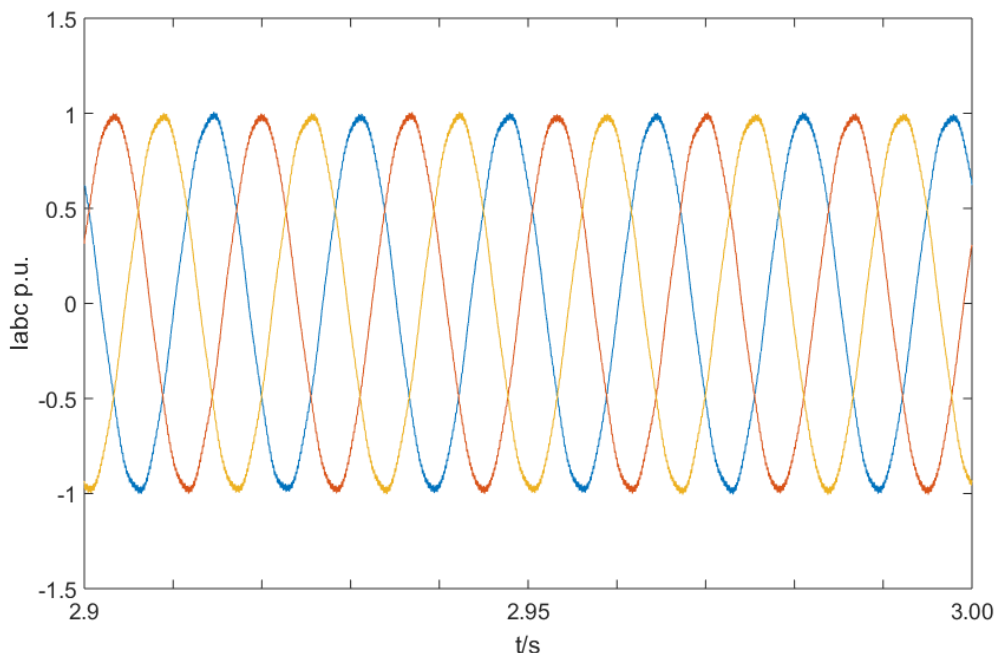
(b) Wave form of grid-side converter current after filter

Fig. 4-6: Wave form of grid-side converter current before and after filter

After the FFT analysis, harmonic characteristics of grid-side converter current is shown in table below:

Table 4-3: Harmonic characteristics of grid-side converter before and after the filter

Harmonic	Before	After
THD	6.51%	1.27%
3	0.07%	0.08%
5	0.14%	0.26%
7	0.17%	0.84%
9	0.02%	0.03%
11	0.03%	0.02%
13	0.01%	0.01%

(a) before the filter　　　　　　　　　(b) after the filter
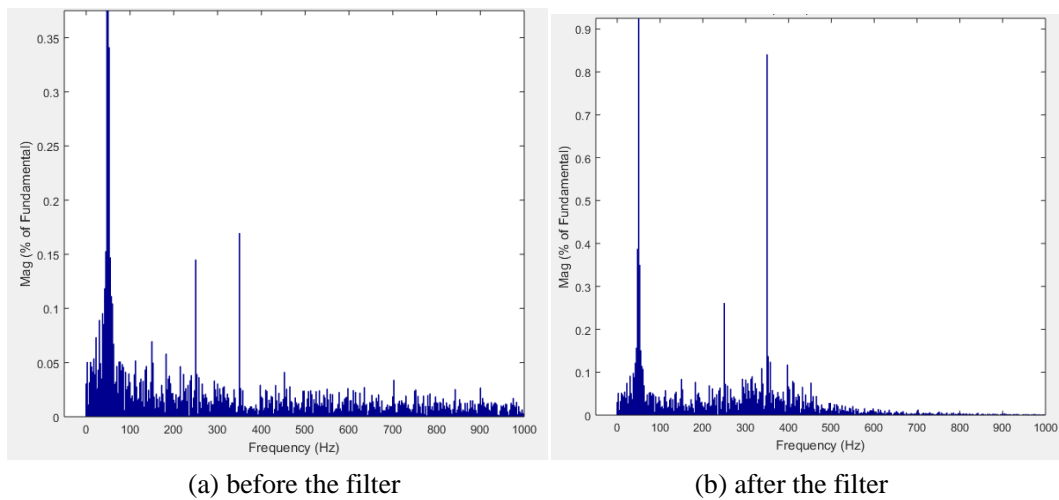
Fig. 4-7: Harmonic characteristics of current before and after filter

From the analysis in figure 4-7, the filter mainly filters the 5th, 7th and 9th harmonic, etc. Furthermore, the filter is more effective to higher harmonic, thus, filter in wind turbine out port has a significant effect in reducing the THD and increasing the power quality.

4.1.4 Summary

Direct Drive PMSG Wind Energy Generation System is introduced in this chapter. Based on the example from MATLAB/Simulink Synchronous Generator and Full Scale Converter (Type 4) Wind Turbine Detailed Model, after analyzing the harmonic characteristics of machine-side converter current, grid-side converter current and current after line filter capacitor, it could be deducted that machine-side converter current is mainly influenced by wind speed and mechanical control system. Grid-side current, which has a lower harmonic to the machine-side current, are mainly affected by PWM control system of converter. Thus, harmonic current injected from PMSG to grid is mainly determined by gird side converter and filter in wind turbine out port.

4.2 Offshore Wind Farm System

4.2.1 System Description

The offshore wind farm system investigated in this report get reference information from the 300MW scale offshore wind farm, which is located in Rudong county, China, built and operated by CHINA HUANENG company from 2015. The collection grid layout, parameters for electric devices are mainly referred to this Rudong OWF. Only scaling down the total capacity of the investigated wind farm to 160MV. The eight 2MW PMSGs are connected in one string type clustering. And total string number is ten. After boosted to 33kV, the chain-linked wind turbine are connected to offshore boost transform station through low and large capacity mid-voltage set cable. When boosted to 230kV, AC or DC transmission strategy are adopted to reach the gird-connection point.

（a）

（b）
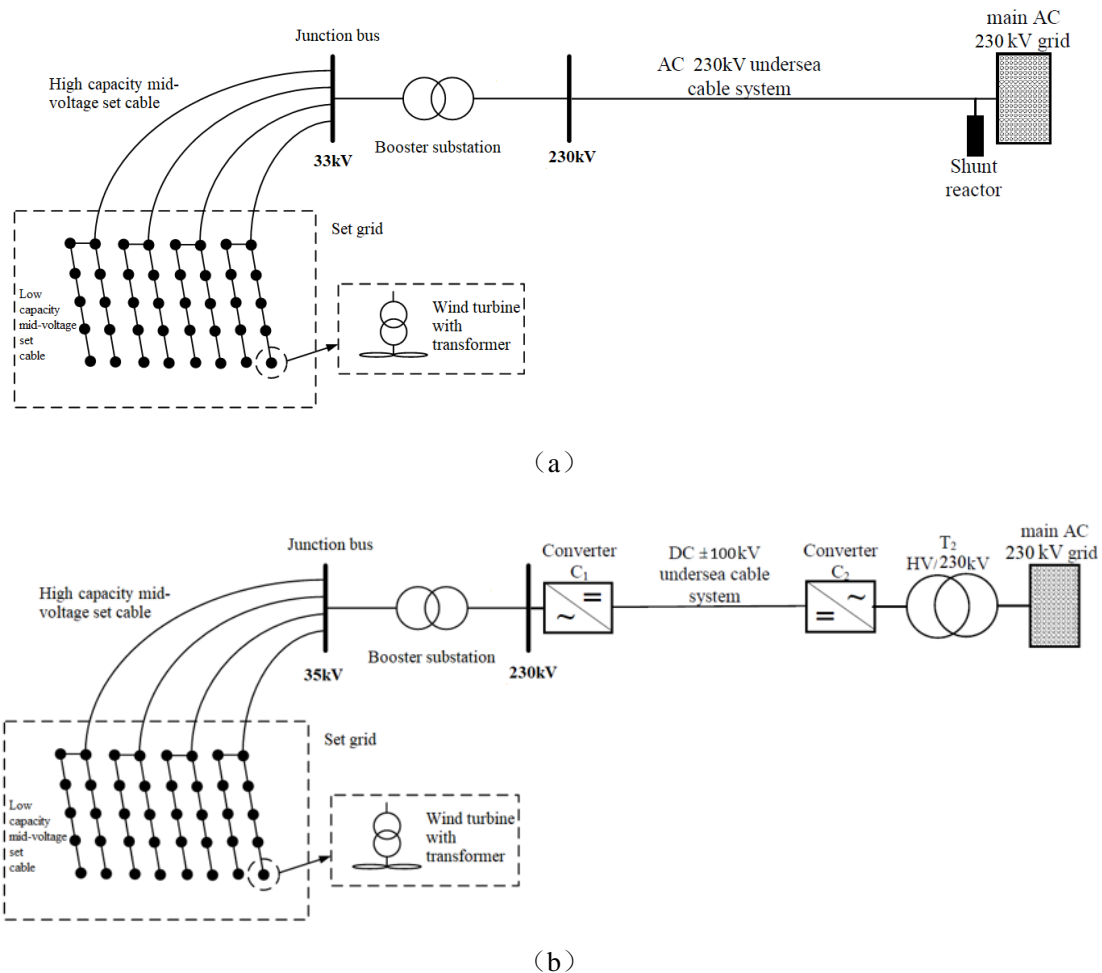
Fig. 4-8: The electrical system for the HVAC (a) and VSC-HVDC (b) transmission system of offshore wind farm

In most cases, the cable type will be a three-core, armored cable with copper or aluminum conductors and XLPE insulation. The cable will have integrated fiber optic

unit for communication purposes.

Each WTG is rated for 2MW. Ideally assuming a power factor of 1, each WTG will supply a current of 35A in the 33kV cable strings. The combined current of the remote end eight turbines will be 280A. Because of the low using time of wind farm, in most cases the current of low capacity mid-voltage set cable is lower than 280A. Hence, the 95 mm^2 cross section cable is picked for the connection for the remote end eight turbines. The maximum current of high capacity mid-voltage set cable is 560A. Hence, the 400 mm^2 cross section cable (rated current 590A) is selected for the feeder section. The parameter comes from the user's guide for XLPE submarine cable system from ABB Ltd, as shown in following table.

As the table D-1 in appendix gives the parameters for 30kV three-core cables with copper wire screen. The chosen 95 mm^2 cross section cable capacitance is 0.18μF/km and its inductance is 0.44 mH/km, resistance (maximum dc resistance at 20℃) is 0.193 Ω/km.The chosen 400 mm^2 cross section cable capacitance is 0.29μF/km and its inductance is 0.35 mH/km, resistance is 0.0991 Ω/km. And 300 mm^2 230kV submarine cable is selected as 230kV AC transmission system. Parameters of AC 230kV submarine cable is shown in table 4-7.

Parameters of Booster Substation is shown in table 4-6. The main parameters of Converter Station is shown in table 4-8.

Table 4-4: Parameters of Low Capacity mid-voltage set cable

Parameter	Area/mm^2	Resistance Ω/km	Inductance mH/km	Capacity μF/km	Charging current A/km
Value	95	0.193	0.44	0.18	1.0

Table 4-5: Parameters of Submarine cable (33kV high capacity mid-voltage set cable)

Parameter	Area/mm^2	Resistance Ω/km	Inductance mH/km	Capacity μF/km	Charging current A/km
Value	400	0.0991	0.35	0.29	1.6

Table 4-6: Parameters of Booster Substation

Parameter	Wire winding resistance/Ω	Eddy current loss resistance/Ω	Leakage/mH
Value	0.036	10.03	0.191

Table 4-7: Parameters of AC 230kV Undersea Cable System

Parameter	Area/mm^2	Resistance Ω/km	Inductance mH/km	Capacity μF/km	Charging current A/km
Value	300	0.00127	0.44	0.14	3.7

Table 4-8: Parameters of Converter Station

Parameter	Length/km	Rated power/MW	DC Capacity/uF	reactor resistance/Ω	reactor inductance/mH
Value	70	200	70	0.0251	8

4.2.2 Simulation Validation of the OWF case

Based on MATLAB/Simulink synchronous generator and full scale converter (Type 4) wind turbine detailed model, the detailed offshore wind farm model was first built according to the OWF configuration design discussed in previous section 4.1. However, the complexity of the control loop of converters causes the simulation running time too long.

In the average type of Type 4 wind turbine model, the IGBT Voltage-sourced converters (VSC) are represented by equivalent voltage sources generating the AC voltage averaged over one cycle of the switching frequency. The average model preserves the dynamics resulting from control system and power system interaction. This model allows using much larger time steps (typically 50 microseconds), thus allowing simulations of several seconds. Thus, by testing both the detailed model and the average model of the Type 4 wind turbine, the harmonic output characteristics from wind turbine unit has no significant difference. In the following wind farm model building, the wind turbine will be applied in the average model, for keeping the simulation test more efficiently.

The 160MW wind farm module in the grid-connected model includes eight rows of wind turbines. Each row of wind turbine is composed of eight wind turbines which are 2MW. After boosted to 33kV, the chain-linked wind turbine are connected to offshore boost transform station through low and large capacity mid-voltage set cable. When boosted to 230kV, AC or DC transmission strategy are adopted to reach the gird-connection point.

VSC-HVDC is selected as one type of transmission system for this offshore wind farm. The flexible DC transmission system studied in this paper is the VSC-HVDC system of ± 100kV, and the AC side is connected to the network of 230kV. The schematic diagram is shown in Fig. 4-9.
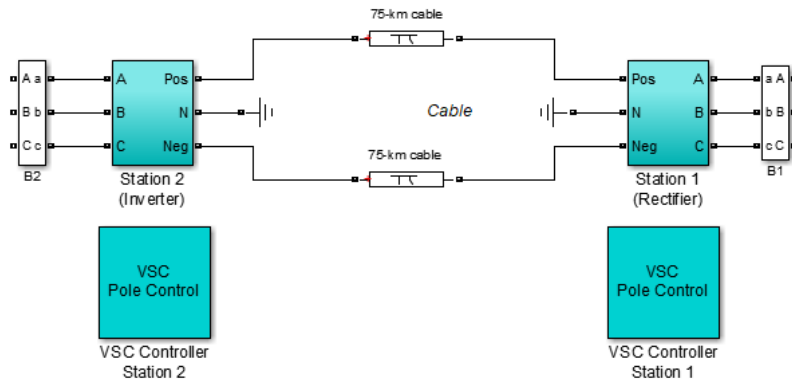
Fig. 4-9: The schematic diagram of the simulation system of VSC-HVDC

The rectifier side adopts the constant active power and constant reactive power control modes, and the inverter side adopts constant AC voltage and constant DC voltage control modes. The structure diagram of the converter station in the system is shown in Fig. 4-10:
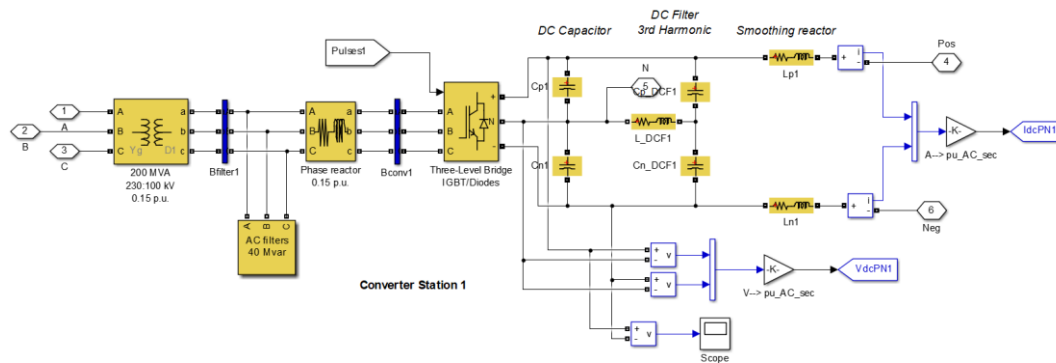
Fig. 4-10: The schematic diagram of the simulation model of converter station in flexible DC system

The transformation ratio of transformer of the converter station is 33kV/230kV, the rated capacity is 200MW, the impedance of the primary side and the secondary side are 0.0025+j23.55p.u. The filter at the exit is used to filter 27 to 54 harmonics with rated power of 18MVar and 22MVar respectively. The impedance of the smoothing reactor on the DC line is 0.0251+j2.512, and the parallel capacitance on the DC side is 70uF.

4.2.3 Simulation Results and Analysis of Harmonic Output Characteristics

As can be seen in previous section, the simulation system includes a large amount of high-frequency power electronic switching elements, thus, much high harmonics will be imported into the system. As a comparative study, the FFT bar plot of offshore wind power grid system at PCC point are shown in the Fig. 4-11, x-axis is the harmonic order.
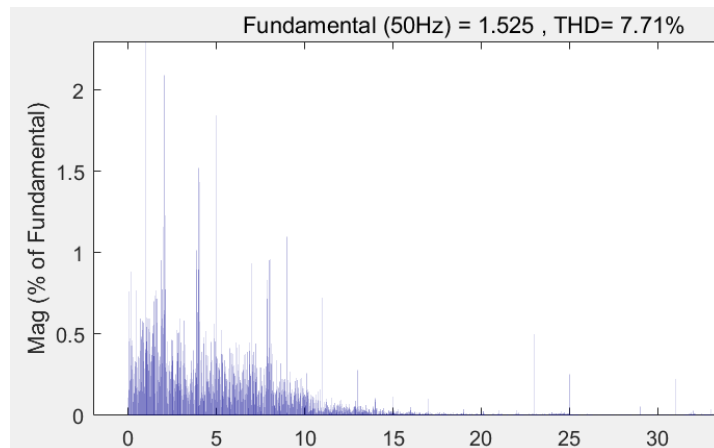
Fig. 4-11: FFT bar plot of offshore wind power grid system at PCC point

The simulation model for the investigated offshore wind farm is validated. Thus the harmonic distribution when no filter is installed at collection node could be illustrated in the spectral diagram Figure 4-11. According to IEEE Std 519-2014, the maximum allowable harmonic distortion level for bus with voltage over 161kV is stated. For the odd harmonic order (h<11), THD should be less than 3.0%. While 11<h<23, THD level should below 1.5%. And for 23<h<35, THD value needs to be smaller than 1.15%. The following figure plot the simulated THD values for the OWF compared with the maximum allowable standard level.
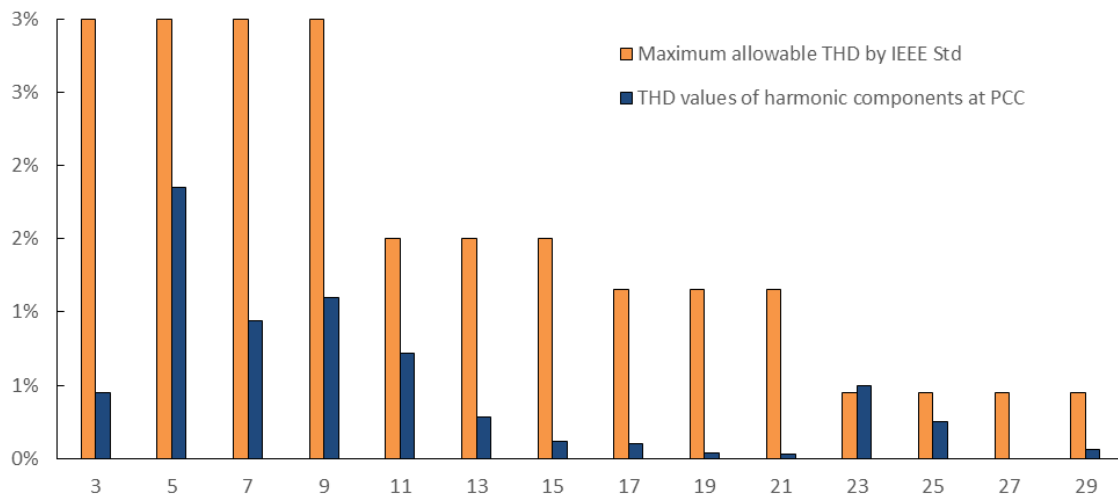
Fig. 4-12: THD bar plot of current harmonics at the connection point to the onshore

As can be seen roughly in spectrum, the harmonic order mainly consists of 3, 5, 7, 9, 23, and relatively severe distortion level around the low frequency range, which could heavily influence the voltage quality at the on-shore grind connection point. This leads us to explore some harmonic suppression strategies, to design effective filters that could erase most of high harmonics.

4.3 Summary

Direct Drive PMSG Wind Energy Generation System is introduced in this chapter. Based on the example from MATLAB/Simulink Synchronous Generator and Full Scale Converter (Type 4) Wind Turbine Detailed Model, after analyzing the harmonic characteristics of machine-side converter current, grid-side converter current and current after line filter capacitor, it could be deducted that machine-side converter current has very high level harmonic distortions, due to the only mechanical control system of the wind turbine rotor. The grid-side current, which has a lower harmonic level, is mainly affected by advanced PWM control system of the voltage sourced converter. Thus, harmonic current injected from PMSG to grid is mainly determined by gird side converter and filter in wind turbine out port.

The simulation model for the investigated 160MW offshore wind farm is validated.

The harmonic order mainly consists of 3, 5, 7, 9, 23, and relatively severe distortion level around the low frequency range, which could heavily influence the voltage quality at the on-shore grind connection point. This leads us to explore some harmonic suppression strategies, to design effective filters that could erase most of high harmonics.

Chapter 5 Harmonic Resonance Analysis in OWF

5.1 Introduction

For small scale systems, the influence of harmonic impedance on the system can be neglected. But for large-scale systems such as offshore wind farms, the existence of harmonic impedance cannot be neglected. The AC system harmonic impedance and the distribution of background harmonic voltage characteristic are important in the domain of power system analysis and design. This section will focus on analyzing the characteristic of harmonic impedance in network components of electric transmission capacitor, discussed the resonance and harmonic current amplification, which may be caused by cables.

Resonance frequency is an important part of harmonic analysis of offshore wind farm. Frequency domain analysis is often used in harmonic resonance analysis. The harmonic resonance problem in OWF requires consideration of the topology of the offshore wind farm collection system. Furthermore, the complexity of the collection grid increases the difficulty of harmonic resonance analysis.

The occurrence of resonance will seriously endanger the safety and stability of the system operation. In this section, the system resonance problem will be analyzed by building the harmonic model of offshore wind farm installation, simulating the system, and then the frequency scan method is applied to detect the influence components which potentially affect the harmonic resonance.

5.2 Theory of Harmonic Models

In order to analyze the harmonic generation mechanism of the wind power field accurately, harmonic models of each component in the OWF installation which are suitable for harmonic analysis should be established. Harmonic models are often linearized in frequency domain analysis.

5.2.1 Harmonic Model of PMSG with full scale converter

This kind of wind power system uses the multi-poles permanent magnet alternator, therefore the wind turbine and the generator does not need to install the speed gearbox, becomes the direct driven turbine generators, as shown in Fig. 5-1. The inverter connects the stator windings of the generator with the power grid, and converts the frequency-changing energy into constant-frequency power with the same frequency as the power grid. Because of the decoupling control of the inverter, the variable-speed wind turbine based on synchronous generator is completely decoupled from the power system, and its characteristics depend entirely on the control strategy of the inverter. At the same time, because the inverter is at the stator side, all the power emitted by

the generator needs to be transformed by the inverter, and the capacity requirement of the inverter is increased significantly for the large capacity wind power system. The advantage of this kind of wind turbine is to omit the lift speed gearbox, to avoid the maintenance and replacement of gear box parts, to improve the stability of the system structure and to enhance the reliability.
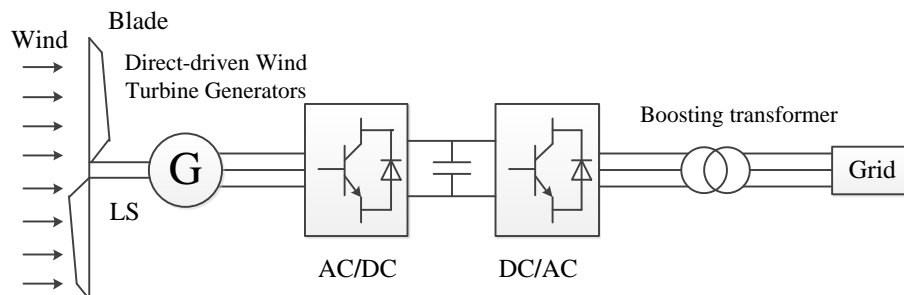
Fig. 5-1: Direct-driven variable speed wind turbine based on permanent magnet synchronous generator

Characteristics of direct-driven permanent magnet synchronous wind power system:(1) The permanent magnet generator has the highest operating efficiency; (2) The excitation of permanent magnet generator is not adjustable, which leads to the change of induction electromotive force with speed and load [52]. With controllable PWM rectifier connecting with DC/AC transform, the DC bus voltage is basically constant and the electromagnetic torque of the generator can be controlled to adjust the speed of the wind wheel; (3) High cost of permanent magnet generator and full-capacity full-control converter; (5) The permanent magnet generator has the locating torque, which is difficult to start the unit.

The power path of direct drive PMSG consists of two parts, the rectifier and the inverter. The operation flow is that: generators emit low-frequency alternating current and becomes DC after rectifier, The DC power passes through the large capacitance filter as the input end of the inverter. The control signal obtained by the power network is transformed to obtain the AC power which can be connected to the grid operation.

The influence of harmonics generated by wind turbines on the power grid is mainly reflected in the grid-side converter of the PMSG. In this section, the grid-side converter is further analyzed on the basis of many research, and the corresponding harmonic model is established according to the harmonic characteristics [53]. This chapter will not go into those details.

- **High Frequency Harmonic Model**

For the grid-side converter, the control strategy can use sinusoidal pulse width modulation (SPWM), space vector pulse width modulation (SVPWM) and so on. The output voltage harmonics is relative to the control strategy that converter applied. There are quite a lot existing literature discussing the harmonic voltage expression under different control methods. Here limited to the direction and length of this thesis,

the discussion will not be listed in details. The harmonic output voltage expression under SVPWM control strategy is given directly:

$$\begin{cases} U_{an} = U_{a0} - U_{n0} \\ U_{n0} = \left(U_{a0} + U_{b0} + U_{c0} \right)/3 \end{cases}$$

(5-3)

In which, U_{n0} is the neutral point voltage of the load to the DC capacitor. U_{a0}, U_{b0}, U_{c0} is the three-phase voltage of abc phases.

In normal working condition, the amplitude of the grid-side converter output harmonic is constant. Therefore, grid-side converter in high frequency section could be equivalent to an independent harmonic voltage source. The high frequency harmonic model including L type filter is shown in Fig. 5.2. In which, U_h is the equivalent harmonic voltage source in high frequency section.
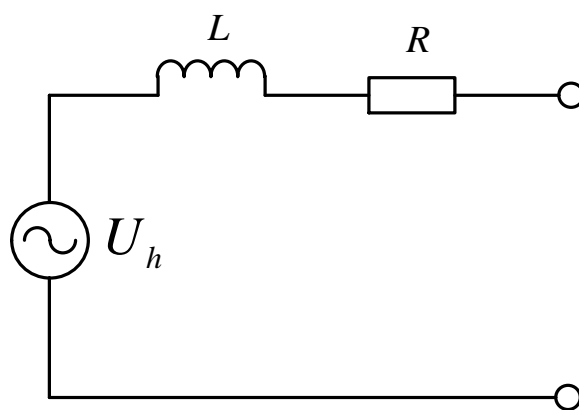
Fig. 5-2: High frequency harmonic model of grid-side converter including L filter

If the grid-side converter contains a LCL filter, the high frequency harmonic model can be equivalent to Fig. 5.3:
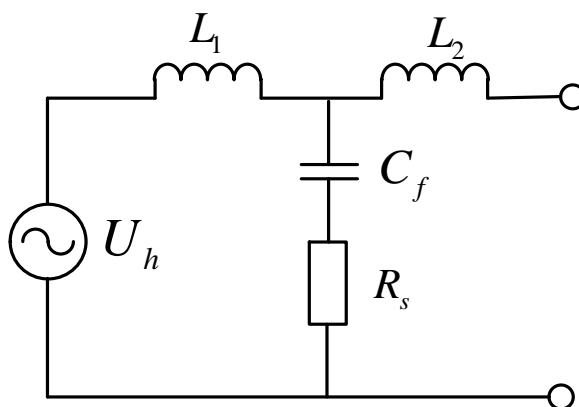
Fig. 5-3: High frequency harmonic model of grid-side converter including LCL filter

Among them, U_h is the equivalent harmonic voltage source for high frequency range, C_f is the filter capacitor, R_s is the damping resistor, L_1 and L_2 are filter inductors.

- **Low frequency harmonic model**

The harmonic characteristics in low frequency range of the grid-side converter is affected by the controller. The output of the phase voltage is also affected by the grid voltage. The harmonic output voltage of the grid-side converter exhibits controlled characteristics. Thus, low frequency harmonic output could be represented by independent controlled voltage source. The derivation of harmonic voltage and wave impedance is quite complex, and the formulas are shown as follows:

$$U_{op}(h) = \frac{U_{bridge}}{1 - C_v(h)} \tag{5-4}$$

$$Z_{eq}(h) = \frac{C_1(h) + Z_L(h)}{1 - C_v(h)} \tag{5-5}$$

Of which U_{bridge} is the extra harmonic from the nonideal state of the component and $C_1(h), C_v(h)$ is the transfer function of the feed-forward current loop or voltage loop.

As can be seen above, the low frequency harmonic model of grid-side converter can be equivalent to Fig. 5.4:
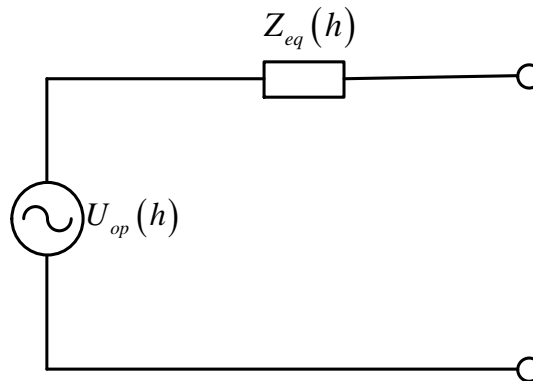
Fig. 5-4: Low frequency harmonic model of grid-side converter

5.2.2 Harmonic Model of Transformer

Offshore wind farms are collected by many wind turbines through the collection grid. And the power is fed to the onshore grid, which contains more transformers during the transmission of power. The transformers can be roughly divided into two kinds. One is the step-up transformer installed on the output of the single wind generator. The other one is step-up transformer on the substation in the sea before high voltage power transmission system. In order to analyze the harmonic of offshore wind farm, an appropriate harmonic model should be set up for the transformers in wind farm.

At present, there already exist many kinds of harmonic models for transformers. Under the condition of power frequency, the influence of excitation branch will not be considered. But when the frequency changes, the influence of excitation branch and

the skin effect of windings cannot be ignored. It is generally believed that the Model 6 is relatively closer to the actual reality in the common harmonic analysis frequency band. Thus, it is commonly accepted that the Model 6 is more accurate harmonic model of transformer. Model 6 (CIGRE model) equations are listed as following:

$$R_s = \frac{X_T}{\tan \phi}, \quad R_p = 10 X_T \tan \phi \quad (5\text{-}11)$$

$$\tan \phi = e^{0.693 + 0.769 \ln S - 0.042 (\ln S)^2} \quad (5\text{-}12)$$

$$Z_T(h) = R_s + \frac{j R_p X_T}{R_p + j X_T} = \frac{X_T}{\tan \phi} + \frac{1}{1 + (h/10 \tan \phi)^2} \left(\frac{h^2 X_T}{10 \tan \phi} + j h X_T \right) \quad (5\text{-}13)$$

Where R_s, R_T is the resistance and eddy current loss of wire winding respectively. Both of them do not change with frequency; S is rated power of the transformer.

The model assumes that the eddy current loss is proportional to the square of frequency, and to consider the demagnetization effect in the case of lower frequency, which can well reflect the working condition of the transformer, and will get higher accuracy in the harmonic analysis. The equivalent harmonic model structure can be seen in Fig. 5.5:
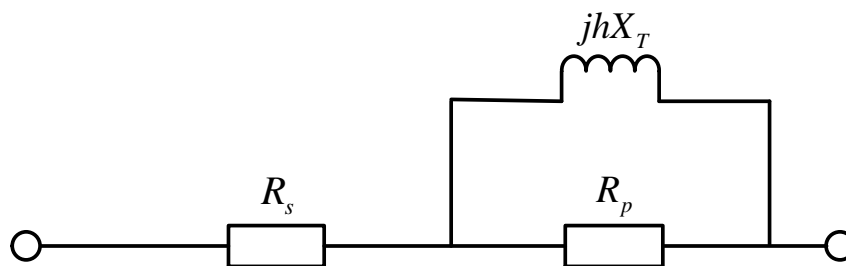
Fig. 5-5: Equivalent circuit for harmonic model of transformer

5.2.3 Harmonic Model of Subsea Cables

Offshore wind farms are integrated by a lot of wind turbines through collection grid and are usually far away from the coast. As a result, a large number of cables with different voltage levels are used in the process of power transmission.

Power cable is different from conventional transmission line, and its distribution capacitance parameter is larger, which will have a great influence on the harmonic resonance of offshore wind farm, such as amplification on harmonic currents. Thus, it is necessary to establish harmonic model of offshore power cables, which will make results of harmonic analysis of OWF more accurate.

Usually, the unit length of submarine cable can be equivalent to a lumped parameter π-equivalent model. But when the length of submarine cable reaches a critical point, considering the long-term effects of submarine cables, a lumped parameter π-equivalent model cannot reflect the influence of skin effect, and thus requires the use of multiple π-equivalent circuit cascades or distributed parameter model.

The π-equivalent circuit is shown as follows:
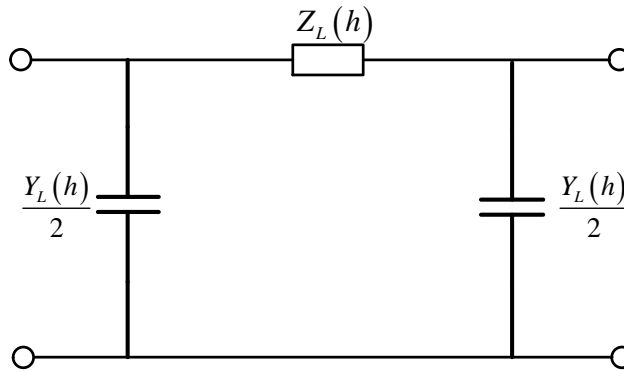
Fig. 5-6: Equivalent circuit for harmonic model of submarine cable

The parameters of the equivalent circuit can be calculated by the following formulas:

$$Z_L(h) = R_L + jhX_L \tag{5-14}$$

$$Y_L(h) = jhB \tag{5-15}$$

When the voltage level is 220kV and above, the equivalent circuit resistance can be calculated by the following formula:

$$R_L(h) = 0.74R_L\left(0.267 + 1.073\sqrt{h}\right) \tag{5-16}$$

When the voltage level is below 220kV, the equivalent circuit resistance can be calculated as below:

$$R_L(h) = R_L\left(0.187 + 0.532\sqrt{h}\right) \tag{5-17}$$

5.2.4 Harmonic Model of VSC- HVDC system

A complete VSC-HVDC system consists of a converter transformer, a converter station and a DC line. The station at the sending end works in the rectifier mode, while the station at the receiving end works in the inverter mode [52]. Taking the two-terminal flexible DC transmission system as an example, the system diagram is shown in Fig. 5.7.
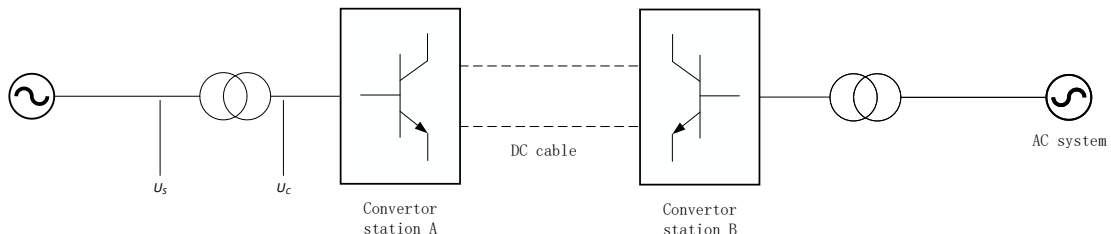
Fig. 5-7: The diagram of the two-terminal flexible DC transmission system

The flexible DC transmission system can adjust the amplitude of the converter output voltage and the power angle of between the converter output voltage and

system voltage by turning on and off power electronic devices so as to independently control the active power and reactive power output.

Considering the assumption of the high symmetry and independent of the two sides of the VSC-HVDC system, the complete system can be represented as two independent systems. Considering the characteristics that the secondary side uses the connection mode ′Δ′ and zero sequence current can not flow in the system, one side of the single line structure of VSC-HVDC can be further simplified as the following circuit.
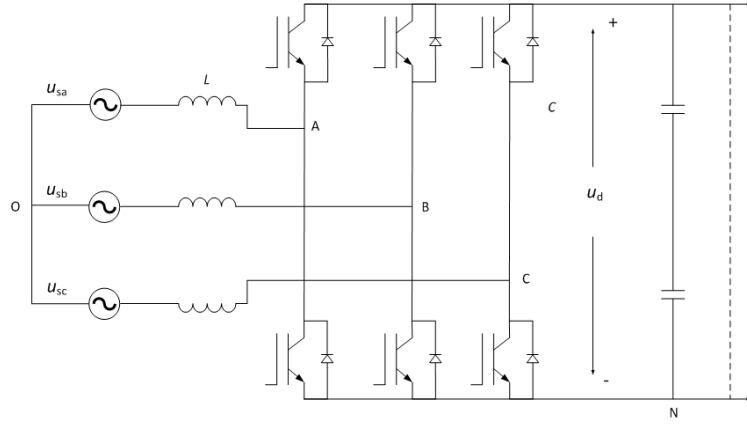
Fig. 5-8: The structure of three-phase VSC

According to the simplified principle and content, if there is no special explanation in the paper, the one-side system of VSC-HVDC is generally used for analysis.

- **The high frequency mathematic model based on switching transfer functions**

By using the Kirchhoff voltage law, the voltage of the A phase in Fig. 5.8 can be written to satisfy the equation:

$$L\left(\frac{di_{sa}}{dt}\right) + R \cdot i_{sa} = u_{sa} - (u_{AN} + u_{NO}) \tag{5-18}$$

It can be assumed that the switching function of the upper arm of the A phase is S_a, and the switch function of the lower bridge arm is S_a'. The switching function S only takes 0 and 1, 0 represents disconnection, and 1 represents conduction. When $S_a=1$、$S_a'=0$, that is, the upper arm of the A phase is connected, and the lower bridge arm is disconnected, which means $u_{AN}=u_d$. When $S_a=0$、$S_a'=1$, that is, the upper arm of the A phase is disconnected, and the lower bridge arm is connected, which means $u_{AN}=0$. Considering that the upper and lower bridge arms can not be switched on or off simultaneously, the switching function must satisfy $S_a + S_a'=1$. By substituting it into the formula (2.6), it can be get that

$$L\left(\frac{di_{sa}}{dt}\right) + R \cdot i_{sa} = u_{sa} - (S_a \cdot u_d + u_{NO}) \tag{5-19}$$

Similarly, the voltage equations for the B and C phases are as follows:

$$L\left(\frac{di_{sb}}{dt}\right) + R \cdot i_{sb} = u_{sb} - (S_b \cdot u_d + u_{NO}) \tag{5-20}$$

$$L\left(\frac{di_{sc}}{dt}\right) + R \cdot i_{sc} = u_{sc} - (S_c \cdot u_d + u_{NO}) \tag{5-21}$$

Considering the characteristics of the three-phase three-wire system, $i_{sa} + i_{sb} + i_{sc} = 0$. When the voltage of each phase of three-phase AC system is balanced, $u_{sa} + u_{sb} + u_{sc} = 0$. By substituting it into the formula (5.19~5.21), it can be get that [52]

$$L\left(\frac{di_{sa}}{dt}\right) + R \cdot i_{sa} = u_{sa} - u_d \cdot (2S_a - S_b - S_c)/3 \tag{5-22}$$

$$L\left(\frac{di_{sb}}{dt}\right) + R \cdot i_{sb} = u_{sb} - u_d \cdot (2S_b - S_a - S_c)/3 \tag{5-23}$$

$$L\left(\frac{di_{sc}}{dt}\right) + R \cdot i_{sc} = u_{sc} - u_d \cdot (2S_c - S_b - S_a)/3 \tag{5-24}$$

The differential equations of the DC side can be written as follows:

$$C\frac{du_d}{dt} = (S_a \cdot i_{sa} + S_b \cdot i_{sb} + S_c \cdot i_{sc}) - i_d = i_{dc} - i_d \tag{5-25}$$

The high frequency mathematical model of VSC is composed of the above four equations. From the expression of the mathematical model, it can be seen that the DC side current in the rectifier or inverter side is determined by the three phases of the switching function, so the switching function belongs to a nonlinear and time-varying mutual coupling system. According to the mathematical model of VSC, the circuit of the VSC in the three-phase stationary coordinate can be equivalent. The DC side and the AC side are equivalent to two independent networks, and the AC side is equivalent to a three-phase controlled voltage source [53], [54]. The DC side is equivalent to a controlled current source, and the AC and DC side are coupled with each other by means of VCCS and CCCS. The characteristic also makes the VSC-HVDC system convenient to form parallel and multi terminal system expediently.

- **The low frequency dynamic model of VSC-HVDC**

As mentioned earlier, the high frequency mathematical model of VSC-HVDC is relatively accurate to describe the switching process of the converter station, but it is difficult to be used for the controller design. The optimization of controller link in VSC-HVDC system plays an important role in improving system reliability and flexibility. In order to establish a mathematical model of a flexible HVDC system with controller design, the switching action need to be simplified, and the main simplification is to ignore the harmonic components produced during the commutation process. According to the formula (5-22~5-24), the low frequency dynamic model of VSC in three phase stationary coordinate system can be obtained:

$$\begin{cases} L \cdot di_{sa}/dt + R \cdot i_{sa} = u_{sa} - v_a \\ L \cdot di_{sb}/dt + R \cdot i_{sb} = u_{sb} - v_b \\ L \cdot di_{sc}/dt + R \cdot i_{sc} = u_{sc} - v_c \\ C \cdot du_d/dt = i_{dc} - i_d \end{cases} \tag{5-26}$$

In the three-phase stationary coordinate system, the mathematical model of VSC-HVDC can clearly and simply represent the principle and operation process of the system. Then harmonic model of VSC-HVDC converter is similar to grid-side converter of PMSG [55].

5.3 Developing the Equivalent Harmonic Model of the OWF

The theory fundamentals are described in the last section. Therefore, the simplified equivalent harmonic model of the investigated OWF could be validated step by step.

- **PMSG with full scale converter**

The influence of harmonics generated by wind turbines on the power grid is mainly reflected in the grid-side converter of the PMSG. As previous description, the grid-side converter could be equivalent to an independent harmonic voltage source.
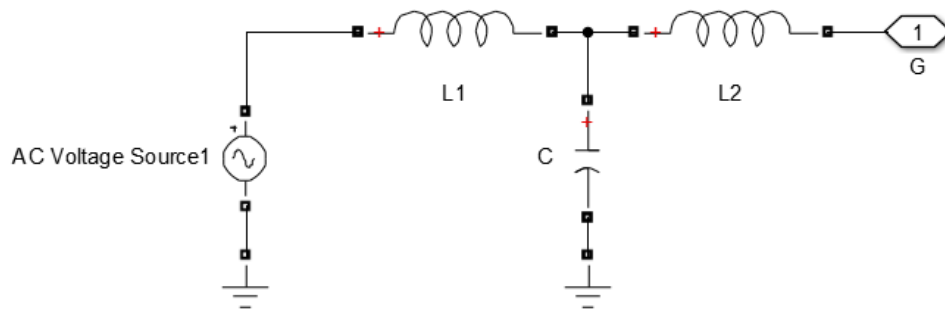
Fig. 5-9: Equivalent circuit for harmonic model of PMSG grid-side converter

- **Transformer**
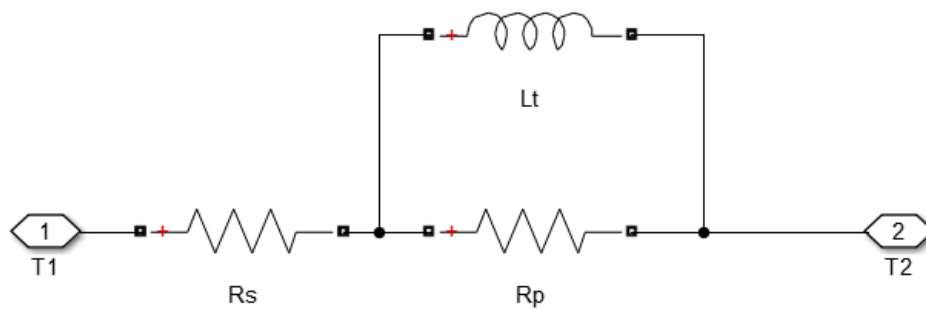
Fig. 5-10: Equivalent circuit for harmonic model of transformer

- **Subsea Cables**
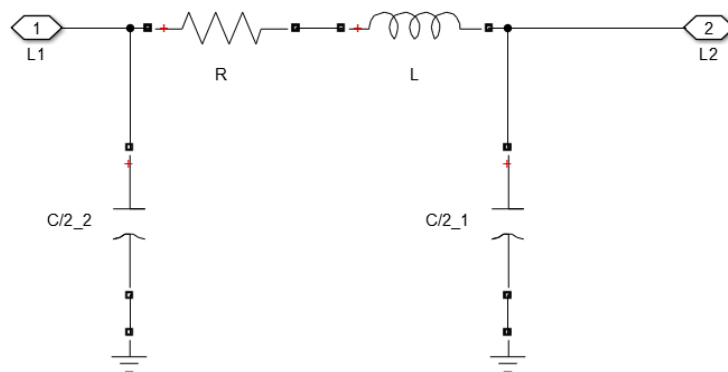
Fig. 5-11: Equivalent circuit for harmonic model of submarine cable

- **VSC- HVDC transmission system**

In the three-phase stationary coordinate system, the mathematical model of VSC-HVDC can clearly and simply represent the principle and operation process of the system. Then harmonic model of of VSC-HVDC converter is similar to grid-side converter of PMSG

Fig. 5-12: Equivalent circuit for harmonic model of VSC-HVDC grid-side converter

- **HVAC transmission system**

HVAC transmission system can be treated as a AC cable, thus the equivalent circuit similar to the subsea cables. The onshore grid can be seen as an ideal voltage source.
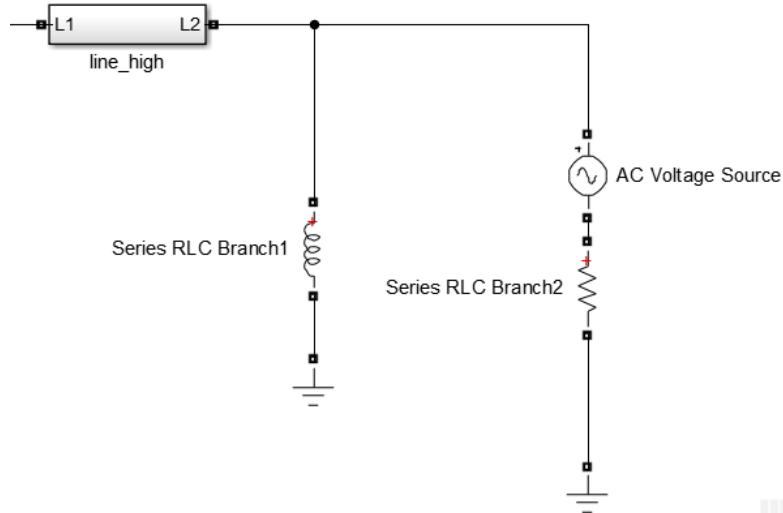
Fig. 5-13: Equivalent circuit for harmonic model of HVAC transmission system and the onshore grid

Establish the equivalent circuit for harmonic model of OWF in MATLAB/Simulink based on the parameters above, and each low capacity mid-voltage cable is 1km, large capacity mid-voltage cable is 3km and high voltage cable is 50km, capacity of shunt reactor installed in PCC point of AC transmission system is 200Mvar. The parameters list is shown in table 5.8, which are converted to 230kV. The equivalent circuit models of OWF with HVAC and HVDC transmission system are shown in appendix fig. A.2

and A.3.

Table 5-1: Offshore wind turbine harmonic model parameters

element		symbol	value
LCL filter	Grid-side inductance	L_{f1}	428.59mH
	Converter-side inductance	L_{f2}	850.79mH
	Capacity	C_{f1}	0.028uF
Wind-turbine transformer (0.575/33kV)	Wire winding resistance	R_{s1}	3.137Ω
	Eddy current loss resistance	R_{p1}	11393Ω
	Leakage	L_{t1}	189.6mH
Small capacity medium pressure set cable	Resistance	R_{cable1}	0.294Ω/km
	Inductance	L_{cable1}	0.647mH/km
	Capacity	C_{cable1}	0.247uF/km
Large capacity medium pressure set cable	Resistance	R_{cable2}	0.11Ω/km
	Inductance	L_{cable2}	0.752mH/km
	Capacity	C_{cable2}	0.728uF/km
Off-shore booster main transformer (33/230kV)	Wire winding resistance	R_{s2}	1.76Ω
	Eddy current loss resistance	R_{p2}	487.02Ω
	Leakage	L_{t2}	29.37mH
230kV High voltage cable	Resistance	R_{cable3}	0.00194Ω/km
	Inductance	L_{cable3}	0.44mH/km
	Capacity	C_{cable3}	0.14uF/km

5.4 Results and Harmonic Resonance Analysis

Frequency scan method was used to find the resonant frequency and frequency

impedance for those equivalent circuit models. Variable-controlling approach is expounded and applied in the following analysis. There are two factors that may influence the resonance phenomenon.

1) The transmission system selected: HVAC or VSC-HVDC.
2) The submarine cable parameters, including the length, inductance and capacitance.

5.4.1 The Influence of Transmission System on Harmonic Resonance in OWF

For HVAC transmission system there are three main resonant frequency at collection grid bus of wind farm: 33Hz, 148Hz and 313Hz as shown in fig 5-14, where the resonant resistance are 8.2Ω, 43Ω and 380Ω. When system is operated under such frequency, the resonance will bring influence to the power quality grid-connection.
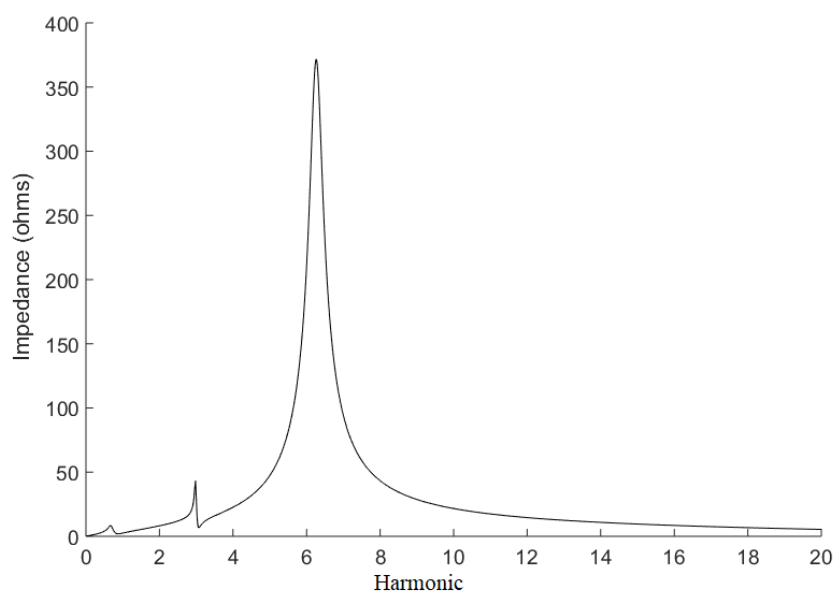
Fig. 5-14: Harmonic Impedance of Offshore Wind Farms with HVAC transmission system

From figure 5-15, in HVDC transmission system, resonance frequency is 310Hz, similar to HVAC system. The resonant resistance is 407 Ω , larger than HVAC transmission system.

The main resonance frequencies are similar at collection grid bus of wind farm in HVAC transmission system and HVDC transmission system, which are between 6 and 7 frequency order.
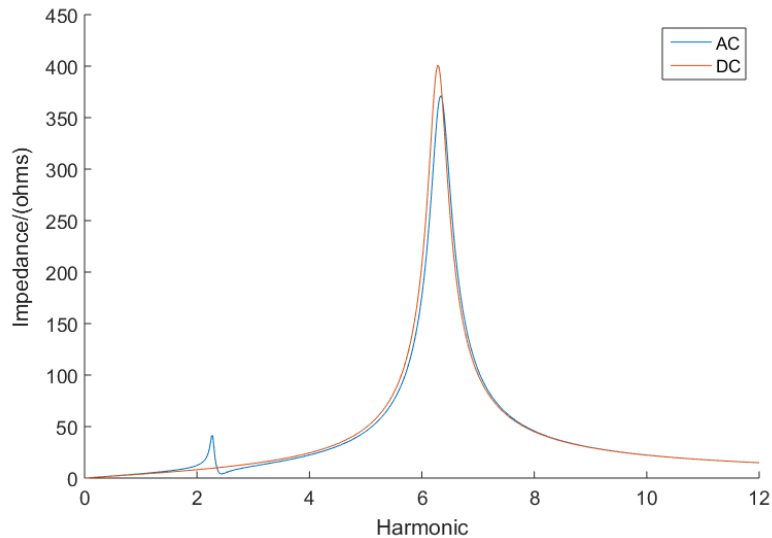
Fig. 5-15: Comparison between HVAC and HVDC Harmonic Model of Offshore Wind Farms

5.4.2 The Influence of Cable on Harmonic Resonance in OWF

Submarine cables contain a lot of distributed capacitance and inductance. Those nonlinear elements will aggravate the harmonic current distortion and distortion rate. More than that, those capacitive elements from cable are very likely interacted with those inductive elements, such as wind turbine windings etc., which then resulting in a resonance circuit, triggering resonance, and endangering the security of the collection grid system. Resonance phenomenon could not only make the electric equipment in the system run abnormally, but also endanger the safety and stable operation of offshore wind farm.

The selection index of a cable can be its cable length, inductance and capacitance value. In this section, three factors from cables that may affect harmonic resonance of wind farm collection grid are simulated and analyzed by Simulink through the impedance scanning method.

Variable-controlling approach is expounded and applied in the following analysis. It means that when looking at the effect of one variable, all other variable predictors are held constant in order to assess or clarify the relationship between the investigated variable and the target result. And how to apply this approach in solving the influence of cable parameters (cable length, inductance and capacitance) will be indicated in below sections in details.

1) The influence of cable length

The length of the cable laid in the offshore wind farm depends on the location of the wind turbines and the distance between the wind turbine export and the grid connection point. The cable lengths required by different wind turbine units are also different. Due to the influence of laying length, the number of capacitor and

inductance leaded in from the marine cable is different, and the electrical parameters will also change accordingly. Therefore, the harmonics generated in offshore the wind farm will vary greatly. It is of great significance to study the different effects of the same type of cable with different lengths on the resonance point in wind farm.

Select the same model cable (such as 33kV cable shown in table 5.4) of different length of 3m, 5km, 7km and 9km, respectively. Record the harmonic frequency at the grid connection point.

From Fig. 5-16, the longer distance of cable laid, the lower resonance frequency happened, and the impedance of the cable at resonance point will slowly increase.
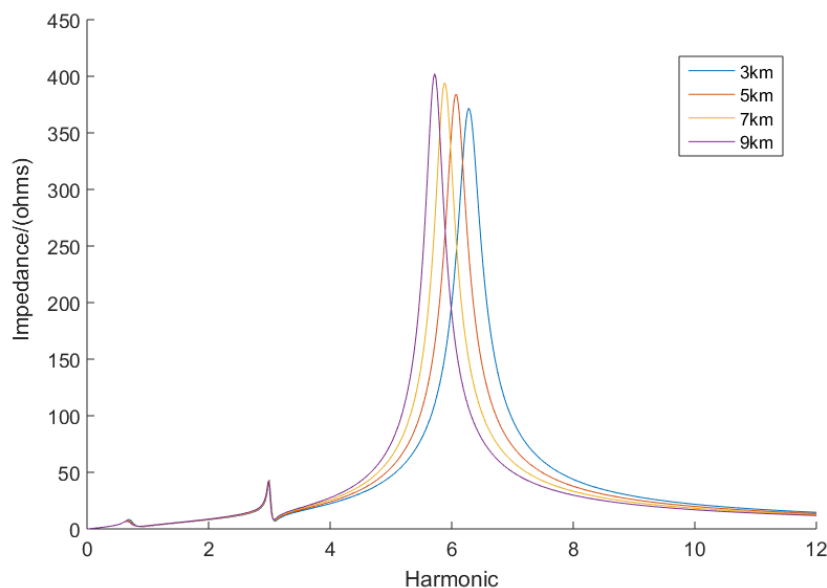
Fig. 5-16: Frequency characteristics of cable impedance with different lengths

The increasing of the cable length leaded in a growth of the distributed capacitance, and the increasing the capacitance value. Therefore, the frequency of resonance, which happened with the inductive element in the system, is shifted to a lower direction.

2) The influence of cable inductance

When studying on the influence of cable inductance on resonance problem, the system is equipped with the same length and the same capacitance value of the cable, changing the inductance value of the cable, then analyze the Simulink simulation results. The formula for the inductance of a cable is shown below：

$$L = \frac{X_L}{\omega_1} = \frac{X_L}{2\pi f_1} \tag{5-27}$$

Where f_1 is the fundamental frequency, and X_L is positive sequence reactance of the system.

Here 4 kinds of cables are selected. And their inductance parameters are 0.6mH/km, 0.52mH/km, 0.45mH/km and 0.32mH/km respectively. They have same length of

3km, the capacitance value of 0.29μF/km, and the positive sequence reactance value is 0.0991Ω/km. Simulation analysis is carried out, and the simulation results are shown in Fig. 5-17.
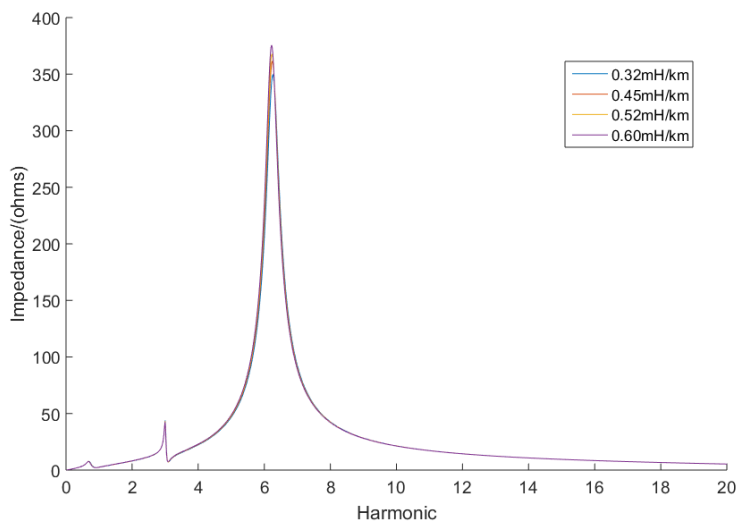
Fig. 5-17 (a) Frequency characteristics of cable impedance with different inductances
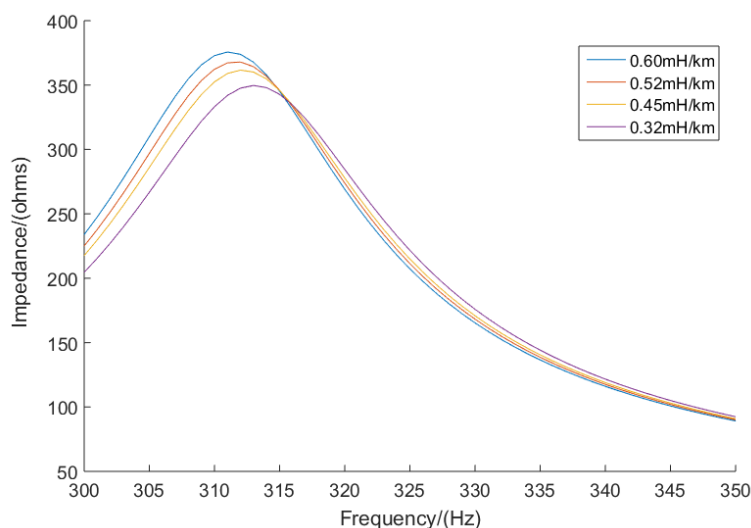
Fig. 5-17 (b) Frequency characteristics of cable impedance with different inductances (detail)

With the gradually increasing of cable inductance, the frequency of resonance will move to a lower frequency accordingly, while the resonant impedance will increase. Therefore, in the design and construction progress of a new offshore wind farm, selecting the reasonable inductance values of the laying cables should be based on the harmonic compatibility test results. At the same time, harmonic adaptability test can also offer reasonable data support and advice for designing proper filters at the later stage.

3) The influence of cable capacitance

Both the length and the inductance value of cable will affect the harmonic resonance characteristics of offshore wind power system. In addition, cable capacitance will also influence the harmonic resonance characteristics, because submarine cables contain a large number of distributed capacitance. The cable with the same length and inductance value is adopted, and the submarine cable with different capacitance is selected to be simulated.

The capacitance values of the 4 cables selected are $0.15\mu F/km$, $0.20\mu F/km$, $0.25\mu F/km$, $0.3\mu F/km$ respectively. The cable length is 3km, the inductance value is $0.32mH/km$, and the positive sequence reactance value is $0.0991\Omega/km$. The simulation result is shown in Fig. 5-18.
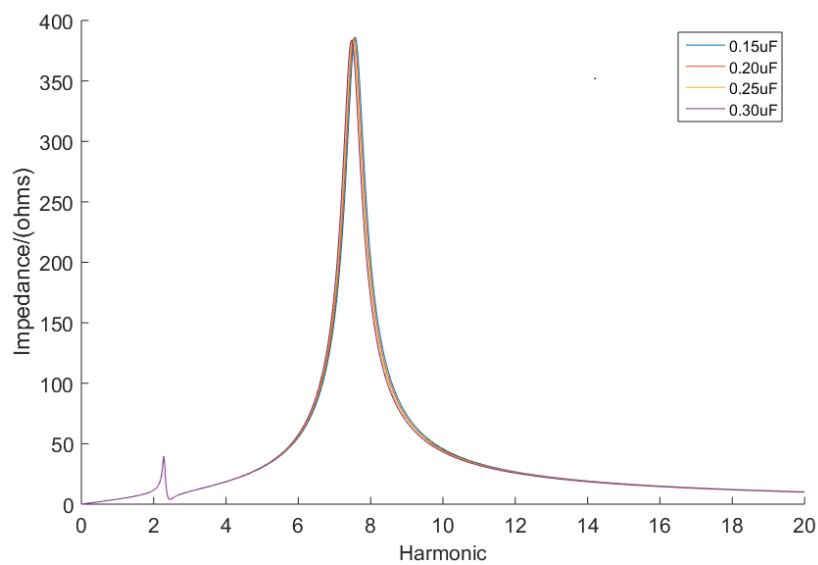
Fig. 5-18(a) Frequency characteristics of cable impedance with different capacitances
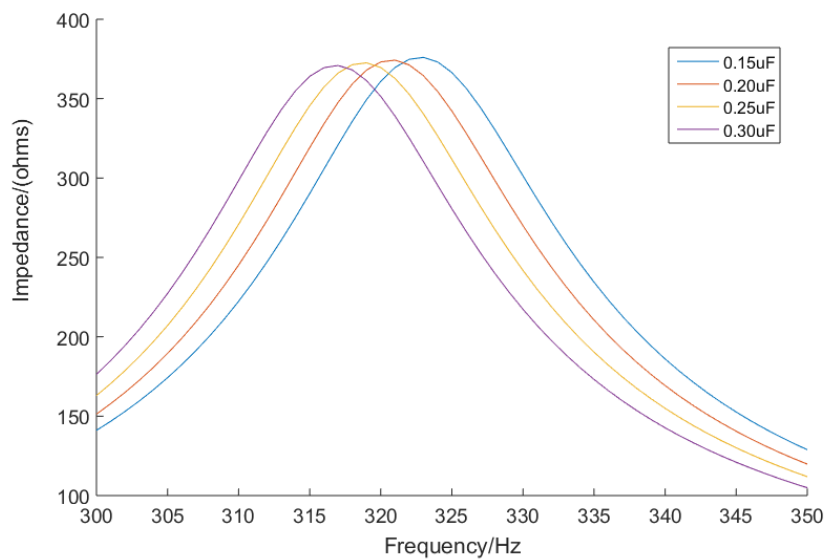
Fig. 5-18(b) Frequency characteristics of cable impedance with different capacitance values (detail)

From above figures, under the variable-controlling approach, the increasing of capacitance can cause the system resonance frequency shift to lower frequency, and resonant impedance increases at the same time.

5.5 Summary

The occurrence of resonance will seriously endanger the safety and stability of the system operation. In this chapter, the system resonance problem is analyzed by building the harmonic model of offshore wind farm installation, simulating the system in equivalent circuit. And then the frequency scan method is applied to detect the influence components which potentially affect the harmonic resonance. Harmonic distortion measured at the WTG terminals is dependent on the network to which it is connected [51]. From the simulation results, the main resonance points are similar at collection grid bus of wind farm in HVAC transmission system and HVDC transmission system, which are around 7th order. Resonance points are also influenced by length, inductance and capacitance of submarine cable, due to the high distributed capacitance of submarine cable. It was shown in chapter 4 that PMSG can generate appreciable level of low order harmonics which are close to resonance point of collection grid in offshore wind farm, so some harmonic suppression strategies should be found.

Chapter 6 Filter Design for Suppressing Harmonics in OWF

6.1 Introduction

Comparing to onshore wind turbine generators, offshore direct-driven PMSG wind turbines have a relatively larger scale and a more complicated construction. Upon multiple wind turbine generators operated in parallel, harmonics amplification occurs easily. This phenomenon exacerbates the harmonics and results in serious voltage distortion that may even exceed the grid limit. In the meantime, a massive implementation of subsea cable and high-power electronic devices greatly increases the number of capacitance and inductance, which is a directly cause of harmonics issue. Therefore, the strategy for suppressing the harmonics at offshore wind farm has become one of the hardest subjects in this field.

Distorted voltage and current cause abnormal operating conditions in a power system. The unwanted harmonics are generated by nonlinear loads, which are loads implemented with semiconductor devices and/or iron-cored devices. Such loads are the power supplies, UPS, motor drive systems, transformers, electronic ballast, electronic appliances, rectifiers, and any other power electronics circuits.

To reduce or eliminate the unwanted harmonic components in a power system, previous researchers have come up with solutions to harmonics issue from several perspectives. One is to introduce filters, including passive filters, active power filters and hybrid filters [56]. The hybrid filters all try to achieve a high performance in the elimination of harmonics while minimizing the costs by combining an active and a passive filter. Any detailed classification of the hybrid filters is out of the scope of this thesis. Based on the current application of filters, the design of one typical type of passive filters and the active power filter (APF) is stated and simulated at the investigated offshore wind farm for suppressing harmonics. Filters can be designed and applied to the system in order to meet better voltage quality requirements.

Besides design of filter, optimization of network structure is another harmonic suppression strategy worth considering. Considering the potential harmonic resonance in advance, the reasonable cable selection and collection grid layout and configuration of system provides better harmonic feature.

6.2 Passive Filter

6.2.1 Fundamental of passive filter

The passive filters are realized with LC components, and active filters are realized using different types of inverter topologies. The filter parameters are set through calculation. The resistance at resonance frequency can be effectively damped by passive filter. The impact caused by harmonics is then reduced, protecting grid from

harmonic pollution. Compared to active filter, passive filter has a larger capacitance, fits for higher voltage and well compensates reactive power. Therefore passive filter is widely implemented in wind farms.

According to working principle and structure, passive filters can be roughly sorted as single turned filters, dual turned filters, second-order high pass filters, C-type high pass filters, etc. Their basic components are shown in figure 6-1 as follows.
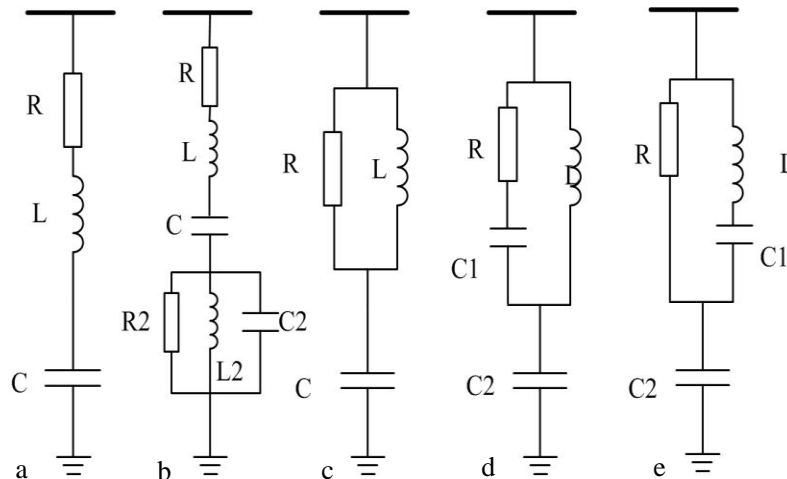
Fig. 6-1: Five common passive filters [57]

a. Single turned filter

Single turned filter is made of a simple serially connected resistance, capacitance and inductance. The cost of single turned filter manufacture and installation is relatively lower. However, subjected to its simple structure, single turned filter only eliminates or suppresses harmonics that occurs at a specific design frequency. The harmonics occurs at other random frequencies cannot be effectively dealt with. Besides, the power consumption of filter increases as higher order harmonics occurs, essentially leads to its low economic performance.

b. Dual turned filter

Differ from single turned filter, dual turned filter has another resistance and inductance in parallel and connected to single turned filter. Dual turned filter suppresses or eliminates harmonics occurs at two design frequencies. Dual turned filter is able to suppress harmonics at two frequencies, one of the harmonic circuit bears lower voltage. The cost of dual turned filter is therefore lower than two single turned filter, and the installation is simpler as well. Thus dual turned filter is an optimum choice for offshore wind farm.

c. Second-order high pass filter

Second-order high pass filter is consisted of a capacitance and a serial connected resistance and inductance. It is usually used to absorb harmonics of multiple orders. The capacitance usage rate of second-order high pass filter is relatively high, but its capability on specific frequency is worse than single turned filter [58]. With a damper configured, on the other hand, the power consumption is reduced, enhancing the

system stability. Therefore second-order high pass filter is widely installed and implemented.

d. Third-order high pass filter

Third-order high pass filter has a capacitance connected with a resistance in series. This capacitance is smaller than the capacitance in the major line, but the resistance at fundamental frequency can be effectively increased.

e. C-type high pass filter

Based on second-order filter, C-type filter installs another capacitance, which reduces fundamental harmonic loss and provides certain amount of reactive power compensation.

Other than the advantages and positive features mentioned above, passive filters exhibits also following disadvantages.

(1) Subjected to the filter features, individual parameter configuration fits only for specific harmonics. Once the system harmonic shifts, previous filter configurations are not applicable. The flexibility and compatibility of passive filter is therefore worse than active filter, it behaves a high reliance on system configuration.

(2) Filter performance is highly subjected to its parameter setting. The harmonic shifts and residual resistance usually leads to unpreventable gap from its ideal performance.

(3) Passive filters are commonly connected with system resistance in series or in parallel and produce harmonics. This harmonics may burn the filter itself and even leads to a series grid accidents.

6.2.2 Design theory of C-type high-pass filter

Due to a massive use of large-scale electronic devices, a large amount of high-order harmonic exists in offshore wind farms. Besides, low-order harmonics are also produced by wind turbine units and the whole wind farm collection grid. Both harmonics endanger severely system stability and economic operation.

C-type high pass filter is effective on suppressing high-order harmonics and also removing harmonic resonance at indicated frequencies. The diagram of C-type filter structure is shown in Fig. 6-2. The damping resistance R is directly connected with the series shunt L-C_1 in order to reduce the fundamental energy loss of the filter [59].
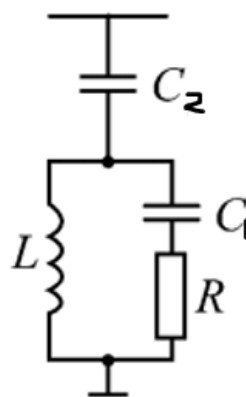
Fig. 6-2: The circuit diagram for C-type high pass filter

The total impedance of the filter is:

$$Z = \frac{(X_L - X_{C_1})^2}{R^2 + (X_L - X_{C_2})^2} R + j(\frac{(X_L - X_{C_1})^2}{R^2 + (X_L - X_{C_2})^2} R - X_{C_1}) \qquad (6\text{-}1)$$

The impedance modulus is:

$$|Z| = \sqrt{\frac{R^2(X_L - X_{C_2} - X_{C_1})^2}{R^2 + (X_L - X_{C_2})^2} + \frac{X_{C_1}{}^2(X_L - X_{C_1})^2}{R^2 + (X_L - X_{C_2})^2}} \qquad (6\text{-}2)$$

According to the above equations, at fundamental frequency, when the inductance L and the capacitance C_2 together generates the series resonance, there is no fundamental power loss at the resistance R and the loss only exists in the harmonic current. Besides, C_1 can be treated as the system voltage support to generate reactive power at the fundamental voltage. Its capacitance value is decided by the required system reactive power [60, 61].

The system rated power angular frequency is ω_1. Limit the L and C_2 to fullfill:

$$\omega_1 = \frac{1}{\sqrt{LC_2}} \qquad (6\text{-}3)$$

When harmonic resonance occurs:

$$X_L - X_{C_2} - X_{C_1} = 0 \qquad (6\text{-}4)$$

Then the frequency of nth-order harmonics is:

$$\omega_n = \sqrt{\frac{C_1 + C_2}{LC_1C_2}} \qquad (6\text{-}5)$$

For this nth-order harmonic, the C-type filter can be equivalent to a RC circuit connected in series, where the filter impedance reaches down to the minimum [62]. The number of major harmonics that needs to be filtered should be set at that point. According to equation (6-3) and (6-5):

$$n_D = \frac{\omega_n}{\omega_1} = \sqrt{1 + \frac{C_2}{C_1}} \qquad (6\text{-}6)$$

According to equation (6-6), the minimum impedance of C-type filter depends on the ratio of C_2 over C_1. When the specific order n_D of harmonics that needs to be eliminated is known, the capacitance of C_2 and C_1 could be obtained by calculation. Then the characteristic equation of filter is obtained as:

$$\frac{|Z|_{min}}{R} = \frac{1}{n^2\omega_1^2 C_1^2 R^2 \sqrt{1 + 1/n^2\omega_1^2 C_1^2 R^2}} \qquad (6\text{-}7)$$

By analyzing and calculating the characteristic equation, the minimum resonance impedance can be adjusted to ensure the safe and stable operation of the filter.

6.2.3 Parameter design of C-type high-pass filter

In order to study the filtering effect of C-type high-pass filter, this section aims to design a proper filter and analyze the harmonics before and after the filter installed in the investigated offshore wind farm system.

From chapter 4, the simulation model for the investigated offshore wind farm is validated. Thus the harmonic distribution when no filter is installed at collection node could be illustrated in the spectral diagram. According to IEEE Std 519-2014, the maximum allowable harmonic distortion level for bus with voltage over 161kV is stated. For the odd harmonic order (h<11), THD should be less than 3.0%. While 11<h<23, THD level should below 1.5%. And for 23<h<35, THD value needs to be smaller than 1.15%. The following figure plot the simulated THD values for the OWF compared with the maximum allowable standard level.
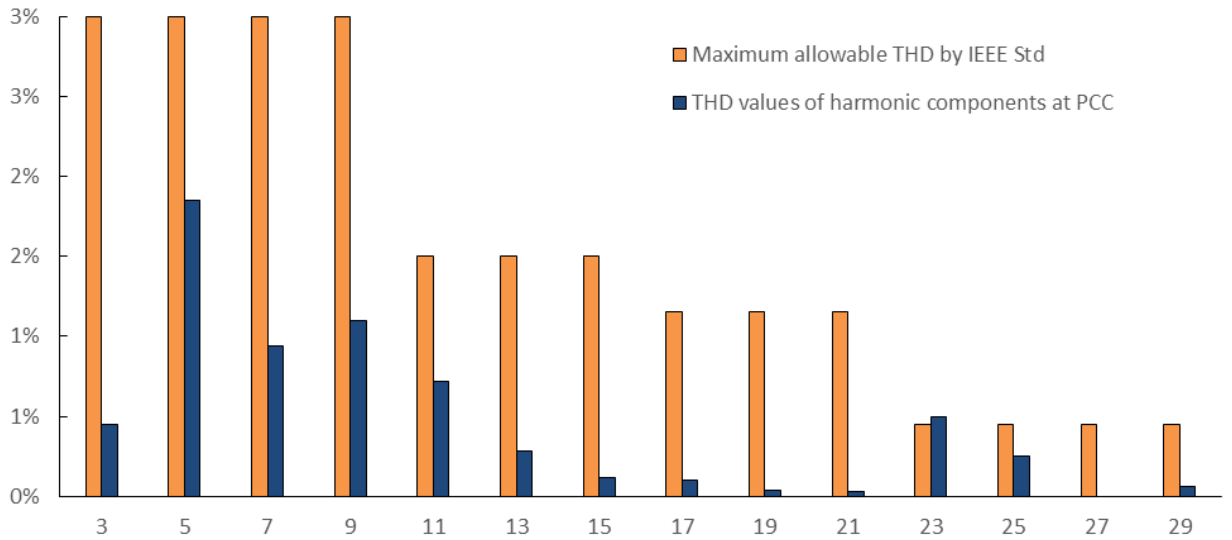
Fig. 6-3: Spectral diagram of current harmonics at PCC without filters

Table 6-1: Simulated system specification

Voltage of the AC network (kV)	230
Frequency (Hz)	50
Fundamental-Freq. Short-circuit reactance (W)	1
dc-side voltage of HVDC converter (kV)	± 100

Based on the previous design equations, we could follow the blow steps to design and calculate the parameters of C-type filter [59-62].

1) The target harmonic order that needs to be eliminated is n_D. In the investigated wind farm model, the target elimination order of harmonics located at 5th order, 7th order and 9th order. Set $n_D = 9$. From equation (6-6), the ratio of C_2 over C_1 is calculated to be 80.

2) The reactive power demanded by an HVDC converter is often expressed in terms of the dc-side power [59]. Based on the reactive power required to compensate the power factor at fundamental frequency, only C_1 could supply reactive power at fundamental frequency:

$$Q_{C1} = U^2 \omega_1 C_1 \tag{6-8}$$

Assume the Q_{C1} is 25MVar, then the capacitance C_1 is 1.5μF.

3) Based on the design value of ratio n_D and C_1, the value of C_2 could be calculated as

$$C_2 = C_1(n_D{}^2 - 1) \tag{6-9}$$

Then the capacitance in the series branch C_2 is 120μF.

4) Based on the limiting condition that

$$\omega_1 = \frac{1}{\sqrt{LC_2}} \tag{6-10}$$

The parameter value of inductance L could be set down.

$$L = \frac{1}{\omega_1{}^2 \cdot C_2} = 84.4\text{mH} \tag{6-11}$$

5) Combined considering of the request of the filtering effect and the system impedance parameter, the first step is to determine the minimum impedance of the filter. The minimum impedance value of the designed filter is assumed to be 1. And then according to formula (6-12) to find the R value,

$$Z_{min} \approx \frac{1}{n_D{}^2 \omega_1{}^2 \cdot C_2{}^2 R} \tag{6-12}$$

The shunt resistance of the C-type filter is 8.68Ω.

Here should note that, when R increases, Z_{min} decreases, but in higher harmonic regions, Z_{min} curve will increase in amplitude [63]. Therefore, in determining the resistance R value, not only should consider Z_{min}, but also take into account the impedance requirements of the entire frequency section.

6) The capacity of capacitance C_2 in the series branch could be calculated as

$$Q_{C2} = Q_{C1} \frac{C_1}{C_2} \tag{6-13}$$

Above all, the design of the C-type filter is realized step by step. Its reactive power compensation capacity is 25MVar. The target harmonic order that needs to be eliminated is set to 9th order. Then parameters of C-type filter can be calculated by equations (6-6) to (6-12). The shunt resistance of the C-type filter is 8.68Ω, the inductance is 84.4mH, the capacitance is 1.5μF, and the capacitance in the series branch is 120μF.

6.2.4 Results analysis

The C type filter is inserted at the grid-connected point, and the model is run on the simulation platform. The model diagram of the model accessing the filter and the topology of the filter are shown in the following figure 6-4.
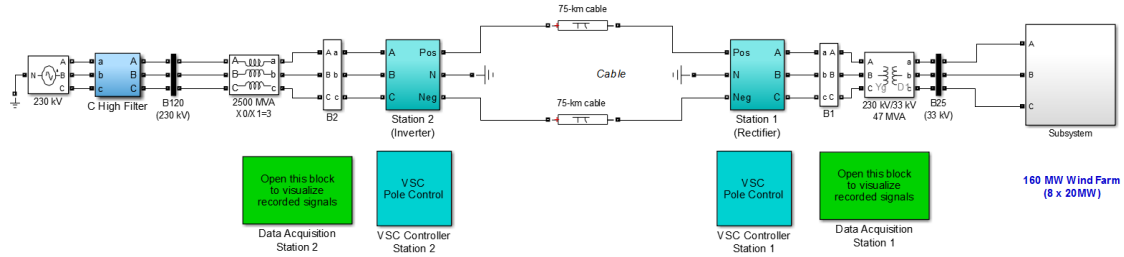
Fig. 6-4: The model of wind farm with the C-type filter

The simulation model of C-type filter established in Matlab is shown as Fig. 6-5.
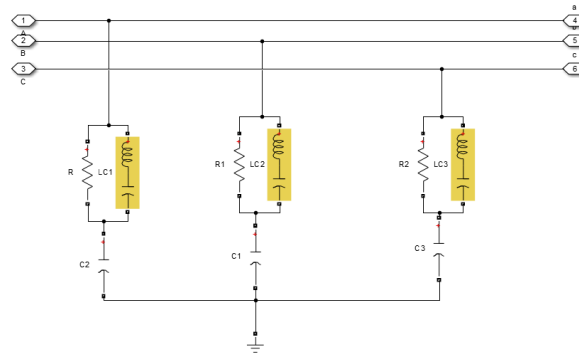
Fig. 6-5: The simulation model of C-type high pass filter

The harmonic spectrum analysis diagram without and with the filter are shown in the following figure. As can be seen from the diagram, the main harmonics in this OWF system are odd order harmonics, especially in the low order range, in which the higher harmonic components are the 5th, 7th, 9th and the 11th order harmonics. And the phenomenon that relatively large THD values at 23rd and 25th order harmonics is also worth to mention. It acts coordinated with the previous chapter 5, which did impedance scanning on the whole system. The x-axis is the harmonic order.
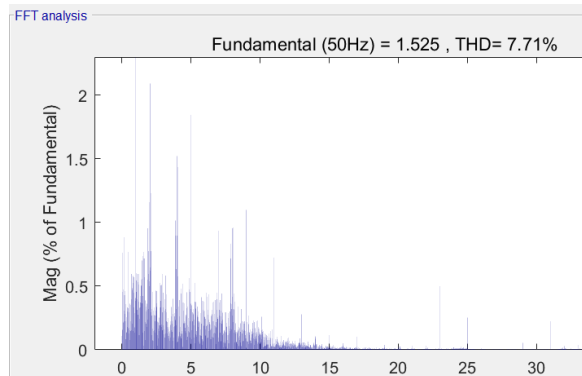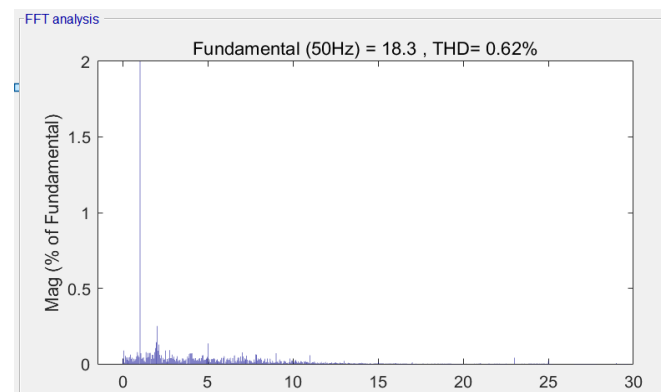
Without the access of filter   With the access of C-type filter

Fig. 6-6: The harmonic spectrum analysis diagram without and with the C-type filter

From the above spectrum analysis diagram, the total harmonic distortion of current at the grid-connected point is reduced from 7.71% to 0.64%. And the THD values for

the low order harmonic are also less than 0.2%, which means the designed filter can weaken the low frequency range of harmonics effectively. The grid-connected current approximates the sine wave reasonably with very high power quality, and the grid-connected point harmonic level meets the requirements of relevant specifications.
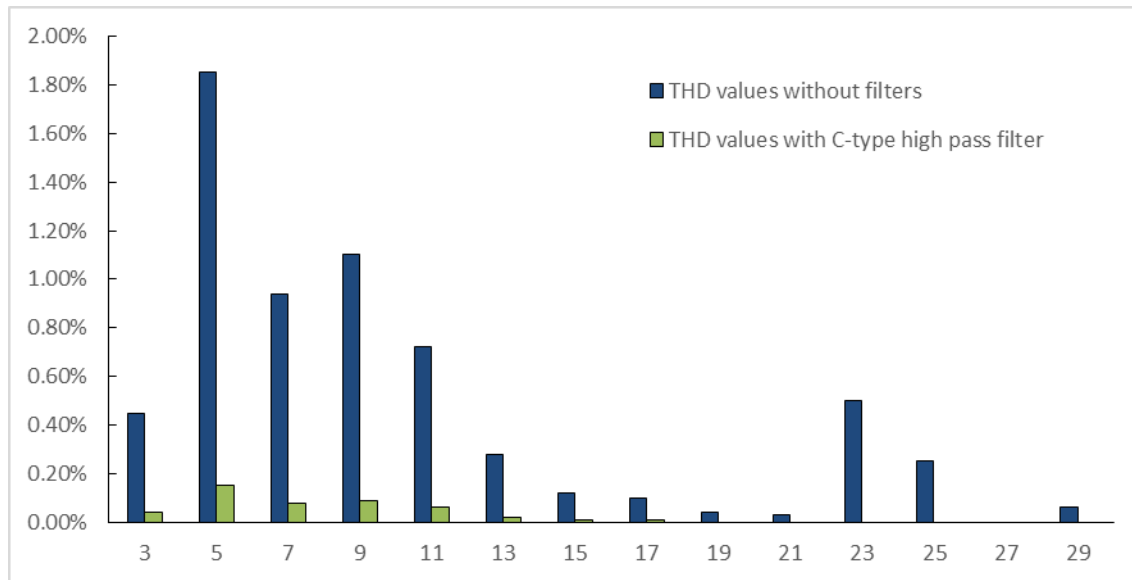
Fig. 6-7: The harmonic spectrum analysis diagram before and after the access of C-type filter

6.3 Active power filter

6.3.1 Fundamental of active power filter

Nowadays, active power filters (APF) are the only solution which is able to improve power quality in contemporary power systems with distributed generation and dynamical changes of supplying current and voltage distortions [64]. The inner power source is the main difference between APF and passive filter. Introducing APF is a compensation for the shortage of passive filter.

Many researchers put a lot attention on APF recent years. Japan has realized APF essentially application, not only on improving harmonic features, but on improving the grid quality compensation. Europe has also put a lot resources on APF research, and some of the offshore wind farm has already introduced APF in their harmonics suppression strategies.

The active filter can be connected in parallel or in series with the load. The main idea of their operation is that they inject currents that are contrary to the harmonics of phase with fundamental currents. In this way they eliminate harmonic fundamental currents. Compared with passive filter, active filter has better performance. It has the advantage of programming to block multiple harmonics rather than just one harmonic. They can also provide reactive power when needed, and can also compensate for neutral currents. A large number of harmonic components can be eliminated by the

same filter. In addition, active filters do not have the risk of resonance with other network components like passive filters. The cost of high power rated converters is the biggest drawback of active filters, even though prices are falling. The design of APF is more complicated and may cost higher power losses with lower reliability. And it can handle lower power compared to the conventional passive filters.

The basic working principle of an active converter works is illustrated in the following diagram. As seen e_s is the AC supply. According to Fig. 6-8, an active power filter consists of 2 part: one is command current operational circuit, the other is compensate current generation circuit. A compensating circuit is made up of a current control tracking circuit, a drive circuit and a main circuit. The main function of operational circuit is to detect the harmonic component at compensating current, while the major function of compensating circuit is to generate proper compensating current according to the operation result [67]. More detail fundamentals about APF model are listed at appendix.
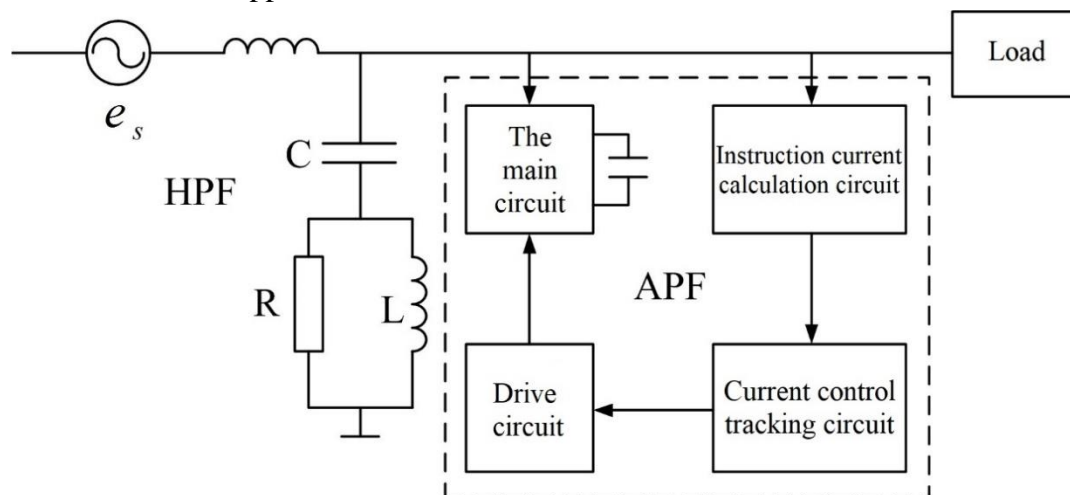
Fig. 6-8: Working principle of a basic APF

6.3.2 Design of LCL active filter

The LCL filter is a new type of active grid-connected filter in recent years, which impedance is inversely proportional to the frequency of the current. Therefore, the suppression of higher order harmonics is more prominent than that of conventional passive filter and it can be well applied to harmonic suppression of the offshore wind farm [66]. The schematic diagram of active filter is shown in the following figure.
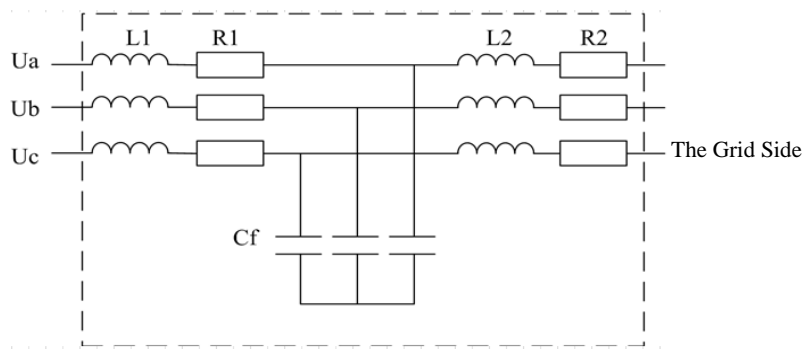
Fig. 6-9: The schematic diagram of active filter

The LCL filter consists of a DC module, an AC module and a power switch module. The fan side of the filter is composed of the resistor R_1 and the inductor L_1, and the grid-side is composed of the resistor R_2 and the inductor L_2. There is a capacitor C_f with a Y-shaped connection between the two sides. The inductor L_1 is used to suppress harmonics of low orders, and the inductance L_2 and capacitor C_f are used to suppress harmonics of high orders as well as improve the stability of the power grid [66]. The overview diagram of structure of LCL APF is shown below.
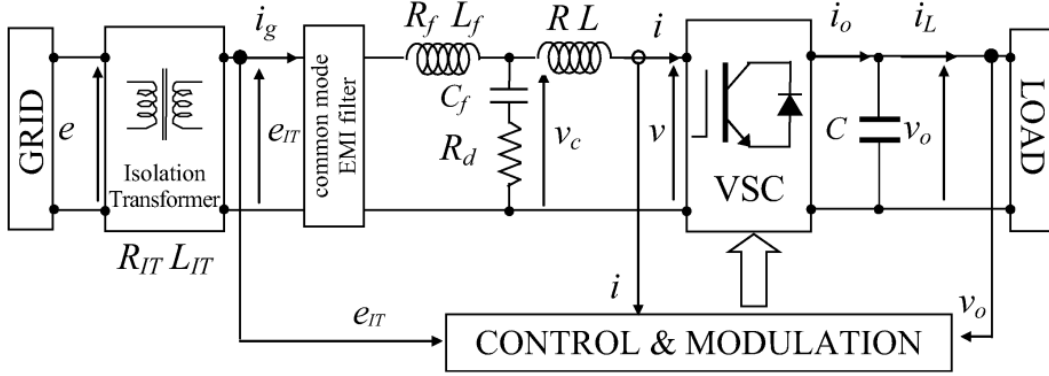
Fig. 6-10: Overview diagram of the LCL active filter [66]

The basic principle of LCL filter is that inductors show low impedance characteristics and capacitor shows high impedance characteristics at low frequency, thus current at fundamental frequency will go through inductors to grid; At high frequency, capacitor has low impedance and inductors shows high impedance, so high frequency harmonics will be filtered out through capacitor. Compared to L filter, LCL filter achieves a higher attenuation with limited values of inductors and capacitors.

In practical applications, large-scale offshore wind farms have a number of wind turbines. Therefore, in order to avoid the resonant oscillation of the LCL filter, it is usually added damping. The LCL filter with damping can also effectively reduce the energy consumption of passive damping and improve the working precision and efficiency of the filter. According to the regulation, the voltage on the inductor is 10% less than the effective value of the system line voltages. This paper takes a ripple current of 20%, and the formula is written as

$$\frac{U_{dc}}{8 f_s L_1} \le 0.2 I_{1N}$$

(6-14)

In the formula, U_{dc} is the system bus voltage, f_s is PMW switch frequency, I_{1N} is the equipment rated current.

For converter side inductance L_1, the constraint is

$$L_1 \le \frac{\sqrt{U_{dc}^2/3 - U_m}}{2\pi f_1 I_m}$$

(6-15)

In the formula, f_1 is the fundamental frequency, U_m is the peak of the phase voltage of the power grid, I_m is the peak of the phase current of the power grid.

Because of the limitation of the filter power factor, in order to prevent the reactive power output of the filter from increasing indefinitely, the reactive power of the LCL filter is set to 95% of the rated capacity of the converter, which is written as

$$C_f \leq \frac{P_N}{6\pi f_1 U_N^2} \times (1 - 95\%)$$

(6-16)

Finally, the damping coefficients are set, as follows:

$$\xi = \frac{K_{cf}}{2} \times \sqrt{\frac{L_2 C_f}{L_1(L_1 + L_2)}}$$

(6-17)

In this way, we can calculate the parameters of the LCL with the active damping filter in the VSC grid-connected mode to achieve the suppression of harmonic resonance.

From equations (6-14) to (6-17), parameters of LCL APF can be set:

1) For L_1, set $0.636 \leq L_1 \leq 2.198mH$, to reduce the weight, volume and building cost, $L_1 = 2mH$ is selected.
2) For C_f, assume $Q = 0.01P_N$, then

$$C_f = \frac{0.01P_N}{6\pi f_1 U_N^2} = 28.34\mu F$$

$C_f = 30\mu F$ is selected to sample the calculation.
(3) Set damping coefficients $\xi = 8\%$, then $L_2 = 1mH$ is selected.

6.3.3 Results analysis

The LCL filter is inserted at the grid-connected point in the simulation model with APF in series. The model diagram of APF for detecting the harmonic component at compensating current and the configuration of the LCL filter are shown in the following figures.
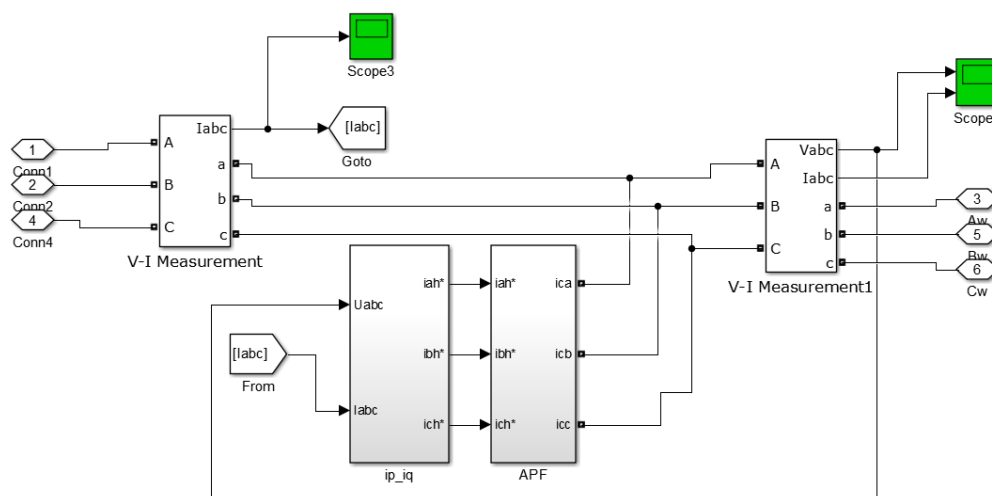
Fig. 6-11: Model diagram of APF's access
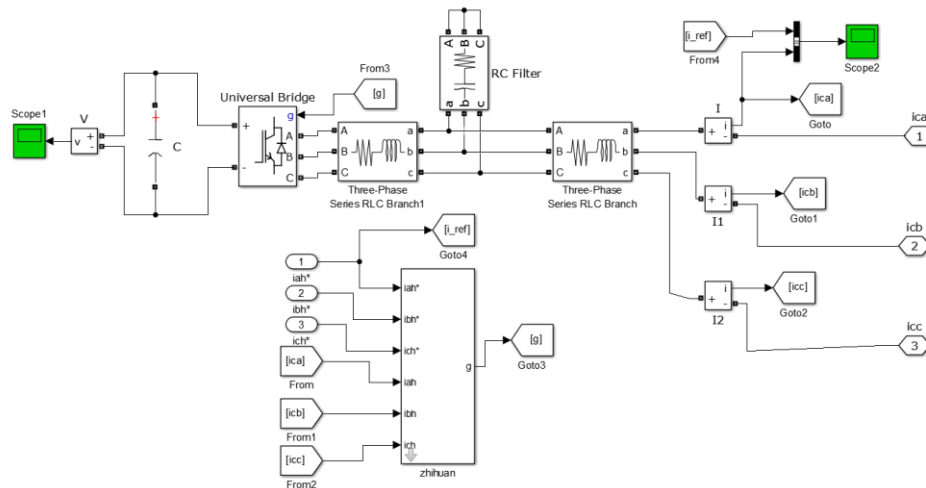
Fig. 6-12: Configuration of the LCL filter
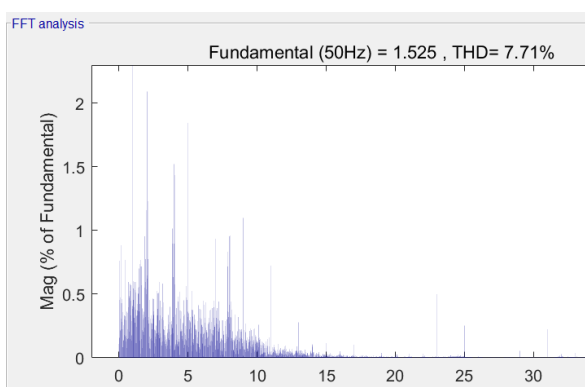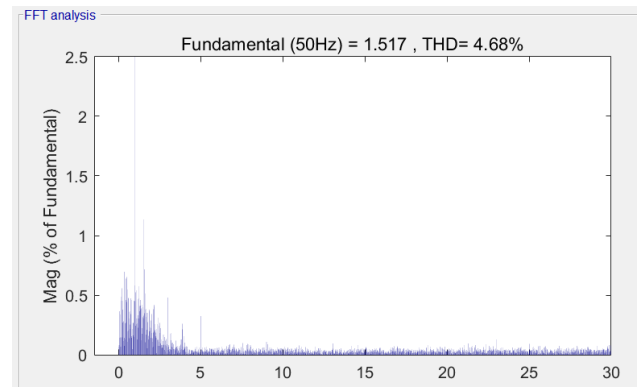
Without the access of filter   With the access of the LCL active filter

Fig. 6-13: The harmonic spectrum diagram without and with the LCL active filter

Harmonic spectrum with the designed LCL active power filter are shown in Fig. 6-13. The total harmonic distortion of current at the grid-connected point is reduced from 7.71% to 4.68%. And the low order harmonics are all suppressed below 0.5%. The result can meet the IEEE harmonic standard. The THD bar plot of the investigated system without and with the designed LCL active filter is drawn as in Fig. 6-14.
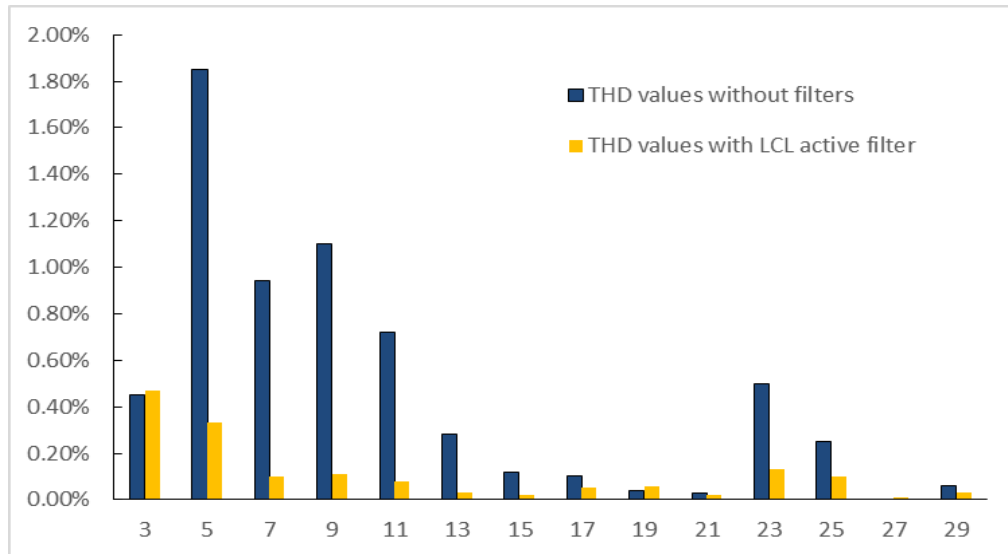
Fig. 6-14: The THD bar plot of the system without and with the LCL active filter

In this work simulation, the direct use of APF in series installed at the end of the VSC-HVDC grid-side converter station. The results for system with the designed APF seem not to be as satisfying as for the system with passive C-type filter. It could be concluded that APF is also a feasible solution for reducing the overall THD level for the OWF system. However, due to the limitation of research and understanding of the design of APF, this thesis work didn't get very persuasive results after the access of the designed LCL type APF. It still need further investigation in the future work.

Now APF is a mature technology with low pressure and small capacity, while the high voltage and large capacity APF is not mature. And the effect of LCL active filter is not very satisfied due to its expensive investment for electronic equipment, especially in large scale offshore wind farm. After further research, the passive filters are the most common and better strategy for the converter station. In addition, the parallel type APF is mainly used in industry, but the series APF is not so commonly applied.

6.4 Summary

Several methods for harmonics suppression are performed in this chapter. Passive filters, active power filters are introduced respectively. Time-domain based simulation methods of offshore wind farm and filters are built in MATLAB/Simulink. The harmonics distribution in cases with C-type filter or active power filter adopted are designed and analyzed with simulation models. Through the simulation case study above, a passive filter with C-type filter combined performed a satisfying results on harmonics suppression, the harmonic distortion of current of the grid-connected point is reduced from 7.71% to 0.64%. And the THD values for the low order harmonic are also less than 0.2%, which means the designed filter can weaken the low frequency range of harmonics effectively. An active power filter solution has also been designed and analysis, however the effect is not very satisfied. The harmonic distortion of

current of the grid-connected point is reduced from 7.71% to 4.68%. In future work, further study on APF design and the optimal parameters of hybrid filters will be chased to improve harmonics suppression.

Chapter 7 Conclusion

7.1 Conclusion

In this thesis work, a comprehensive harmonic analysis in offshore wind farm was studied. Firstly, the fundamental of the offshore wind farm installation and basics of harmonic are described. Secondly, a suitable model of one offshore wind farm is built and validated in Simulink, based on the type 4 wind turbine example and VSC-HVDC transmission system example in MATLAB. Moreover, the equivalent circuit is calculated for the components in the aggregated wind farm based on their harmonic model. And then the resonance problems are analyzed by frequency scan method to calculate the potential resonance impedance and frequency. As well, the two types of transmission system and the cable parameter selection are simulated to evaluate the various influence on the resonance issue. Afterwards, based on the self-built system model, potential harmonic issues that arise in the system are investigated in time domain to interpret the THD at PCC between the OWF collection grid and the onshore grid. At last, a C-type filter and an LCL active power filter are designed and performed a satisfying results on harmonics suppression.

1) Simulation models of offshore wind farm system is established. The harmonic current injected from PMSG to grid is mainly determined by gird side converter and filter in wind turbine out port. The harmonics are mainly influenced by the converter control strategy and switching frequency of electronic devices. Only some relatively high emission occurs at higher harmonic orders, which is lack of enough power to influence the voltage quality of the whole grid system, and for other frequencies where the distortion levels are traditionally lower. The overall THD level of harmonic output from wind energy generation system is relatively small.

2) System resonance problem of OWF was analyzed in equivalent circuit models. And then the frequency scan method is applied to detect the influence components which potentially affect the harmonic resonance. From the simulation results, the main resonance points are similar at collection grid bus of wind farm in transmission system of HVAC and VSC-HVDC, which are both around 7th order. Resonance points are also influenced by length, inductance and capacitance of submarine cable, due to the high distributed capacitance of submarine cable.

3) Time-domain based simulation of offshore wind farm and filters are built in MATLAB/Simulink. The harmonics distribution in cases with C-type filter and active power filter adopted are designed and analyzed in simulation models. A passive filter with C-type filter combined performed a satisfying results on harmonics suppression. The designed LCL active power filter has also been proved to be effective on filtering the harmonics, but not very suitable for such large scale capacity system.

7.2 Future Work

This project is just a simple trial to build the large scale offshore wind farm model in numerical simulation software. To pursue the possible factors resulting in harmonic and resonance issues in the collection grid, various cases are performed in Matlab/Simulink. There are quite a lot shortages and interest points that may promote future work.

- In this work, the harmonics analysis only focus at the grid connected terminal with considering of power quality to the onshore grid. However, the harmonics not only affect the power grid, but also can affect the HVDC transmission system. This direction is another interesting research scope which may be for further work.

- Due to large cable system involved, it is important that switching over-voltage is considered, and appropriate over-voltage protection is needed for the collection grid design [68].

- The modeling of harmonic propagation and damping is still a very difficult subject. This may not be a serious research challenge by itself. Estimating harmonic voltage and current levels remains a serious challenge when there is limited amount of network or component data available. Detailed models exist but are often not applicable due to lack of data [69].

- Due to the limitation of this research and understanding of the design of APF, this thesis work didn't get very persuasive results after the access of the designed LCL type APF. It still need further investigation in the future work.

- For the harmonic suppression strategy, the combination application of the active filter and passive filter has not been considered in this paper. Only the single type filter is studied and simulated. Further study of the combination of the two filter strategy helps to make up for the shortcomings of a single type filter and to eliminate harmonics more effectively.

Appendix

A. Offshore Wind Farm Test Case
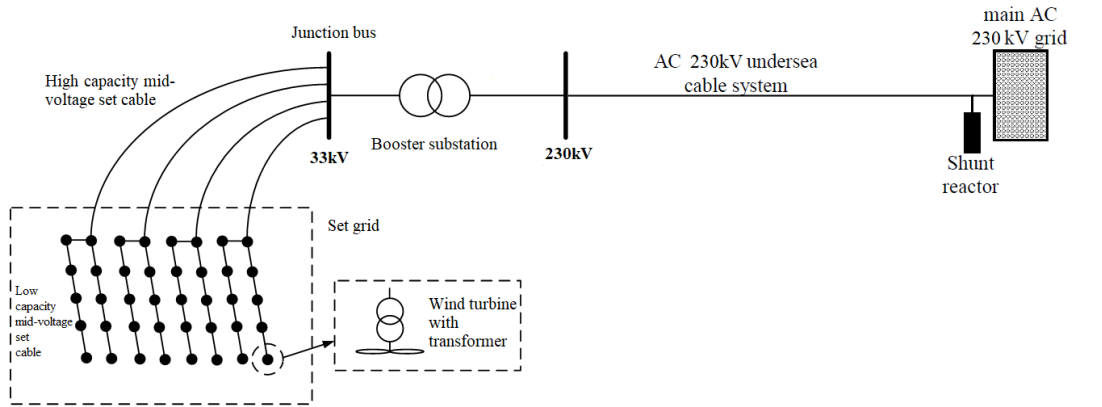
（a）

（b）

Fig. A-1: The electrical system for the HVAC (a) and HVDC (b) connection of the 160 MW offshore wind farm
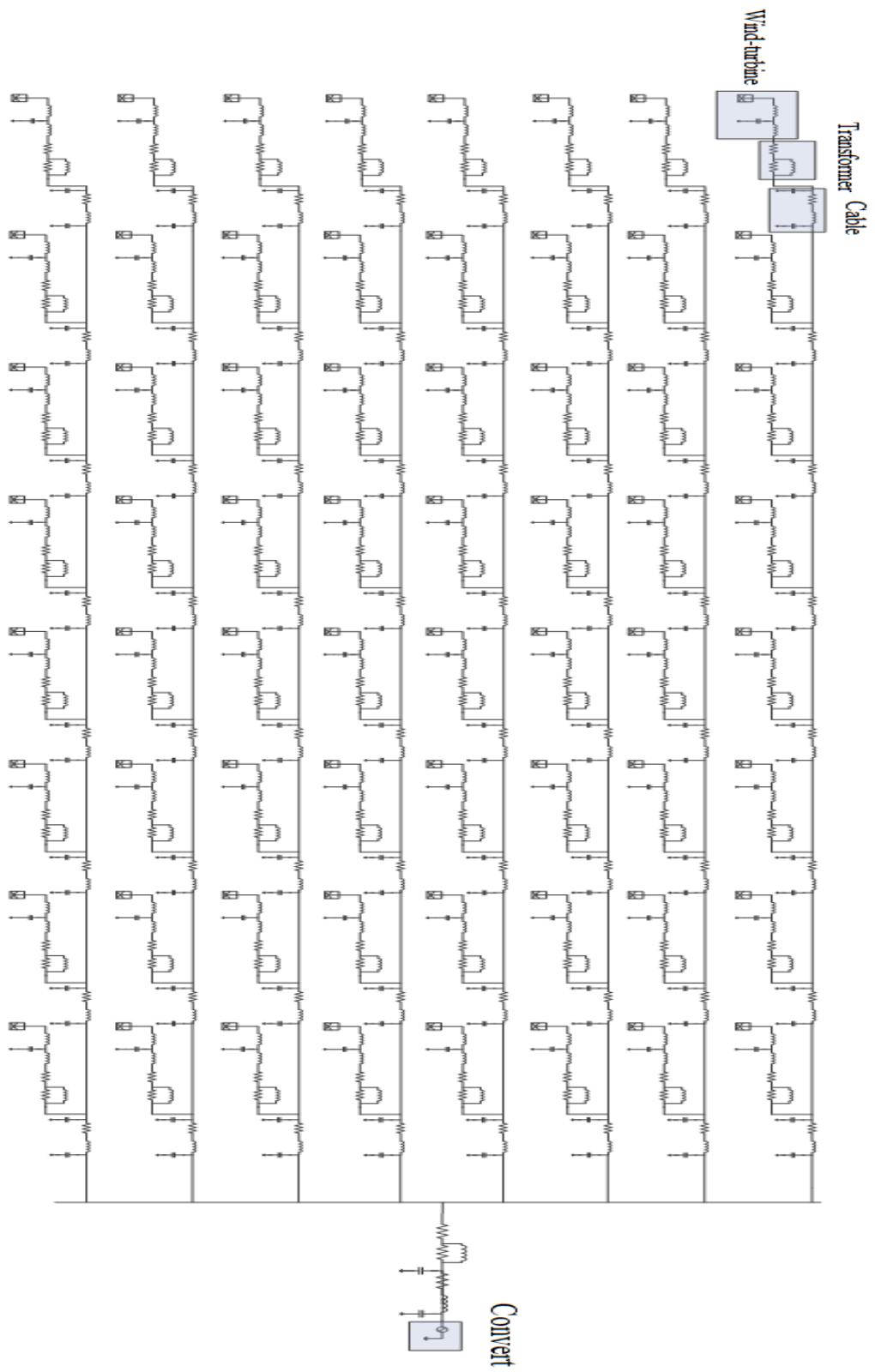
Fig. A-2: harmonic model of HVAC transmission system in OWF
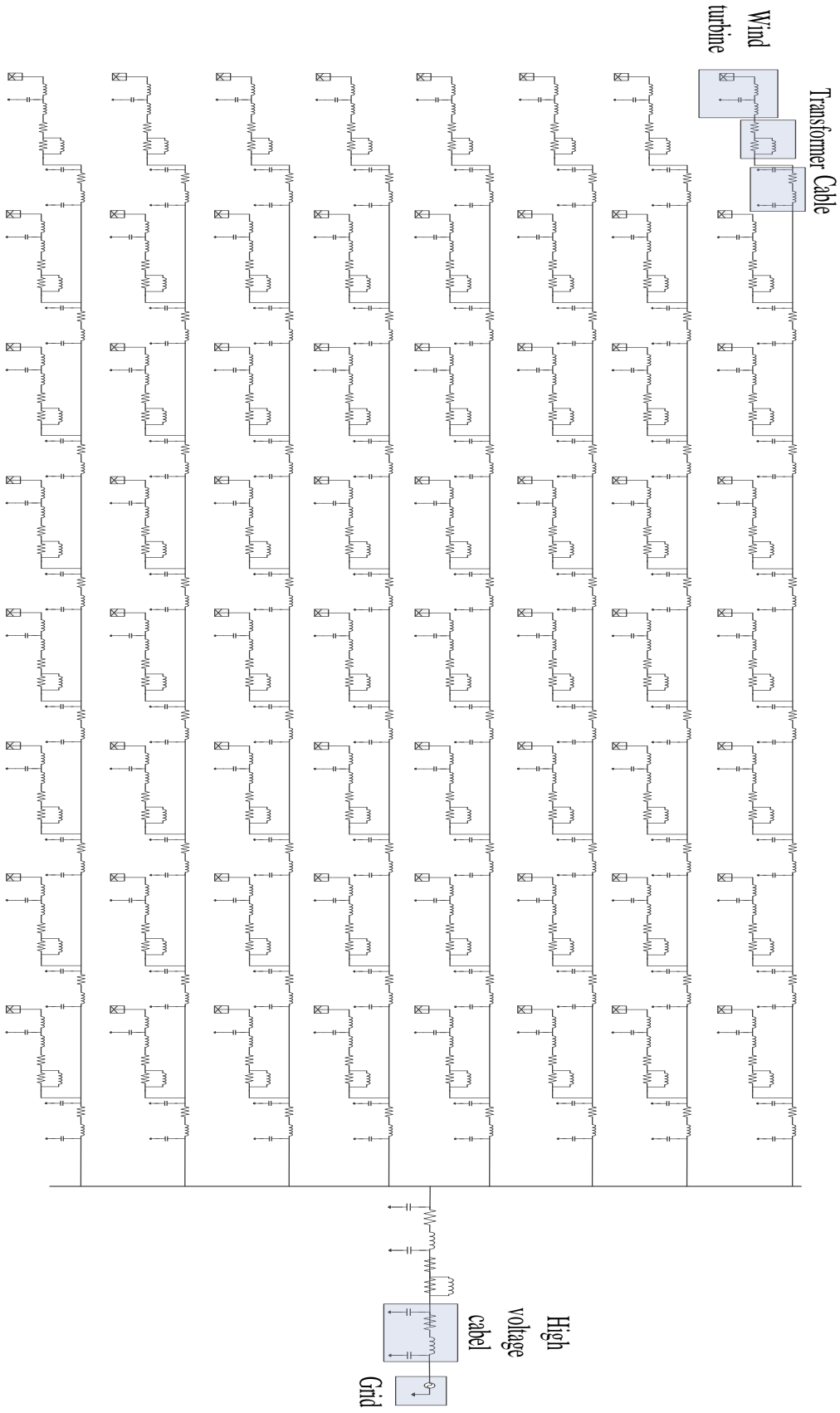
Fig. A-3: harmonic model of HVAC transmission system in OWF

B. Mathematical model of APF in ip-iq detection algorithm

ip-iq algorithm is deducted from the basis of H.Akagi's instantaneous power theory. The algorithm is able to measure the harmonic current and voltage precisely when grid voltage is asymmetry.
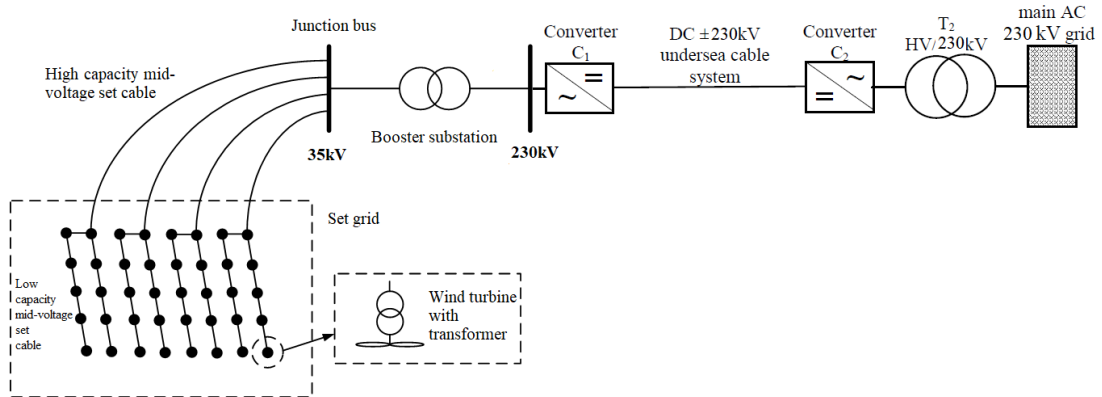
Take voltage vector u and it's vertical direction vector as a basis of phasor, orthogonal decompose the current vector i on the basis, define the i_p, current in the direction of u, as the instantaneous active current in three-phase circuit, and the i_q, current in the vertical direction of u, as the instantaneous reactive current in three-phase circuit, i_p, i_q are expressed as below:

$$i_p = i\cos\varphi \tag{B-1}$$

$$i_q = i\sin\varphi \tag{B-2}$$

Vector diagram between i_p, i_q, u and i in α-β coordinate system is shown in fig.E-1.
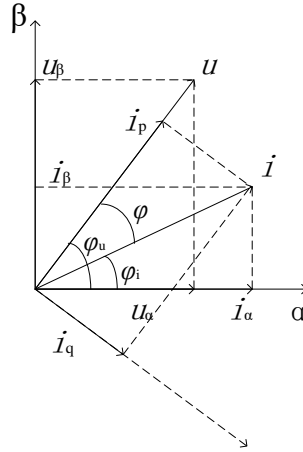
Fig. B-1: Vector diagram between ip, iq in α-β coordinate system

$$\begin{bmatrix} i_p \\ i_q \end{bmatrix} = \begin{bmatrix} \dfrac{u_\alpha}{u} & \dfrac{u_\beta}{u} \\ \dfrac{u_\beta}{u} & -\dfrac{u_\alpha}{u} \end{bmatrix} \begin{bmatrix} i_\alpha \\ i_\beta \end{bmatrix} = \begin{bmatrix} \sin(wt) & -\cos(wt) \\ -\cos(wt) & -\sin(wt) \end{bmatrix} \begin{bmatrix} i_\alpha \\ i_\beta \end{bmatrix} \tag{B-3}$$

ip-iq harmonic detection principle block diagram is shown in Fig. B-2, The phase-locked loop is used to determine the frequency of the a-phase voltage to get the positive sequence voltage phasors, harmonic command current are named after i_{ab}, i_{bb} i_{cb}. After multiplied by matrix C32, three phase current are transformed to i_α and i_β, which are i_p and i_q after multiplied by matrix C. After the low pass filter process, DC component corresponding to the three-phase current in the fundamental current, $\bar{i}_p$ and $\bar{i}_q$, can be deducted. Subtracting the fundamental current with the compensated three-phase load current is the final harmonic command current.
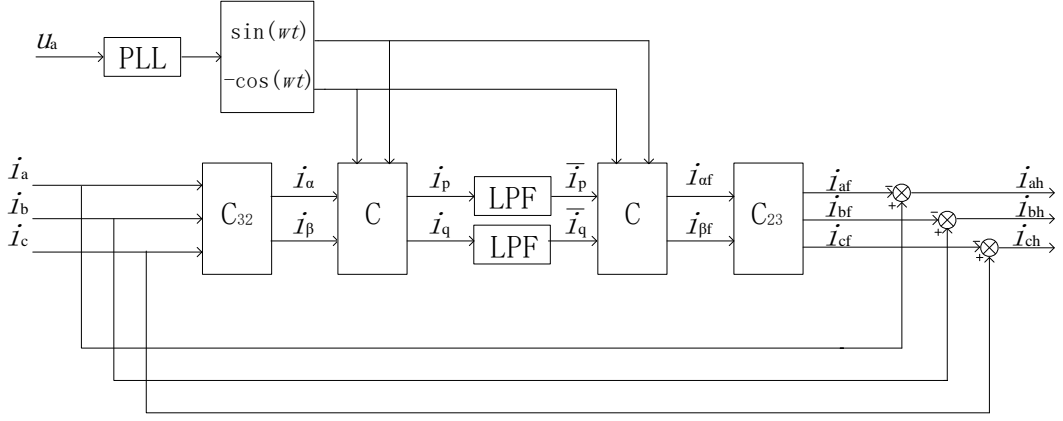
Fig. B-2: ip-iq harmonic detection schematic

Where

$$\mathbf{C}_{23} = \mathbf{C}_{32}^{\mathrm{T}}$$

(B-4)

$$\mathbf{C} = \begin{bmatrix} \sin(wt) & -\cos(wt) \\ -\cos(wt) & -\sin(wt) \end{bmatrix}$$

(B-5)

C. Control modes adopted in the converter station

The main control modes adopted in the converter station include voltage amplitude control and power angle control:

(1) The bus voltage amplitude control in wind farms

In the $d\text{-}q$ synchronous rotating coordinate system, the shaft d is positioned on the wind farm bus voltage vector $\dot{U}_S$. It can be get that

$$\begin{cases} L\dfrac{di_d}{dt} = U_S - U\cos\delta - Ri_d - \omega L i_q \\ L\dfrac{di_q}{dt} = -U\sin\delta - Ri_q + \omega L i_d \end{cases}$$

（C-1）

Assume that the converter output voltage amplitude $\dot{U}$ remains unchanged, $U=U_0$, when i_d, i_q and δ produce a small disturbance at the point of operation, the linearization and Laplace transform are applied to them in the neglect of disturbance of angular frequency. It can be get that

$$\begin{cases} \Delta i_d = U_0 \dfrac{\omega L \cos \delta_0 + (sL+R)\sin \delta_0}{(sL+R)^2 + (\omega L)^2} \Delta \delta \\[4mm] \Delta i_q = U_0 \dfrac{\omega L \sin \delta_0 + (sL+R)\cos \delta_0}{(sL+R)^2 + (\omega L)^2} \Delta \delta \end{cases} \tag{C-2}$$

The instantaneous power disturbance is that

$$\Delta P = \begin{bmatrix} I_{d0} \\ I_{q0} \end{bmatrix}^T \begin{bmatrix} \Delta U_d \\ \Delta U_q \end{bmatrix} + \begin{bmatrix} U_{d0} \\ U_{q0} \end{bmatrix}^T \begin{bmatrix} \Delta i_d \\ \Delta i_q \end{bmatrix} \tag{C-3}$$

By means of necessary calculation and simplification, the linearized transfer function between active power and power angle can be obtained, additional high-pass filter is added in the control to effectively suppress resonance. The magnitude of the output AC voltage of the converter U is controlled as

$$\begin{cases} U = U_0 - G(s)I \\ G(s) = Ks/(s+\lambda) \end{cases} \tag{C-4}$$

In the formula (C-4), $G(s)$ is the high-pass filter, I is current. After applying the control, the linearized transfer function between the active power and the power angle is

$$\Delta P = \dfrac{as^2 + bs + c}{(sL+R+G(s))^2 + (\omega L)^2} \Delta \delta \tag{C-5}$$

In the formula (C-5),

$$\begin{cases} a = \dfrac{L}{\omega}(U_{s0}U_0 \cos \delta_0 - U_0^2) \\[3mm] b = \dfrac{R+G(s)}{\omega}(U_{s0}U_0 \cos \delta_0 - U_0^2) \\[3mm] c = \omega U_{s0}U_0 \cos \delta_0 + [R+G(s)]U_{s0}U_0 \sin \delta_0 \end{cases} \tag{C-6}$$

In order to keep the bus voltage of the wind farm stable, the voltage amplitude controller shown in Fig. C-1 is used. U_{sref} is the reference value of the bus voltage and U_{0ref} is the reference value of the convert output voltage.
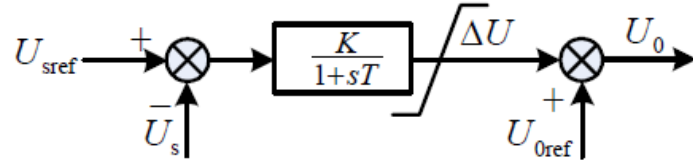
Fig. C-1: The AC voltage amplitude controller (AVAC)

According to the formula (C-4) in the above control principle, the component of $d\text{-}q$ axis of the output voltage of the converter is controlled by the following formulas:

$$\begin{cases} U_d = U_0 - G(s)i_d \\ U_q = -G(s)i_q \end{cases}$$

(C-7)

(2) The power angle control

The phase difference between the bus voltage of the wind farm and the output voltage of the converter is the power angle. When the wind farm is connected to grid through the AC / DC hybrid transmission system, the VSC-HVDC must adopt the constant active power control, and the fluctuation of the wind power will lead to the change of the power in the AC transmission line. The active power control(APC) shown in Fig. F-2 is adopted in order to maintain the constant power control of the VSC-HVDC when the power flow changes.
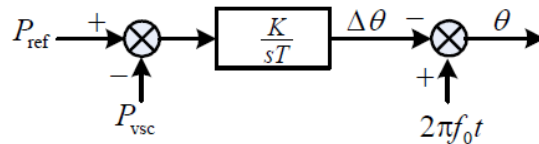
Fig. C-2: The active power controller

The angle deviation $\Delta\theta$ can be get after integrating the deviation between the active power reference value P_{ref} and the transmission power of VSC-HVDC P_{vsc}. With the reference of the given frequency of the controller's built-in clock f_0 and phase $2\pi f_0 t$, the d-axis orientation position of the converter output voltage and the angle of Park inverse transformation θ can be get by shifting angle. The d-axis orientation position is shown as Fig. C-3.
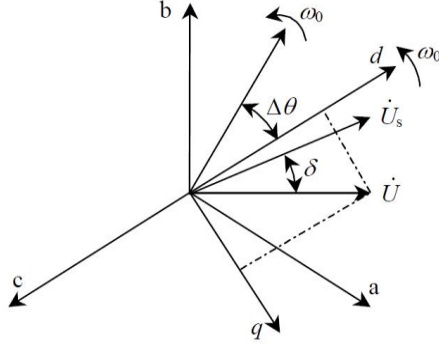
Fig. C-3: The d-axis orientation position

Therefore, the angle deviation will be adjusted to change the relative position of the d-q axis orientation by the integral link when there is a deviation between the transmission active power and the given value. In essence, the power angle is adjusted so that the VSC-HVDC transmission power is kept at a given reference value and the constant active power control is realized.

When the grid-connected wind farm is purely flexible, the voltage of the wind farm is kept stable by the amplitude controller, and the frequency of the wind farm is controlled by the built-in clock of the controller. According to the above active power control link, it can be get that

$$\theta = \omega t = 2\pi [f_0 - \frac{K(P_{ref} - P_{VSC})}{2\pi}]t \tag{C-8}$$

In the formula (C-8), the frequency of the wind farm is adjusted as follows.

$$f = f_0 - \frac{K(P_{ref} - P_{VSC})}{2\pi} \tag{C-9}$$

Therefore, the wind farm bus is controlled as a power point whose voltage amplitude is stable and the frequency is f , which realizes the synchronous transmission of wind power.

Due to the fluctuation of wind power, there is a deviation between the given reference value of active power P_{ref} and the transmission power P_{VSC} . According to the formula (C-9), the deviation between the frequency of the wind farm and built-in clock frequency of the given controller will exist because of the fluctuation of wind power. The reference value of active power P_{ref} is generally given according to the average output of the wind farm, so the deviation between P_{ref} and the

real-time output of the wind farm.is less. Therefore, when the wind farm output changes, the frequency of wind farm f will fluctuate in the range of allowable deviation of the frequency f_0.

D. Subsea cable parameters from ABB

Table D-1: Parameters for 30kV three-core cables with copper wire screen

Cross section of conductor	Diameter of conductor	Insulation thickness	Diameter over insulation	Cross section of screen	Outer diameter of cable	Cable weight(Alumi-num)	Cable weight(Copper)	Capacitance	Charging current per phase at 50hz	Inductance
mm^2	mm	mm	mm	mm^2	mm	kg/m	kg/m	uf/km	A/km	mH/km
Three-core cables, nominal voltage 30kV(Um=36kV)										
70	9.6	8.0	28.0	16	100.6	16.9	18.2	0.16	0.9	0.46
95	11.2	8.0	29.6	16	104.0	17.7	19.5	0.18	1.0	0.44
120	12.6	8.0	31.0	16	107.0	18.4	20.7	0.19	1.0	0.42
150	14.2	8.0	32.6	16	110.5	19.3	22.1	0.21	1.1	0.41
185	15.8	8.0	34.2	16	114.0	20.1	23.6	0.22	1.2	0.39
240	18.1	8.0	36.5	16	118.9	21.4	25.9	0.24	1.3	0.38
300	20.4	8.0	38.8	16	123.9	22.6	28.2	0.26	1.4	0.36
400	23.2	8.0	41.6	16	123.9	24.6	32.0	0.29	1.6	0.35
500	26.2	8.0	45.0	16	137.3	26.7	36.0	0.32	1.7	0.34
630	29.8	8.0	48.6	16	145.1	29.2	40.9	0.35	1.9	0.32
800	33.7	8.0	52.5	16	154.4	32.2	47.2	0.38	2.1	0.31

Table D-2: 10-90kV XLPE 3-core cables

10-90kV XLPE 3-core cables		
Cross section mm2	Copper conductor	Aluminum conductor
	A	A
95	300	235
120	340	265
150	375	300
185	420	335
240	480	385
300	530	430
400	590	485
500	655	540
630	715	600
800	775	660
1000	825	720

Reference

[1]M. Amin, M. Molinas, and L. Jing, "Oscillatory phenomena between wind farms and HVDC systems: The impact of control," in *Proc. COMPEL. IEEE,* 2015, pp. 1-8.

[2]K. W. Louie, P. Wilson, R. W. Wachal, et al., "HVDC Power System Harmonic Analysis in the Time and Frequency Domains," in Proc. *International Conference on Power System Technology, 2006. Powercon. IEEE,* 2007, pp. 1-8.

[3]R. Zheng, M. H. J. Bollen, and J. Zhong, "Harmonic resonances due to a grid-connected wind farm," in *Proc. International Conference on Harmonics and Quality of Power IEEE,* 2010, pp. 1-7.

[4]A. G. Sanchez, M. G. Molina, and A. M. R. Lede, "Dynamic model of wind energy conversion systems with PMSG-based variable-speed wind turbines for power system studies," *International Journal of Hydrogen Energy,* vol. 37, no. 13, pp. 10064-10069, 2012.

[5]A. Medina, et al., "Harmonic Analysis in Frequency and Time Domain," *IEEE Transactions on Power Delivery,* vol. 28, no. 3, pp. 1813-1821, 2013.

[6]L. H. Kocewiak, J. Hjerrild, and C. L. Bak, "Harmonic Analysis of Offshore Wind Farms with Full Converter Wind Turbines," in *Proc. 8th International Conference on Large-Scale Integration of Wind Power into Power Systems,* 2009.

[7]K. N. M. Hasan, K. Rauma, P. Rodriguez, et al., "An overview of harmonic analysis and resonances of large wind power plant," in *Proc. IECON 2011 -, Conference on IEEE Industrial Electronics Society. IEEE,* 2012, pp. 2467-2474.

[8]M. H. J. Bollen and K. Yang, "Harmonic aspects of wind power integration," *Journal of Modern Power Systems & Clean Energy*, vol. 1, no. 1, pp. 14-21, 2013.

[9]M. D. Prada-Gil, et al., "Offshore Wind Power Plants (OWPPS): For Offshore and Supergrid of the Future," in *HVDC Grids,* 2016.

[10]G. W. Chang, et al., "Measuring power system harmonics and interharmonics by an improved fast Fourier transform-based algorithm," *Generation Transmission & Distribution Iet,* vol. 2, no. 2, pp. 193-201, 2008.

[11]J. B. Glasdam, "Harmonics in Offshore Wind Power Plants: Application of Power Electronic Devices in Transmission Systems," Ph.D. dissertation, Dept. Elect. Eng., Barry Univ., 2005.

[12]D. Schwanz and R. C. Leborgne, "Comparative harmonic study of a wind farm: Time vs frequency domain simulation," in *Proc. International Conference on Harmonics and Quality of Power. IEEE,* 2014, pp. 793-797.

[13]J. A. Carta, "Wind Power Integration," in *Comprehensive Renewable Energy,* 2012, pp. 569-622.

[14]L. Sevgi, "Numerical Fourier transforms: DFT and FFT," *IEEE Antennas & Propagation Magazine*, vol. 49, no. 3, pp. 238-243, 2007.

[15]J. Li Jun, N. Samaan, and S. Williams, "Modeling of large wind farm systems for dynamic and harmonics analysis," in *Proc. T&D. IEEE/PES IEEE,* 2008, pp. 1-7.

[16]J. Arrillaga, et al., "Introduction," in *Power System Harmonic Analysis*, 2013.

[17]H. V. Haghi and M. T. Bina, "Complete harmonic domain modeling and performance evaluation of an optimal-PWM-modulated STATCOM in a realistic distribution network," in *Proc. International School on Nonsinusoidal Currents and Compensation. IEEE,* 2008, pp. 1-7.

[18]M. R. Abedi and K. Y. Lee, "Modeling, operation and control of wind turbine with direct drive PMSG connected to power grid," in *Proc. PES General Meeting / Conference & Exposition. IEEE,* 2014, pp. 1-5.

[19]M. Chinchilla, S. Arnaltes, and J. C. Burgos, "Control of Permanent-Magnet Generators Applied to Variable-Speed Wind-Energy Systems Connected to the Grid," *IEEE Transactions on Energy Conversion,* vol. 21, no. 1, pp. 130-135, 2006.

[20]A. Uehara, A. Pratap, T. Goya, et al., "A Coordinated Control Method to Smooth Wind Power Fluctuations of a PMSG-Based WECS," *International Journal of Emerging Electric Power Systems,* vol. 26, no. 2, pp. 550-558, 2011.

[21]M. V. Chavez-Baez, O. Anaya-Lara, K. L. Lo, et al., "Review of harmonics in offshore wind farms," in *Proc. UPEC. IEEE,* 2014, pp. 1-5.

[22]G. S. Stavrakakis, "Electrical Parts of Wind Turbines," in *Comprehensive Renewable Energy,* 2012.

[23]K. Yang and M. H. J. Bollen, "Interharmonic currents from a Type-IV wind energy conversion system," *Electric Power Systems Research,* vol. 143, pp. 357-364, 2017.

[24]D. Jenkins, "Renewable energy systems," in *Proc. IEEE International Conference on Industrial Technology IEEE,* 2013, pp. 650-652.

[25]M. G. Molina and P. E. Mercado, "Chapter 16 Modelling and Control Design of Pitch-Controlled Variable Speed Wind Turbines," in *Wind Turbines,* InTech, 2006.

[26]M. G.Molina, A. G. Sanchez, and A. M. R. Lede. "Dynamic modeling of wind farms with variable-speed direct-driven PMSG wind turbines," in *Proc. T&D-LA. IEEE/PES,* 2010, pp. 816-823.

[27]A. Uehara, A. Pratap, T. Goya, et al., "A Coordinated Control Method to Smooth Wind Power Fluctuations of a PMSG-Based WECS," *IEEE Transactions on Energy Conversion,* vol. 26, no. 2, pp. 550-558, 2011.

[28]F. lov, M. Ciobotaru, and F. Blaabjerg, "Power electronics control of wind energy in distributed power systems," in *Proc. International Conference on Optimization of Electrical and Electronic Equipment. IEEE,* 2008, pp. XXIX-XLIV.

[29]A. D. Hansen and M. Gabriele, "Modelling and control of variable-speed multi-pole permanent magnet synchronous generator wind turbine," *Wind Energy,* vol. 11, no. 5, pp. 537-554, 2008.

[30]J. Ivanqui, H. Voltolini, R. Carlson, et al., ""pq theory" control applied to wind turbine trapezoidal PMSG under symmetrical fault," in *Proc. Electric Machines & Drives Conference. IEEE,* 2013, pp. 534-540.

[31]T. A. Haskew and S. Li, "Transient and Steady-State Simulation Study of Decoupled d-q Vector Control in PWM Converter of Variable Speed Wind Turbines," in *Proc. Industrial Electronics Society, IECON, Conference of the IEEE,* 2007, pp. 2079-2086.

[32]S. M. Tripathi, A. N. Tiwari, and D. Singh, "Optimum design of proportional-integral controllers in grid-integrated PMSG-based wind energy conversion system: Optimum Design of PI Controllers," *International Transactions on Electrical Energy Systems,* vol. 26, no. 5,

pp.1006-1031, 2016.

[33] M. Ben Smida and A. Sakly, "Differen conventional strategies of pitch angle control for variable speed wind turbines," in *Proc. 15th International Conference on Sciences and Techniques of Automatic Control and Computer Engineering. IEEE,* 2014, pp. 803-808.

[34]S. L. Feng, H. X. Zhao, and W. S. Wang, "Studies on the Variable Speed Wind Turbine Control System Based on PSCAD/EMTDC," in *Proc. International Conference on Power System Technology. Powercon. IEEE,* 2007, pp. 1-9.

[35]H. Xiao, Y. Liu, and H. Liu. "Harmonic Analysis by Modelling and Simulation of the Wind Farm Based on DFIG," *Electronics and Electrical Engineering,* vol. 19, no. 7, pp. 17-21, 2013.

[36]T. M. Blooming, and D. J. Carnovale, "Application of IEEE STD 519-1992 Harmonic Limits," in *Proc. Pulp and Paper Industry Technical Conference, 2006. Conference Record of IEEE,* 2006, pp. 1-9.

[37]F. Blaabjerg, M. Liserre, and K. Ma. "Power electronics converters for wind turbine systems," *IEEE Transactions on Industry Applications,* vol. 48, no. 2, pp. 708-719, 2011.

[38]J. O. Tande, "Power Quality Standards for Wind Turbines," in *Wind Power in Power Systems,* 2012, pp. 79-95.

[39]Y. Zhu, M. Cheng, W. Hua, et al., "A Novel Maximum Power Point Tracking Control for Permanent Magnet Direct Drive Wind Energy Conversion Systems," *Energies,* vol. 5, no. 5, pp. 1398-1412, 2012.

[40]H. Li and Z. Chen, "Design optimization and site matching of direct-drive permanent magnet wind power generator systems," *Renewable Energy,* vol. 34, no. 4, pp. 1175-1184, 2009.

[41]H. Huang, G. W. Chang, P. K. Wang, et al., "A study of submarine power grid planning for offshore wind farm," *IEEE Power and Energy Society General Meeting,* vol. 19, no. 5, pp. 1-5, 2011.

[42]P. Bresesti, W. L. Kling, R. L. Hendriks, et al., "HVDC Connection of Offshore Wind Farms to the Transmission System," *IEEE Transactions on Energy Conversion,* vol. 22, no. 1, pp. 37-43, 2007.

[43]S. S. Gjerde and T. M. Undeland, "Control of direct driven offshore wind turbines in a DC-collection grid within the wind farms," in *Proc. Trondheim PowerTech. IEEE,* 2011, pp. 1-7.

[44]A. Thomas, O. Antje, and R. Krzysztof, "14. Transmission Systems for Offshore Wind Power Plants and Operation Planning Strategies for Offshore Power Systems," in *Wind Power in Power Systems,* 2012, pp. 293-327.

[46]M. Amin, M. Molinas, and L. Jing, "Oscillatory phenomena between wind farms and HVDC systems: The impact of control," in *Proc. COMPEL. IEEE,* 2015, pp. 1-8.

[47]C. Kim, V. K. Sood, G. Jang, et al., "Trends for HVDC Applications," in *HVDC Transmission: Power Conversion Applications in Power Systems,* John Wiley & Sons, Ltd., 2009, pp. 352.

[48]R. Blasco-Gimenez, N. Aparicio, S. Ano-Villalba, et al., "LCC-HVDC Connection of Offshore Wind Farms With Reduced Filter Banks," *IEEE Transactions on Industrial Electronics,* vol. 60, no. 6, pp. 2372-2380, 2013.

[49]H. Liu and J. Sun, "Voltage Stability and Control of Offshore Wind Farms With AC Collection and HVDC Transmission," *IEEE Journal of Emerging and Selected Topics in Power Electronics,* vol. 2, no. 4, pp. 1181-1189, 2014.

[50]N. M. Kirby, L. Xu, M. Luckett, et al., "HVDC transmission for large offshore wind farms," *Power Engineering Journal,* vol. 16, no. 3, pp. 135-141, 2002.

[51]B. Badrzadeh, M. Gupta, N. Singh, et al., "Power system harmonic analysis in wind power plants — Part I: Study methodology and techniques," in *Proc. Industry Applications Society Annual Meeting. IEEE,* 2012, pp. 1-11.

[52]D. Mehrzad, J. Luque, and M. C. Cuenca, "Vector control of PMSG for grid-connected wind turbine applications," Project for Master's Thesis, Institute of Energy Technology, Alborg University, 2009.

[53]T. H. Nguyen and D. C. Lee. "Control of offshore wind farms based on HVDC," in *Proc. ECCE. IEEE,* 2012, pp. 3113-3118.

[54]H. Abniki, S. Nateghi, R. Ghandehari, et al., "Harmonic analyzing of wind farm based on harmonic modeling of power system components," in *Proc. International Conference on Environment and Electrical Engineering. IEEE,* 2012, pp. 667-672.

[55]M. Madrigal, and E. Acha. "Harmonic modelling of voltage source converters for HVDC stations," in *Proc. Ac-Dc Power Transmission, Seventh International Conference on IET,* 2001, pp. 125-131.

[56]A. Reznik, M. G. Simoes, A. Al-Durra, et al. "LCL Filter Design and Performance Analysis for Grid-Interconnected Systems," *IEEE Transactions on Industry Applications,* vol. 50, no. 2, pp. 1225-1232, 2014.

[57] T. Qian, K. Liu, Z. Li, et al., "The Suppression of Resonance by a New Hybrid Power Filter," in *Proc. Conference on Industrial Electronics and Applications. IEEE,* 2006, pp. 1-5.

[58] J. Ji, G. Zeng, H. Liu, et al., "Research on selection method of Passive Power Filter topologies," in *Proc. IPEMCC. IEEE,* 2012, pp. 2844-2848.

[59]M. A. Zamani, M. Moghaddasian, M. Joorabian, et al., "C-type filter design based on power-factor correction for 12-pulse HVDC converters," in *Proc. Industrial Electronics, IECON, Conference of IEEE,* 2009, pp. 3039-3044.

[60]R. Klempka, "A New Method for the C-Type Passive Filter Design," *Przeglad Elektrotechniczny,* vol. 88, no. 7a, pp. 277-281, 2012.

[61]Y. Xiao, J. Zhao, and S. Mao, "Theory for the design of C-type filter," in *Proc. International Conference on Harmonics and Quality of Power. IEEE,* 2004, pp. 11-15.

[62] J. Wen, W. Meng, W. Y. Yin, et al., "Optimizing design of AC filters of ±800 kV UHVDC transmission projects," *High Voltage Engineering,* vol. 36, no. 4, pp. 912-917, 2010.

[63] S. H. E. A. Aleem, A. F. Zobaa, and M. M. A. Aziz, "Optimal C-Type Passive Filter Based on Minimization of the Voltage Harmonic Distortion for Nonlinear Loads," *IEEE Transactions on Industrial Electronics,* vol. 59, no. 1, pp. 281-289, 2011.

[64] D. Grabowski, M. Pasko, et al., "Compensation based on active power filters – The cost minimization," *Applied Mathematics and Computation,* vol. 267, no. C, pp. 648-654, 2015.

[65]K. L. Koo, "Harmonic assessments for filter design specifications at U.K. National Grid electricity transmission system for large wind farms," in *Proc. Universities Power Engineering Conference. IEEE,* pp. 1-6, 2010.

[66] Liserre M, Blaabjerg F, Hansen S, "Design and control of an LCL-filter-based

three-phase active rectifier," in *IEEE Transactions on Industry Applications,* vol. 41, no. 5, pp. 1281-1291, 2005.

[67] Badkubi, Salman, et al., "Reducing the current harmonics of a wind farm generation based on VSC-HVDC transmission line by shunt active power filters," in *Energy Procedia,* vol. 14, pp. 861-866, 2012.

[68]B. Franken, H. Breder, M. Dahlgren, et al., "Collection grid topologies for off shore wind parks," *Iet Digital Library,* pp. 1-5, 2005.

[69]M. Bollen, J. Meyer, H. Amaris, et al., "Future work on harmonics - some expert opinions Part I - wind and solar power," in *Proc. International Conference on Harmonics and Quality of Power. IEEE,* 2014, pp. 904-908.